Legacy contaminant release from the cryosphere to downstream systems

by

Katarzyna Joanna Staniszewska

A thesis submitted in partial fulfillment of the requirements for the degree of

Master of Science

Department of Earth and Atmospheric Sciences
University of Alberta

ABSTRACT

Anthropogenic climate warming is degrading the cryosphere. Retreating alpine glaciers and thawing permafrost pose the risk of releasing previously sequestered legacy contaminants to downstream environments, with potential negative consequences for downstream aquatic ecosystems. In this thesis I present the results of high temporal resolution hydrochemistry monitoring and modeling from proglacial Sunwapta River, which is fed by glacial melt in the Canadian Rocky Mountains, and Old Crow River in arctic Yukon, which is underlain by continuous permafrost. Relations between the hydrochemistry dataset and high-resolution monitoring data (e.g. discharge, conductivity, turbidity) were used to model daily contaminant concentrations and estimate annual fluxes and yields. Nutrient and trace element contaminant concentrations, fluxes, and yields were low, dominated by particulate phases, and positively related to discharge in both systems. In the Sunwapta River, two chemically and temporally distinct sources to melt were distinguished: a subglacial component characterized by dissolved elements associated with carbonate, and an englacial component which contained potential legacy contaminants predominantly in particulate form and at low concentrations. In the Old Crow River, contaminant concentrations peaked during the high-discharge spring freshet. Thaw slumps and thermokarst-connected tributaries to the Old Crow River did not significantly raise contaminant concentrations during the summer period of peak ground thaw, which was associated with very low contaminant fluxes. The annual yield of mercury was low (3.2 g/km^2/yr at Sunwapta River; 0.8 g/km^2/yr at Old Crow River) and comparable to natural temperate streams. Positive trends in historic water yield at both study sites suggest contaminant fluxes have increased over the past > 40 years. Collectively, the results suggest that other glaciers in the Canadian Rocky Mountains, and degrading permafrost in moderately sized arctic watersheds,

release low levels of particle-bound contaminants to their downstream environments that predominantly augment sedimentary contaminant stocks.

PREFACE

This thesis contains four chapters. Chapters two and three are collaborative works prepared as standalone manuscripts:

Chapter 2 is a manuscript prepared for submission as: “Quantifying meltwater sources and contaminant fluxes from the Athabasca Glacier, Canada”, coauthored by me, Colin A. Cooke, and Alberto V. Reyes. CAC designed the project concept and coordinated the fieldwork and sonde maintenance. KJS carried out fieldwork and was responsible for all data processing and analysis. KJS led the data interpretation with guidance from CAC and AVR. The manuscript was written by KJS with editorial contributions from CAC and AVR.

Chapter 3 is a manuscript being prepared for submission as: “Thaw features in continuous permafrost contribute minor amounts of mercury and other trace elements to downstream environments in the Old Crow River, Yukon”, coauthored by me, Alberto V. Reyes, Colin A. Cooke, and Grant D. Zazula. KJS, AVR, and CAC designed the project concept. KJS conducted monthly field research, laboratory analyses, data processing, and data analysis. GDZ coordinated aspects of the field work and provided geological context for the study. The manuscript was written by KJS with editorial contributions from AVR and CAC.

ACKNOWLEDGMENTS

Thank you to my kind and supportive supervisors, Dr. Colin Cooke and Dr. Alberto Reyes who provided guidance, freedom, thoughtful feedback, were present, encouraging, patient, respectful, genuine, and encouraged my personal and academic growth. I eagerly await our future collaborations.

This thesis is written with deep gratitude to the Vuntut Gwitchin First Nation and Community of Old Crow, Kathie Charlie, Caleb Charlie, Megan Williams, Sophia Flather, David Moses, and Josepth Tetlichi, the Yukon Government Palaeontology team: Dr. Grant Zazula and Elizabeth Hall, and the Alberta Environment and Parks Aquatic Monitoring and Science Division. I am grateful to my defense committee: Dr. Suzanne Tank and Dr. Martin Sharp for insightful defense questions and thesis feedback. I am also grateful to past and current mentors, including Dr. Duane Froese, Dr. Britta Jensen, Dr. Grant Zazula, Dr. Lauren Davies, Sasiri Bandara, Dr. Thomas Stachel, and Dr. John Waldron who have guided, inspired, and taught me so much in the lab, field, classroom, and beyond. I am grateful to Ella Lassu, Ruby Prinsen, Casey Buchanan, Serhiy Buryak, Matthew Bolton, Patrick Williams, Sophie Norris, Nicholas Heida, Brielle Andersen, Adam Halverson, Shaun Woudstra, Libby Tunney, Jordan Harvey, and Nathan Polard-Yopek who animated these two years with pandemic-virtual-office, inspiring conversations, collaborative story telling, sports, hikes, coffees, encouragement, and many moments of laughter and joy.

Most of all, thank you to my husband, Corey, and my brother, Konrad. Your uplifting kindness, friendship, love, and support mean the world.

Funding was provided by Alberta Environment and Parks (Cooke), NSERC Discovery Grants (Reyes), NSERC Canada Graduate Scholarship-Master's (Staniszewska), Norther Scientific Training Program (Staniszewska), University of Alberta Northern Research Award (Staniszewska), Polar Continental Shelf Program (Zazula); in-kind support was also provided by Yukon Government Palaeontology and Alberta Environment and Parks.

TABLE OF CONTENTS

LIST OF TABLES

LIST OF FIGURES

CHAPTER 1. Legacy Contaminant Release from the Cryosphere to Downstream Systems

1.1. Introduction

The cryosphere contains large stocks of legacy contaminants (Stern et al., 2012; Miner et al., 2017; Gao et al., 2018; Olson et al., 2018; Schuster et al., 2018; Lim et al., 2020). Legacy contaminants are compounds which were emitted to the earth system by natural and anthropogenic activity during the past that have persisted in the environment. Legacy contaminants include trace elements (e.g., mercury, lead, arsenic, chromium, cadmium, copper), nutrients from fertilizers, hydrocarbons, and pesticides including organochlorines and polychlorinated biphenyls. Perennial ice bodies and permafrost regions have accumulated these legacy contaminants from wet and dry atmospheric deposition over millennia (Stern et al., 2012; Zhang et al., 2016). Now, as anthropogenic climate warming accelerates the retreat of glaciers and the thaw of permafrost ground (IPCC, 2013), these components of the cryosphere have become potential sources of legacy contaminants to downstream aquatic systems (Brighenti et al., 2019). The following thesis aims to quantify the magnitude of legacy contaminant release to lotic systems: (1) downstream of a glacier, and (2) in a watershed underlain by continuous permafrost.

1.2. Background

The history of anthropogenic contaminant emissions is as old as human history, but contaminant emissions increased multifold over the industrial revolution (Nriagu, 1990;

Hammerschmidt, 2011; Streets et al., 2011; Horowitz et al., 2014). For example, atmospheric mercury inputs to western North American lakes (Fitzgerald et al., 2005; Phillips et al., 2011; Drevnick et al., 2016) and nitrogen fluxes of global rivers (Green et al., 2004) have risen 3- to 5-fold from natural background concentrations. Similarly, ice cores record a changing history of 20th Century lead emissions to the atmosphere beginning with coal mining and then leaded gasoline usage from the 1920s – 80s (Barbante et al., 2004; Schwikowski et al., 2004; McConnell and Edwards, 2008; Eichler et al., 2012; Beal et al., 2015). Emissions of many anthropogenic contaminants have decreased sharply since the 1970s alongside the introduction of NO_x and SO_x capture technologies, reduction in coal emissions worldwide, and heightened environmental regulation (Beijer Institute et al., 1987; Dudka and Adriano, 2010; Zhang et al., 2016). Cumulatively, however, anthropogenic chalcophile element emissions far surpass natural emissions from, for example, biogenic emissions, forest fire, or volcanism (Nriagu, 1979, 1990; Schuster et al., 2002; Beal et al., 2015).

Together, contaminants released naturally and anthropogenically to the atmosphere have accumulated through wet- and dry deposition in components of the cryosphere, including alpine glaciers and permafrost. In glacier settings, contaminants which settle with dry deposition and precipitation can become stored in the accumulation area for long time frames, and released through seasonal melt decades to centuries later (Blais et al., 2001; Lafrenière et al., 2006; Bogdal et al., 2010; Stern et al., 2012; Niu et al., 2017). In permafrost, and particularly permafrost peatland settings, contaminants accumulate in vegetation as the permafrost table aggrades. Over millennia, this can lead to vast quantities of contaminants being stored in permafrost, though the magnitude of the permafrost contaminant reservoir is an area of active research. For example, Schuster et al. (2018) estimated that northern hemisphere permafrost

regions contain 1656 ± 962 Gg Hg in the top 3 m of material; this is more than double the amount of mercury stored in non-permafrost soils, the ocean, and the atmosphere combined. In contrast, Lim et al. (2020) estimated that 597 Gg Hg resides in the top 3 m of northern permafrost regions. Lim et al. (2020) further estimated that the upper 30 cm of the global soil Hg pool contains 1086 Gg Hg of which 7% (72 Gg Hg) resides in northern permafrost soils. Gao et al. (2018) estimate that permafrost regions also contain significant stocks of nitrogen and phosphorus.

Global warming is directly leading to the degradation of many components of the cryosphere (IPCC, 2013). By 2100, glacier cover is predicted to decrease by 60 – 90% in the Canadian Rockies (Marshall et al., 2011; Clarke et al., 2015) and permafrost in the northern hemisphere is predicted to shrink by 30 – 99% (Koven, Riley and Stern, 2013). As a result of this melt and thaw, potentially hazardous levels of legacy contaminants may be released to downstream aquatic systems. Synthetic contaminants such as polychlorinated biphenyls and organochlorine pesticides have been recorded in alpine glacier-fed lakes in the Arctic (Miner et al., 2017; Lehmann-Konera et al., 2019; Sun et al., 2020), Asia (Li et al., 2017), Canadian Rocky Mountains (Blais et al., 2001; Lafrenière et al., 2006; Miner et al., 2017), and Alps (Villa et al., 2006; Ferrario, Finizio and Villa, 2017). Similarly, elevated mercury and nutrient concentrations have been recorded in glacier- and permafrost-fed streams (Baron, Schmidt, and Hartman, 2009; Barnes et al., 2014; Heath and Baron, 2014; Mast et al., 2014; Vermilyea et al., 2017; St. Pierre et al., 2018; X. Sun et al., 2018) and lakes (Hobbs, Vinebrooke and Wolfe, 2011; Burke et al., 2018; Zdanowicz et al., 2018; Colombo et al., 2019; Lafrenière and Lamoureux, 2019; Lehnherr et al., 2018). Thus, there is evidence that high stocks of legacy contaminants in cryosphere

reservoirs may be a significant source of contaminant release to downstream environments (Stern et al., 2012; Colombo et al., 2018; Brighenti et al., 2019).

The reintroduction of these legacy contaminants to aquatic systems is concerning due to their persistent, bioaccumulative, and toxic qualities, especially in certain speciations and at high concentrations. The reintroduction, if in bioavailable forms, may lead to ecosystem wide effects due to biomagnification with increasing trophic level (Brighenti et al., 2019). Thus, the speciation, concentration, and overall release flux (mass) and yield (mass normalized to land area) of contaminants is important for the assessment of contaminant persistence, bioaccumulation potential, and toxicity to aquatic biotic life. Excessive phosphorus and nitrogen can lead to eutrophication; additionally, nitrite and ammonia are toxic. Many trace element contaminants can form organometallic complexes (including with methyl groups) that are several times more toxic to aquatic organisms than their inorganic counterparts (US Environmental Protection Agency, 2009). Organometallic complexes such as methylmercury are especially susceptible to bioaccumulate in the fatty tissues of living organisms, and biomagnify through food webs (Kidd, Clayden and Jardine, 2012). Bioaccumulation is the process by which an organism's body accumulates increasing concentrations of a chemical over its lifespan; biomagnification is the process by which high trophic level organisms, (e.g., large fish) accrue high concentrations of a chemical with increasing trophic level (Kidd, Clayden and Jardine, 2012). Bioavailability describes a species' immediate uptake potential to organisms, whereas bioaccessiblility describes the potential for a chemical species to become bioavailable given its physical or chemical state (Semple et al., 2004). For example, dissolved methylmercury is immediately bioavailable while particulate methylmercury, which is sorbed to the outside of organic matter, may be bioaccessible. In contrast, inorganic mercury is typically considered not

to be bioaccessible. Of those trace elements and nutrient contaminants examined in this thesis, mercury is of particular concern. The fate of mercury release is a pressing research area given that mercury rises may pose a risk to future water quality, aquatic ecosystem health, food security, and human health (Järup, 2003; AMAP/UNEP, 2013; Eagles-Smith et al., 2016; Laird et al., 2018).

1.3. Problem and Significance

Research over the 1990s – 2020s has led to an emerging body of knowledge suggesting that degrading glacier and permafrost systems contribute dangerous legacy contaminants to their downstream reach. The pervasive hypothesis is that the high stocks of contaminants stored in glaciers and permafrost regions will lead to release of labile and environmentally impactful quantities and species of contaminants to downstream systems as the cryosphere degrades. However, there are contrasting reports of the rate and lability of legacy contaminant release from these systems, and the downstream transport of the contaminants.

In glaciated catchments, recent work by Vermilyea et al. (2017) and Paudyal et al. (2017) points to high concentrations and/or fluxes of mercury from small glaciated catchments. These studies contrast with the low mercury concentrations and fluxes reported by St. Pierre et al. (2019), Sun et al. (2017, 2018), and Søndergaard et al. (2012). Baron, Schmidt and Hartman (2009), and Barnes et al. (2014) determined that permafrost thaw and alpine glacier melt significantly increased nutrient flux in the Colorado Mountains, but this was contested by Mast et al. (2014) who instead suggested that increased rainfall following a drought led to the observed increased nutrient fluxes. In terms of organic pollutants, Blais et al. (2001), found that

50 – 97% of organochlorines and polychlorinated biphenyls measured in an alpine lake originated from alpine glaciers. Lafrenière et al. (2006) found that alpine glacier runoff was enriched in organochlorine compounds relative to snowpacks in one of two study years, and Villa et al. (2006) found that alpine glacier runoff-fed streams generally had higher organochlorine concentrations than non-glacier fed streams. These synthetic compounds are bioavailable and toxic at extremely low concentrations and their mere presence is concerning. However, inferences based on synthetic organic compounds do not translate directly to inferences which can be made about trace elements and nutrients which are naturally present, at various concentrations, in the environment.

In permafrost regions, Gao et al. (2018) suggested that nutrients are not labile and are sediment bound. However, St. Pierre et al. (2018) found that retrogressive thaw slumps in the Peel Basin, NWT, contributed over 1000 ng/L of total mercury downstream. This total mercury concentration was predominantly in particulate form with low bioavailability. Klaminder et al. (2008) found that thawing palsa mires release 40 – 90% of stored mercury as they degrade, and a number of studies (Schuster et al., 2011; Emmerton et al., 2013; Sonke et al., 2018; Zolkos et al., 2020) have reported a large range of mercury yields in large arctic river basins underlain by extensive permafrost. Inferences which could be drawn from previous studies have been hampered by: (1) uncertainties inherent to sampling resolution or duration; (2) being conducted at zero-order stream scales, limiting assessment of downstream effects; or (3) being conducted at the outlets of large rivers, limiting the identification of upstream contaminant sources and cycling.

The degree to which alpine glaciers and permafrost regions currently release legacy contaminants to lotic aquatic systems has been studied in limited geographic regions and for a

small simultaneously-analyzed suite of contaminants. A large portion of studies which found significant anthropogenic contamination were conducted in lentic systems—lakes, ponds, and wetlands (Blais et al., 2001; Klaminder et al., 2008; Hobbs, Vinebrooke and Wolfe, 2011; Burke et al., 2018; Colombo et al., 2019; Lehnherr et al., 2018)—where longer water residence times promote contaminant accumulation and physiochemical and biotic conditions promote organometallic complexation (including methylation). These physiochemical and biotic differences may result in lentic systems responding more sensitively to legacy contaminant inputs than lotic systems. In addition, few studies have investigated hydrochemistry drivers, and thereout modeled past and future trends in contaminant release using long term data records.

At the global scale, rivers draining glaciated and permafrost basins supply a significant portion of sediments and associated organic matter, nutrients, and contaminants to the Arctic Ocean (Leitch et al., 2007; Fisher et al., 2012; Amos et al., 2014; Sonke et al., 2018), where the concentrations of certain contaminants have increased in the decades following the 1970s and global reduction of mercury emissions (AMAP/UNEP, 2013; Sunderland and Selin, 2013; Zhang et al., 2016). Numerous studies have shown increasing levels of mercury (and organochlorine) exposure in Arctic fish, wildlife, and Northern-Canadian populations who consume traditional foods (Donaldson et al., 2010; Laird et al., 2018). Identifying whether thawing permafrost or melting glaciers are at the root of increasing contaminant levels in the Arctic ecosystem is key to predicting future trends in legacy contaminant concentrations in the Arctic environment. Canada has the third largest reservoir of renewable freshwater on Earth, but climate change is threatening to lower the quality of this resource (Schindler and Donahue, 2006; Schindler and Smol, 2006; Sprague, 2007; Brahney et al., 2017). Assessing the water quality of rivers which sustain vast ecosystems, Canadian communities, and agriculture is mounting in importance as a result of the

rapid acceleration of climate warming. Put together, numerous literature reviews and environmental assessment panels have pointed to legacy contaminants released from the cryosphere as a potential hotspot of contamination, and a pressing future research topic (Stern et al., 2012; AMAP/UNEP, 2013; Dubé et al., 2013; Sunderland and Selin, 2013; Andrews et al., 2016; Colombo et al., 2018).

1.4. Purpose and Questions

The research gaps, environmental impacts, and societal implications described above provide a clear motivation for the thesis research presented here. The objective of this thesis is to assess how melting glaciers and thawing permafrost impact downstream water quality in western Canada. I analyzed water quality downstream of the Athabasca Glacier, in proglacial Sunwapta River, Alberta, and across the permafrost-dominated Old Crow River basin in arctic Yukon. Specifically, I monitored and analyzed river hydrochemistry by measuring the concentration and speciation of nutrients and trace elements contaminants, and modeled their flux and yield at the watershed scale. Using these data, I aim to answer the following questions:

(1) Does the Athabasca Glacier (and by extension, the Columbia Icefield, and other glaciers in the Rocky Mountains) release legacy contaminants to downstream environments?

(2) Do permafrost thaw features along the Old Crow River (and other Arctic rivers) release legacy contaminants to downstream environments?

(3) Are there any temporal patterns in contaminant release in these two systems?

(4) How do the annual yields of mercury of the Sunwapta and Old Crow rivers compare to other rivers?

1.5. Research Design and Methods

In order to answer these questions, I conducted two studies which analyzed a broad suite of physical and chemical water quality parameters in two watersheds where cryosphere degradation is actively occurring. The Sunwapta and Old Crow rivers were selected as examples of fluvial systems sourced from alpine-glacial settings and continuous permafrost, respectively. Sunwapta River originates from a small stream which flows from the Athabasca Glacier, one of eight outlet glaciers of the Columbia Icefield, Canada. The catchment area at the monitoring station is approximately 30 km^2 (Water Survey of Canada, 2020). The site essentially represents a point source of discharge dominated by melt of snow, subglacial, englacial, and supraglacial ice. The Old Crow River's 13,900 km^2 watershed is underlain by continuous permafrost (Yukon Ecoregion Working Group, 2004), a region where more than 90% of the material below the active layer has remained at or below 0 °C for a minimum of two years (Van Everdingen, 1998). These two rivers are relatively untouched by localized anthropogenic activity and are distant from potential major points sources of contamination from urban emissions, coal and ore-processing, fossil-fuel burning, agriculture, or oil-sands development. The Sunwapta River is protected within Jasper National Park, and the Old Crow River's entire watershed is undeveloped and within the traditional territory of the Vuntut Gwitchin First Nation (The Government of Canada, The Vuntut Gwitchin First Nation and The Government of the Yukon, 1993).

River water samples were collected for a broad suite of total, dissolved, and field water chemistry parameters at both sites. At Sunwapta River, ~monthly water sampling was supplemented by continuous monitoring of water physiochemical parameters using a stream gauge and sondes (OTT Hydromet, 2020; YSI Inc., 2020) for turbidity and conductivity. At Old Crow River, ~weekly water samples were supplemented with stream gauge data. I also collected samples of Old Crow River tributary waters, and thaw slump stream and sediment samples, across the basin during the summer period of peak permafrost thaw to further assess point sources of permafrost degradation, such as retrogressive thaw slumps and tributaries affected by thermokarst lakes. Samples were collected in accordance with standard US Environmental Protection Agency (U.S. Environmental Protection Agency, 1996) and Alberta Environment and Parks (Kerr and Cooke, 2017) methodologies. Continuous measurements of river water physiochemical properties lend insight into daily and seasonal river dynamics that may otherwise be missed by grab samples collected at weekly or monthly frequencies (Wade et al., 2012; Vermilyea et al., 2017; Kneib et al., 2020). Thus, I incorporated sonde and discharge gauge data to increase process understanding, and to model contaminant flux and yield.

A broad suite of field and chemical parameters were collected at both rivers across their respective open water seasons. I used principal components analysis to assess the broad parameter suites comprehensively, and to gain process understanding of covaried physical and chemical drivers of hydrochemistry. In both study systems, I estimated annual legacy contaminant fluxes and yields using the product of daily discharge and contaminant concentrations modeled by simple linear regression with strongly correlated continuous parameters. Trends in historic discharge data were investigated as a means of interpreting past and future contaminant release.

The major result of this thesis research is that the concentrations of trace element contaminants were low and predominantly particle-bound in both study locations. Nutrient concentrations were low in the glacier-fed watershed, but high in the permafrost-fed watershed. The annual flux and yield of mercury from both rivers were low and comparable to non-regulated, non-cryosphere-fed rivers globally (Domagalski et al., 2016). The particle-bound nature of the contaminants suggests that they are not bioavailable to aquatic ecosystems, but do augment sedimentary contaminant stocks where the potential to bioaccumulate is controlled by conditions at the ultimate sites of long-term sediment deposition.

1.6. References

AMAP/UNEP (2013) *Technical Background Report for the Global Mercury Assessment*, *Arctic Monitoring and Assessment Programme*. Oslo, Norway/UNEP Chemicals Branch, Geneva, Switzerland. doi: 10.1088/1751-8113/45/44/444010.

Amos, H. M. *et al.* (2014) 'Global Biogeochemical Implications of Mercury Discharges from Rivers and Sediment Burial', *Environmental Science and Technology*, 48, pp. 9514–9522. doi: 10.1021/es502134t.

Andrews, T. D. *et al.* (2016) 'Permafrost Thaw and Aboriginal Cultural Landscapes in the Gwich'in Region, Canada', *Journal of Preservation Technology*, 47, 15–22. doi: 10.1017/CBO9781107415324.004.

Barbante, C. *et al.* (2004) 'Historical record of European emissions of heavy metals to the atmosphere since the 1650s from alpine snow/ice cores drilled near Monte Rosa', *Environmental Science and Technology*, 38, pp. 4085–4090. doi: 10.1021/es049759r.

Barnes, R. T. *et al.* (2014) 'Thawing glacial and permafrost features contribute to nitrogen export from Green Lakes Valley, Colorado Front Range, USA', *Biogeochemistry*, 117, pp. 413–430. doi: 10.1007/s10533-013-9886-5.

Baron, J. S., Schmidt, T. M. and Hartman, M. D. (2009) 'Climate-induced changes in high elevation stream nitrate dynamics', *Global Change Biology*, 15, pp. 1777–1789. doi: 10.1111/j.1365-2486.2009.01847.x.

Beal, S. A. *et al.* (2015) 'Ice Core Perspective on Mercury Pollution during the Past 600 Years', *Environmental Science and Technology*, 49, pp. 7641–7647. doi: 10.1021/acs.est.5b01033.

Blais, J. M., Schindler, D. W., Muir, D.C.G., *et al.* (2001) 'Melting Glaciers: A Major Source of Persistent Organochlorines to Subalpine Bow Lake in Banff National Park, Canada', *AMBIO: A Journal of the Human Environment*, 30, pp. 410–415. doi: 10.1579/0044-7447-30.7.410.

Bogdal, C. *et al.* (2010) 'Release of legacy pollutants from melting glaciers: Model evidence and conceptual understanding', *Environmental Science and Technology*, 44, pp. 4063–4069. doi: 10.1021/es903007h.

Brahney, J. *et al.* (2017) 'Evidence for a climate-driven hydrologic regime shift in the Canadian Columbia Basin', *Canadian Water Resources Journal*, 42, pp. 179–192. doi: 10.1080/07011784.2016.1268933.

Brighenti, S. *et al.* (2019) 'Ecosystem shifts in Alpine streams under glacier retreat and rock glacier thaw: A review', *Science of the Total Environment*, 675, pp. 542–559. doi: 10.1016/j.scitotenv.2019.04.221.

Burke, S. M. *et al.* (2018) 'Patterns and controls of mercury accumulation in sediments from three thermokarst lakes on the Arctic Coastal Plain of Alaska', *Aquatic Sciences*, 80, pp. 1–15. doi: 10.1007/s00027-017-0553-0.

Clarke, G. K. C. C. *et al.* (2015) 'Projected deglaciation of western Canada in the twenty-first

century', *Nature Geoscience*, 8, pp. 372–377. doi: 10.1038/ngeo2407.

Colombo, N. *et al.* (2018) 'Review : Impacts of permafrost degradation on inorganic chemistry of surface fresh water', *Global and Planetary Change*, 162, pp. 69–83. doi: 10.1016/j.gloplacha.2017.11.017.

Colombo, N. *et al.* (2019) 'Influence of permafrost, rock and ice glaciers on chemistry of high-elevation ponds (NW Italian Alps)', *Science of the Total Environment*, 685, pp. 886–901. doi: 10.1016/j.scitotenv.2019.06.233.

Domagalski, J. *et al.* (2016) 'Comparison of mercury mass loading in streams to atmospheric deposition in watersheds of Western North America: Evidence for non-atmospheric mercury sources', *Science of The Total Environment*, 568, pp. 638–650. doi: 10.1016/j.scitotenv.2016.02.112.

Donaldson, S. G. G. *et al.* (2010) 'Environmental contaminants and human health in the Canadian Arctic', *Science of The Total Environment*, 408, pp. 5165–5234. doi: 10.1016/j.scitotenv.2010.04.059.

Drevnick, P. E. *et al.* (2016) 'Spatiotemporal patterns of mercury accumulation in lake sediments of western North America', *Science of the Total Environment*, 568, pp. 1157–1170. doi: 10.1016/j.scitotenv.2016.03.167.

Dubé, M. G. *et al.* (2013) 'Accumulated state of the Yukon River watershed: Part I critical review of literature', *Integrated Environmental Assessment and Management*, 9, pp. 426–438. doi: 10.1002/ieam.1360.

Dudka, S. and Adriano, D. C. (2010) 'Environmental Impacts of Metal Ore Mining and Processing: A Review', *Journal of Environment Quality*, 26, pp. 590–602. doi: 10.2134/jeq1997.00472425002600030003x.

Eagles-Smith, C. A. *et al.* (2016) 'Spatial and temporal patterns of mercury concentrations in freshwater fish across the Western United States and Canada', *Science of the Total Environment*, 568, pp. 1171–1184. doi: 10.1016/j.scitotenv.2016.03.229.

Eichler, A. *et al.* (2012) 'Three centuries of Eastern European and Altai lead emissions recorded in a Belukha ice core', *Environmental Science and Technology*, 46, pp. 4323–4330. doi: 10.1021/es2039954.

Emmerton, C. A. *et al.* (2013) 'Mercury export to the Arctic Ocean from the Mackenzie River, Canada', *Environmental Science and Technology*, 47, pp. 7644–7654. doi: 10.1021/es400715r.

Van Everdingen, R. O. (1998) 'Glossary of Permafrost and Related Ground-Ice Terms', *Arctic and Alpine Research*, 21, p. 213. doi: 10.2307/1551636.

Ferrario, C., Finizio, A. and Villa, S. (2017) 'Legacy and emerging contaminants in meltwater of three Alpine glaciers', *Science of the Total Environment*, 574, pp. 350–357. doi: 10.1016/j.scitotenv.2016.09.067.

Fisher, J. A. *et al.* (2012) 'Riverine source of Arctic Ocean mercury inferred from atmospheric observations', *Nature Geoscience*, 5, pp. 499–504. doi: 10.1038/ngeo1478.

Fitzgerald, W. F. *et al.* (2005) 'Modern and historic atmospheric mercury fluxes in northern Alaska: Global sources and arctic depletion', *Environmental Science and Technology*, 39, pp. 557–568. doi: 10.1021/es049128x.

Gao, L. *et al.* (2018) 'Yields and Characterization of Dissolved Organic Matter From Different Aged Soils in Northern Alaska', *Journal of Geophysical Research: Biogeosciences*, 123, pp. 2035–2052. doi: 10.1029/2018JG004408.

Green, P. A. *et al.* (2004) 'Pre-industrial and contemporary fluxes of nitrogen through rivers: A global assessment based on typology', *Biogeochemistry*, 68, pp. 71–105. doi: 10.1023/B:BIOG.0000025742.82155.92.

Hammerschmidt, C. R. (2011) 'Mercury and carbon dioxide emissions: Uncoupling a toxic relationship', *Environmental Toxicology and Chemistry*, 30, pp. 2640–2646. doi: 10.1002/etc.702.

Heath, J. and Baron, J. S. (2014) 'Climate, Not Atmospheric Deposition, Drives the Biogeochemical Mass-Balance of a Mountain Watershed', *Aquatic Geochemistry*, 20, pp. 167–181. doi: 10.1007/s10498-013-9199-2.

Hobbs, W. O., Vinebrooke, R. D. and Wolfe, A. P. (2011) 'Biogeochemical responses of two alpine lakes to climate change and atmospheric deposition, Jasper and Banff national parks, Canadian rocky mountains', *Canadian Journal of Fisheries and Aquatic Sciences*, 68, pp. 1480–1494. doi: 10.1139/f2011-058.

Horowitz, H. M. *et al.* (2014) 'Historical Mercury Releases from Commercial Products: Global Environmental Implications', *Environmental Science & Technology*, 48, pp. 10242−10250. doi: dx.doi.org/10.1021/es501337j.

IPCC (2013) *IPCC, 2013: Climate Change 2013: The Physical Science Basis. Contribution of Working Group I to the Fifth Assessment Report of the Intergovernmental Panel on Climate Change*, *the Fifth Assessment Report*. Edited by T. F. Stocker et al. Cambridge, United Kingdom and New York, NY, USA: Cambridge University Press.

Järup, L. (2003) 'Hazards of heavy metal contamination', *British Medical Bulletin*, 68, pp. 167–182. doi: 10.1093/bmb/ldg032.

Kerr, J. G. and Cooke, C. A. (2017) 'Erosion of the Alberta badlands produces highly variable and elevated heavy metal concentrations in the Red Deer River, Alberta', *Science of the Total Environment*, 596–597, pp. 427–436. doi: 10.1016/j.scitotenv.2017.04.037.

Kidd, K., Clayden, M. and Jardine, T. (2012) 'Part IV Bioaccumulation, Toxicity, and Metallomics; Chapter 14. Bioaccumulation and Biomagnification of Mercury Through Food Webs', in Liu, G., Cai, Y., and O'Driscoll, N. (eds) *Environmental Chemistry and Toxicology of Mercury*. 1st edn. John Wiley & Sons, Inc.

Klaminder, J. *et al.* (2008) 'An explorative study of mercury export from a thawing palsa mire', *Journal of Geophysical Research: Biogeosciences*, 113, pp. 1–9. doi: 10.1029/2008JG000776.

Kneib, M. *et al.* (2020) 'Glacier retreat changes diurnal variation intensity and frequency of hydrologic variables in Alpine and Andean streams', *Journal of Hydrology*, 583, pp. 1–11. doi: 10.1016/j.jhydrol.2020.124578.

Koven, C. D., Riley, W. J. and Stern, A. (2013) 'Analysis of permafrost thermal dynamics and response to climate change in the CMIP5 earth system models', *Journal of Climate*, 26, pp. 1877–1900. doi: 10.1175/JCLI-D-12-00228.1.

Lafrenière, M. J. *et al.* (2006) 'Organochlorine pesticide and polychlorinated biphenyl concentrations in snow, snowmelt, and runoff at Bow Lake, Alberta', *Environmental Science and Technology*, 40, pp. 4909–4915. doi: 10.1021/es060237g.

Lafrenière, M. J. and Lamoureux, S. F. (2019) 'Effects of changing permafrost conditions on hydrological processes and fluvial fluxes', *Earth-Science Reviews journal*, 191, pp. 212–223. doi: 10.1016/j.earscirev.2019.02.018.

Laird, M. J. *et al.* (2018) 'Mercury and omega-3 fatty acid profiles in freshwater fish of the Dehcho Region, Northwest Territories: Informing risk benefit assessments', *Science of the Total Environment*, 637–638, pp. 1508–1517. doi: 10.1016/j.scitotenv.2018.04.381.

Lehmann-Konera, S. *et al.* (2019) 'Concentrations and loads of DOC, phenols and aldehydes in a proglacial arctic river in relation to hydro-meteorological conditions. A case study from the southern margin of the Bellsund Fjord – SW Spitsbergen', *Catena*, 174, pp. 117–129. doi: 10.1016/j.catena.2018.10.049.

Lehnherr, I. *et al.* (2018) 'The world's largest High Arctic lake responds rapidly to climate warming', *Nature Communications*, 9, pp. 1–9. doi: 10.1038/s41467-018-03685-z.

Leitch, D. R. *et al.* (2007) 'The delivery of mercury to the Beaufort Sea of the Arctic Ocean by the Mackenzie River', *Science of the Total Environment*, 373, pp. 178–195. doi: 10.1016/j.scitotenv.2006.10.041.

Li, J. *et al.* (2017) 'Evidence for persistent organic pollutants released from melting glacier in the central Tibetan Plateau, China', *Environmental Pollution*, 220, pp. 178–185. doi: 10.1016/j.envpol.2016.09.037.

Lim, A. G. *et al.* (2020) 'A revised pan-Arctic permafrost soil Hg pool based on Western Siberian peat Hg and carbon observations', *Biogeosciences*, 17, pp. 3083–3097. doi: 10.5194/bg-17-3083-2020.

Marshall, S. J. *et al.* (2011) 'Glacier water resources on the eastern slopes of the Canadian Rocky Mountains', *Canadian Water Resources Journal*, 36, pp. 109–134. doi: 10.4296/cwrj3602823.

Mast, M. A. *et al.* (2014) 'Links between N deposition and nitrate export from a high-elevation watershed in the Colorado front range', *Environmental Science and Technology*, 48, pp. 14258–14265. doi: 10.1021/es502461k.

McConnell, J. R. and Edwards, R. (2008) 'Coal burning leaves toxic heavy metal legacy in the Arctic', *Proceedings of the National Academy of Sciences of the United States of America*, 105, pp. 12140–12144. doi: 10.1073/pnas.0803564105.

Miner, K. R. *et al.* (2017) 'Legacy organochlorine pollutants in glacial watersheds: A review', *Environmental Science: Processes and Impacts*, 19, pp. 1474–1483. doi: 10.1039/c7em00393e.

Nriagu, J. O. (1979) 'Global inventory of natural and anthropogenic emissions of trace metals to the atmosphere', *Nature*, 279, pp. 409–411. doi: 10.1038/279409a0.

Nriagu, J. O. (1990) ‘Global Metal Pollution Poisoning the Biosphere’, *Environment: Science and Policy for Sustainable Development*, 32, pp. 7–33. doi: doi: 10.1080/00139157.1990.9929037.

Olson, C. *et al.* (2018) ‘Mercury in Active-Layer Tundra Soils of Alaska: Concentrations, Pools, Origins, and Spatial Distribution’, *Global Biogeochemical Cycles*, 32, pp. 1058–1073. doi: 10.1029/2017GB005840.

OTT Hydromet (2020) *Hydrolab HL4 Multiparameter Sonde*. Available at: https://www.ott.com/products/water-quality-2/hydrolab-hl4-multiparameter-sonde-54/ (Accessed: 28 April 2020).

Paudyal, R. *et al.* (2017) ‘Insights into mercury deposition and spatiotemporal variation in the glacier and melt water from the central Tibetan Plateau’, *Science of the Total Environment*, 599–600, pp. 2046–2053. doi: 10.1016/j.scitotenv.2017.05.145.

Phillips, V. J. A. *et al.* (2011) ‘Increased mercury loadings to Western Canadian Alpine Lakes over the past 150 years’, *Environmental Science and Technology*, 45, pp. 2042–2047. doi: 10.1021/es1031135.

Schindler, D. W. and Donahue, W. F. (2006) ‘An impending water crisis in Canada’s western prairie provinces’, *Proceedings of the National Academy of Sciences of the United States of America*, 103, pp. 7210–7216. doi: 10.1073/pnas.0601568103.

Schindler, D. W. and Smol, J. P. (2006) ‘Cumulative effects of climate warming and other human activities on freshwaters of Arctic and subarctic North America’, *Ambio*, 35, pp. 160–168. doi: 10.1579/0044-7447(2006)35.

Schuster, P. F. *et al.* (2002) ‘Atmospheric mercury deposition during the last 270 years: A glacial ice core record of natural and anthropogenic sources’, *Environmental Science and Technology*, 36, pp. 2303–2310. doi: 10.1021/es0157503.

Schuster, P. F. *et al.* (2011) ‘Mercury export from the Yukon River Basin and potential response to a changing climate’, *Environmental Science and Technology*, 45, pp. 9262–9267. doi: 10.1021/es202068b.

Schuster, P. F. *et al.* (2018) ‘Permafrost Stores a Globally Significant Amount of Mercury’, *Geophysical Research Letters*, 45, pp. 1463–1471. doi: 10.1002/2017gl075571.

Schwikowski, M. *et al.* (2004) ‘Post-17th-Century Changes of European Lead Emissions Recorded in High-Altitude Alpine Snow and Ice’, *Environmental Science and Technology*, 38, pp. 957–964. doi: 10.1021/es034715o.

Semple, K. T. *et al.* (2004) ‘Defining Bioavailability and Bioaccessibility of Contaminated Soil and Sediment is Complicated’, *Environmental Science & Technology*, 38, pp. 228A-231A. doi: 10.1021/es040548w.

Søndergaard, J. *et al.* (2012) ‘Mercury transport in a low-arctic river in Kobbefjord, West Greenland (64° N)’, *Water, Air, and Soil Pollution*, 223, pp. 4333–4342. doi: 10.1007/s11270-012-1198-1.

Sonke, J. E. *et al.* (2018) ‘Eurasian river spring flood observations support net Arctic Ocean

mercury export to the atmosphere and Atlantic Ocean', *Proceedings of the National Academy of Sciences of the United States of America*, 115, pp. E11586–E11594. doi: 10.1073/pnas.1811957115.

Sprague, J. B. (2007) 'Great Wet North? Canada's Myth of Water Abundance', in Bakker, K. (ed.) *Eau Canada*. 1st edn. Vancouver: UBC Press, pp. 23–36.

St Pierre, K. A. *et al.* (2018) 'Unprecedented Increases in Total and Methyl Mercury Concentrations Downstream of Retrogressive Thaw Slumps in the Western Canadian Arctic', *Environmental Science and Technology*, 52, pp. 14099–14109. doi: 10.1021/acs.est.8b05348.

St Pierre, K. A. *et al.* (2019) 'Drivers of Mercury Cycling in the Rapidly Changing Glacierized Watershed of the High Arctic's Largest Lake by Volume (Lake Hazen, Nunavut, Canada)', *Environmental Science and Technology*, 53, pp. 1175–1185. doi: 10.1021/acs.est.8b05926.

Stern, G. A. *et al.* (2012) 'How does climate change influence arctic mercury?', *Science of The Total Environment*, 414, pp. 22–42. doi: 10.1016/j.scitotenv.2011.10.039.

Streets, D. G. *et al.* (2011) 'All-Time Releases of Mercury to the Atmosphere from Human Activities', *Environmental Science & Technology*, 45, pp. 10485–10491. doi: 10.1021/es202765m.ALL-TIME.

Sun, X. *et al.* (2017) 'The role of melting alpine glaciers in mercury export and transport: An intensive sampling campaign in the Qugaqie Basin, inland Tibetan Plateau', *Environmental Pollution*, 220, pp. 936–945. doi: 10.1016/j.envpol.2016.10.079.

Sun, X. *et al.* (2018) 'Mercury speciation and distribution in a glacierized mountain environment and their relevance to environmental risks in the inland Tibetan Plateau', *Science of the Total Environment*, 631–632, pp. 270–278. doi: 10.1016/j.scitotenv.2018.03.012.

Sun, Y. *et al.* (2020) 'Glacial Melt Inputs of Organophosphate Ester Flame Retardants to the Largest High Arctic Lake', *Environmental Science and Technology*, 54, pp. 2734–2743. doi: 10.1021/acs.est.9b06333.

Sunderland, E. M. and Selin, N. E. (2013) 'Future trends in environmental mercury concentrations: Implications for prevention strategies', *Environmental Health: A Global Access Science Source*, 12, pp. 1–5. doi: 10.1186/1476-069X-12-2.

Beijer Institute *et al.* (1987) *Environmental impacts of coal mining and utilization.* In Chadwick M.J., Highton N.H., and Lindman N (eds). Pergamon Press, pp. 171–217. doi: 10.1016/b978-0-08-031427-3.50002-5.

The Government of Canada, The Vuntut Gwitchin First Nation and The Government of the Yukon (1993) *Vuntut Gwitchin First Nation Final Agreement*. doi: 10.1017/CBO9781107415324.004.

U.S. Environmental Protection Agency (1996) *Method 1669 Sampling Ambient Water for Trace Metals at EPA Water Quality Criteria Levels 20460*. Washington, D. C.

US Environmental Protection Agency (2009) 'Environmental Chemistry, Transport and Fate', *Guidance for Reporting on the Environmental Fate and Transport of the Stressors of Concern in Problem Formulations*, p. 30.

Vermilyea, A. W. *et al.* (2017) 'Continuous proxy measurements reveal large mercury fluxes from glacial and forested watersheds in Alaska', *Science of the Total Environment*, 599–600, pp. 145–155. doi: 10.1016/j.scitotenv.2017.03.297.

Villa, S. *et al.* (2006) 'Organochlorine compounds in ice melt water from Italian Alpine rivers', *Ecotoxicology and Environmental Safety*, 63, pp. 84–90. doi: 10.1016/j.ecoenv.2005.05.010.

Wade, A. J. *et al.* (2012) 'Hydrochemical processes in lowland rivers: Insights from in situ, high-resolution monitoring', *Hydrology and Earth System Sciences*, 16, pp. 4323–4342. doi: 10.5194/hess-16-4323-2012.

Water Survey of Canada (2020) *Daily Discharge Graph for SUNWAPTA RIVER AT ATHABASCA GLACIER (07AA007) [AB] - Water Level and Flow - Environment Canada*. Available at: https://wateroffice.ec.gc.ca/report/historical_e.html (Accessed: 28 April 2020).

YSI Inc. (2020) *Multiparameter water quality instrument - YSI EXO - EXO2 Sonde*. Available at: https://www.ysi.com/exo2 (Accessed: 28 April 2020).

Yukon Ecoregion Working Group (2004) 'Old Crow Flats', in *Ecoregions of the Yukon Territory*, pp. 115–122.

Zdanowicz, C. *et al.* (2018) 'Snowmelt, glacial and atmospheric sources of mercury to a subarctic mountain lake catchment, Yukon, Canada', *Geochimica et Cosmochimica Acta*, 238, pp. 374–393. doi: 10.1016/j.gca.2018.06.003.

Zhang, Y. *et al.* (2016) 'Observed decrease in atmospheric mercury explained by global decline in anthropogenic emissions', *Proceedings of the National Academy of Sciences of the United States of America*, 113, pp. 526–531. doi: 10.1073/pnas.1516312113.

Zolkos, S. *et al.* (2020) 'Mercury Export from Arctic Great Rivers', *Environmental Science & Technology*, 54, pp. 4140–4148. doi: 10.1021/acs.est.9b07145.

CHAPTER 2. Quantifying meltwater sources and contaminant fluxes from the Athabasca Glacier, Canada

2.1. Introduction

Glaciers around the world are shrinking as a result of persistent negative net mass balance (Stocker et al., 2013; Zemp et al., 2019). In the Canadian Rocky Mountains, the area of glacier ice-cover was ~2200 km^2 in 2005 (Bolch, Menounos and Wheate, 2010) but is predicted to decrease by 60–90% by 2100 (Marshall et al., 2011; Clarke et al., 2015). As the Canadian Rocky Mountains lose their ice, freshwater supply to many of western Canada's major prairie river systems will likely decline during the warmest summer months (Schindler and Donahue, 2006; Huss and Hock, 2018). There is also concern that glacial meltwater will release contaminants, accumulated over millennia and currently sequestered in glacier ice (Miner et al., 2017), to downstream ecosystems (Stern et al., 2012; Brighenti et al., 2019). These legacy contaminants were emitted by distal natural and anthropogenic sources and transported to glaciated mountains by atmospheric circulation, where they then accumulated in ice via wet- and dry-deposition (Zhang, Wright and Blanchard, 2009; Huang et al., 2015). Some of these legacy contaminants are priority pollutants (e.g. Hg, Pb, As, Cu, Cd, Zn, and Cr) which, when released to aquatic ecosystems, can bioaccumulate in organisms and biomagnify in food webs. Many of these trace elements readily form highly toxic and bioavailable organometallic complexes under specific physiochemical and biotic conditions (US Environmental Protection Agency, 2009). Mercury is a trace element of particular concern because it can convert to the neurotoxin methylmercury in the presence of sulfur-reducing microbes, organic matter, and anoxic conditions, with potential

harm to downstream ecosystems even at extremely low methylmercury concentrations (Ullrich, Tanton and Abdrashitova, 2001).

A range of legacy contaminants—including heavy metals (Sheppard, Deely and Edgerley, 1997; Carling, Tingey and Fernandez, 2013; Carling et al., 2017; Paudyal et al., 2017; Sun et al., 2017; Vermilyea et al., 2017; S. Sun et al., 2018; X. Sun et al., 2018; Li et al., 2019; Lone et al., 2019), nutrients (Baron, Schmidt and Hartman, 2009; Hobbs, Vinebrooke and Wolfe, 2011; Holtgrieve et al., 2011; Barnes et al., 2014; Mast et al., 2014; VanLooy and Vandeberg, 2019), organochlorine pesticides (Blais et al., 2001; Lafrenière et al., 2006; Villa et al., 2006; Geisz et al., 2008; Bogdal et al., 2010; Miner et al., 2017), polychlorinated biphenyls (Blais et al., 2001; Lafrenière et al., 2006; Bogdal et al., 2010; Sharma et al., 2015; Steinlin et al., 2016), polycyclic aromatic hydrocarbons (Sharma et al., 2015; Li et al., 2017), and pharmaceuticals (González-Alonso et al., 2017)—have been reported in supra- and proglacial stream and lake waters around the globe. However, no comprehensive studies have been conducted on the concentrations of nutrients, mercury, or other heavy metals in proglacial streams of the Canadian Rockies. Glaciers in the Canadian Rockies supply water to millions of people, and flows are declining (Schindler and Donahue, 2006; Brahney et al., 2017). Yet the concentration, flux, and fate of legacy contaminants in these glacier-fed systems have yet to be quantified.

Here we characterize the source and magnitude of contaminant flux and yield in glacial meltwater from Athabasca Glacier, in the Canadian Rocky Mountains. We monitored proglacial stream meltwater throughout the 2017 and 2018 hydrological seasons at a high temporal resolution using sonde measurements, then paired sonde data with chemical analyses of grab samples to model trace element concentrations at high resolution. We show that concentrations

and fluxes of legacy contaminants are low, and that proglacial stream chemistry reflects mixed input from glacial ice and subglacial weathering products.

2.2. Study Site

The Sunwapta River is a small proglacial river draining the Columbia Icefield (~200 km^2) in the Canadian Rocky Mountains (Figure 2.1). Meltwater from the Columbia Icefield drains into three continental-scale watersheds: east to Hudson Bay, west to the Pacific Ocean, and north to the Arctic Ocean. Climate in the region is continental, with mean annual air temperature and precipitation of 4.1 ˚C and 600 mm, respectively (years 1981-2010) (Environment and Climate Change Canada, 2020). The terminus of Athabasca Glacier is currently retreating by ~20 m/yr, with an annual mass balance of –1.0 m water equivalent (Tennant and Menounos, 2013; Ednie, Demuth and Shepherd, 2017). Meltwater flows along supraglacial streams, englacially, and subglacially through a seasonally-evolving drainage network (Arendt, Stevenson and Aciego, 2016). Bedrock beneath Athabasca Glacier and in the recently deglaciated forefield is largely Cambrian limestone, dolomite, and shale; these lithologies also dominate the till and colluvium that locally mantle the forefield (Swennen and Vandeginste, 2003; Hart, 2006; Arendt, Stevenson and Aciego, 2016). From the glacier terminus, meltwater flows into Sunwapta Lake (Gilbert and Shaw, 1981), a small proglacial lake in the forefield of Athabasca Glacier, before exiting through the lake outlet into Sunwapta River (Figure 2.1). The study area is in southernmost Jasper National Park, which is roughly midway (~100 km) between the towns of Banff and Jasper and > 130 km southwest of industrial facilities (including a large pulp mill) in the town of Hinton, AB. The sampling site is ~300 m from Hwy

93, and the Athabasca Glacier is a popular tourist attraction that includes motorized guided tours onto the glacier. From its headwaters at Sunwapta Lake, Sunwapta River's 29.3 km^2 catchment is ~70% glaciated, including Athabasca Glacier and three small cirque glaciers (Tennant and Menounos, 2013; Water Survey of Canada, 2020). After flowing ~50 km Sunwapta River joins the Athabasca River, the largest unregulated river in Alberta, which ultimately drains to the Arctic Ocean via the Mackenzie River.

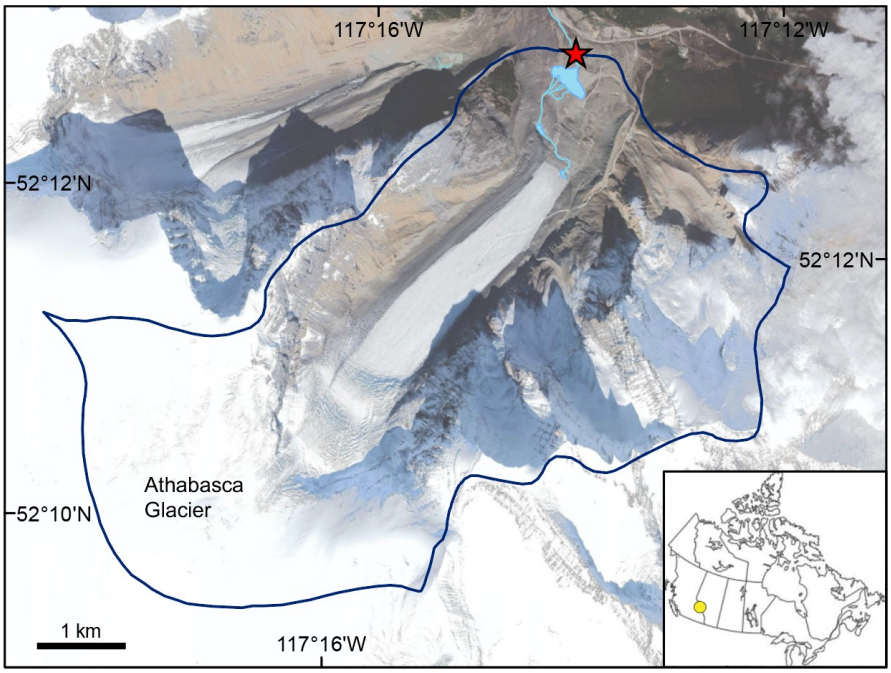

Figure 2.1. Location of the Athabasca Glacier (yellow circle in inset), the Sunwapta River monitoring station co-located with the Water Survey of Canada stage gauge station 07AA007 (red star on main map), and the outlined drainage basin above the monitoring station (Water Survey of Canada, 2020). Satellite imagery (October 3, 2016) from Google Earth Pro.

2.3. Methods

2.3.1. Water Quantity and Quality

The Water Survey of Canada has operated a hydrometric station (07AA007; 1950 m a.s.l.) at Sunwapta River seasonally since 1948. Hydrolab HL4 (OTT Hydromet, 2020) and EXO2 (YSI Inc., 2020) sondes were deployed at the Sunwapta River hydrometric station in continuous flow, >10 cm below the water surface and ~2 m from the bank from May 10 to October 11, 2017, and May 7 to October 2, 2018. The river was frozen outside of these dates. The sondes recorded dissolved oxygen, pH, electrical conductivity, temperature, and turbidity at 30-minute intervals. Sondes were serviced, replaced, and calibrated monthly (Appendix A). Sonde data were smoothed using a 4-point mean (i.e., 2-hour window) due to high variability in some of the sonde parameters.

Grab samples were collected at the hydrometric station following EPA Method 1669 (U.S. Environmental Protection Agency, 1996). Samples were collected monthly on 12 separate occasions during the 2017 and 2018 open-water season, with two full sets of field duplicates (Laceby et al., 2019) collected in August 2017 and 2018, yielding a total sample set of 14 grab samples. Most parameters were analyzed for both filtered (i.e., dissolved) and unfiltered (i.e., total) fractions. For the purpose of this study filtered phases are referred to as dissolved but are operationally defined as any particle or ion with diameter <0.45 µm, which therefore includes both colloidal and ionic phases. Samples intended for total analysis were preserved immediately in the field using either trace-metal-grade HNO_3 to 0.1 % v/v (for major, minor, and trace elements) or HCl to 0.2 % v/v (for mercury samples). Samples intended for dissolved trace elements were kept at 4 °C and returned to the laboratory within 48 hours, then filtered and

acidified. Data quality was assessed as part of the Government of Alberta Tributary Monitoring Network (Kerr and Cooke, 2017; Laceby et al., 2019).

Dissolved and total concentrations of 31 elements were quantified by inductively coupled plasma mass spectrometry following acidification to 1 % v/v HNO_3 for > 16-hours and total microwave digestion at 180 ºC and 200 psi. Cations (Ca^{2+}, K^{+}, Mg^{2+}, Na^{+}) were measured by inductively coupled plasma optical emission spectroscopy; anions ($SO_4^{2-,}$ Cl^{-}, NO_2^{-}, and NO_3^{-}) were measured by ion chromatography. Total and dissolved mercury were analyzed by cold vapour atomic fluorescence spectrometry, following EPA Method 1631E (U.S. Environmental Protection Agency, 2002). Total and dissolved phosphorus, soluble reactive phosphorus, total and dissolved ammonia, kjeldahl nitrogen, and total and dissolved organic carbon were determined colourimetrically. Filterable and nonfilterable residue concentrations (i.e., total dissolved and total suspended solids; TDS and TSS) were derived from masses of, respectively, evaporated and dried materials of known original volumes. Stable hydrogen and oxygen isotopes were determined by cavity ring-down spectroscopy on a Picarro L2130-I isotope analyzer, and presented in standard δ-notation relative to Vienna Standard Mean Ocean Water (VSMOW).

2.3.2. Statistical Methods

2.3.2.1. Principal Component Analysis

Principal component analysis (PCA) was used to examine relations among the Sunwapta River grab sample, sonde, and discharge results. The grab sampling event from May 7, 2018 was discarded from analyses due to sonde and discharge data logger malfunction concurrent with grab sampling. Data were checked for normality using quantile-quantile plots, which revealed

that turbidity and discharge displayed strongly right-skewed behaviour (Figure A.3); the other parameters were normally distributed. Discharge and sonde data were down-sampled to match the time of grab sampling events, and were centered and standardized (Table A.1). Data below method detection limits (MDL) were substituted with zero for PCA which relies on complete pairwise observations. Chemical parameters for which >25% of analyses were below the MDL were not included in the PCA.

2.3.2.2. Flux and Yield Calculations

We modeled concentrations of select chemical parameters at 1-hour resolution using simple linear regression of grab sample data and correlated sonde parameters, (conductivity or turbidity; Table A.1). Regression was computed on down-sampled sonde data concurrent with grab sampling. Grab sample data below MDL were left blank. Missing sonde or discharge data were linearly interpolated. Modeled hourly trace element, TSS, and TDS concentrations were multiplied by concurrent hourly discharge to obtain a time series of instantaneous flux (e.g., (Vermilyea et al., 2017)). Annual fluxes and yields are based on the ~150 day open-water season for each of 2017 and 2018. Annual flux was divided by watershed area to obtain annual yield. We also calculated flux in two other ways: as the product of mean annual grab sample concentration and mean annual discharge, and as the product of linearly-interpolated grab sample concentration and mean hourly discharge (Appendix A; Table A.4).

2.4. Results

2.4.1. Discharge and Sonde Results

Sunwapta River has a glacial flow regime characterized by peak discharge during July/August (Figure 2.2A). Discharge during 2017 (median 6.2 m^3/s) was high compared to historic values, with both median annual discharge (4.3 m^3/s) and peak discharge decreasing in 2018. Annual water yield increased by ~30% between 1949 and 2018 (Figure 2.3).

Turbidity closely tracked discharge ($r = 0.48$, $p < 0.05$), with higher turbidity during periods of higher flow (Figure 2.2B). In contrast, conductivity was high during low flow following break-up and preceding freeze-up, and low during the high flow summer meltwater season ($r = 0.51$, $p < 0.05$; Figure 2.2C). On shorter timescales, conductivity had clear diurnal and multi-day cycles (amplitude: ~15 µS/cm). Sunwapta River pH varied between 8.1 and 9.0 (Figure A.1), and was negatively correlated with conductivity ($r = –0.79$, $p < 0.05$) and positively correlated with discharge ($r = 0.67$, $p < 0.05$). Water temperature averaged 2.5°C (maximum 6.8 °C) and dissolved oxygen concentrations averaged 11 mg/L with waters remaining near saturation (68 – 96%) throughout the open-water season (Figure A.1). Dissolved oxygen underwent pronounced diurnal cycles and varied on average by ~0.2 mg/L, or 3% in terms of saturation.

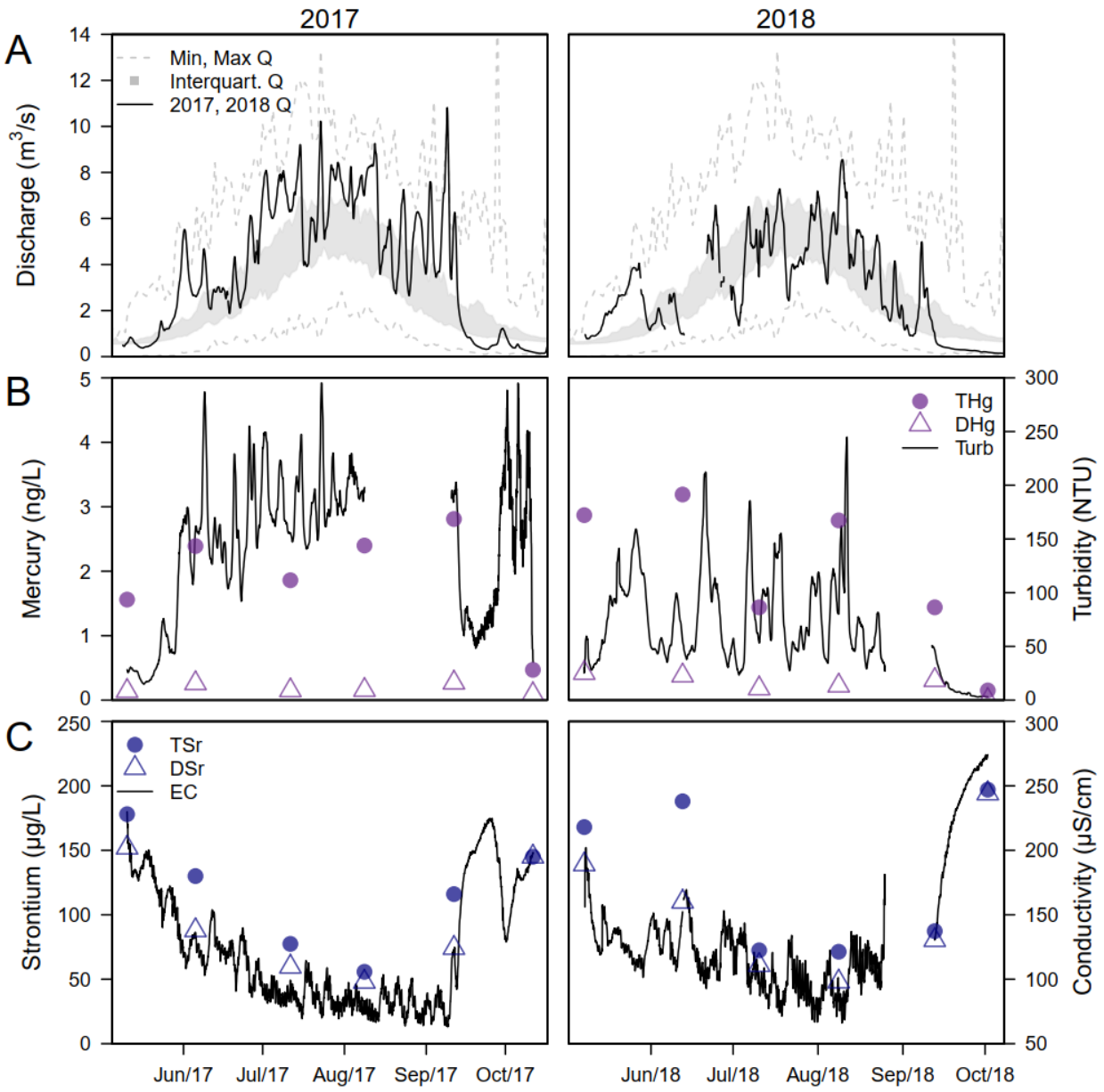

Figure 2.2. Sunwapta River sonde and grab sample time series for the 2017 and 2018 open water seasons. (A) Discharge (black line; smoothed at 24 h) with 1948–2015 minima, interquartile range, and maxima. (B) Turbidity (smoothed at 24 h) measured by sonde, and total and dissolved mercury concentrations from grab samples. (C) Conductivity (smoothed at 1 h) measured by sonde, and total and dissolved strontium concentrations from grab samples. Samples collected as field duplicates (August 2017 and August 2018) are presented as their mean value.

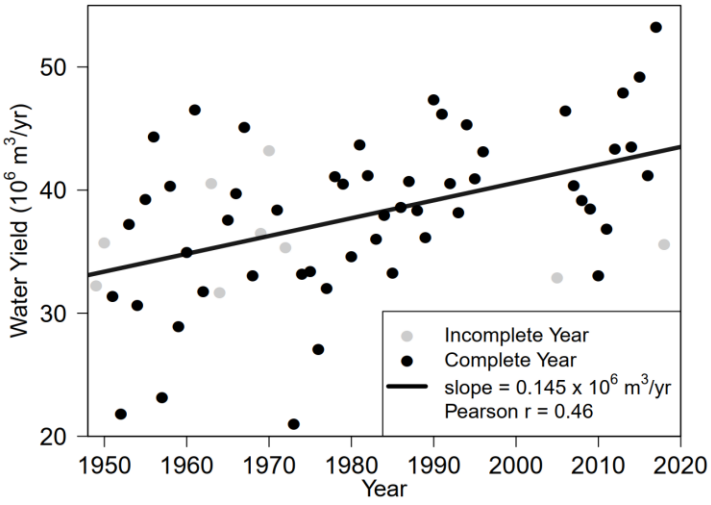

Figure 2.3. Trends in annual water yield between 1949 and 2018. Point shading reflects years for which gaps were identified in the daily-discharge data during the open water season.

2.4.2. Water Chemistry

Sunwapta River is carbonate-rich, and poor in organics, nutrients, and evaporites (Table 2.1; Figure A.2). Nutrient concentrations in Sunwapta River had no clear seasonal pattern. Total nitrogen ranged from <0.055 to 0.22 mg/L and was primarily nitrate, while ammonia, nitrite, TKN, and DKN were generally below detection. Total phosphorus was mostly in the particulate phase and ranged from <0.003 to 0.03 mg/L. In contrast, TSS and TDS had clear seasonal trends. TSS ranged from <1 to 240 mg/L, with highest concentrations in the late spring. TDS was 60–160 mg/L and peaked during low-flow. TOC and DOC were below the MDL of 0.5 mg/L. Ions associated with evaporite and chemically-weathered silicate minerals (Cl^-, Na^+, K^+) were extremely low during low-flow and below the MDL during high-flow. Concentration of ions associated with carbonate and sulphate chemical weathering (SO_4^{2-}, CO_3^{2-}, Ca^{2+}, Mg^{2+}) were 3–120 mg/L and, like conductivity and TDS, had a seasonal trend of dilution during high-flow and increased concentration during low-flow. Sunwapta River $\delta^{18}O$ and δ^2H increased through the

openwater season from most depleted values in May (respectively, –22.5 ‰ and –171 ‰) to least depleted in September (respectively, –20.0 ‰ and –150 ‰) of both years (Figure A.2; Table A.1).

Table 2.1. Summary of grab sample chemistry results (n=14). The "% <MDL" category represents the percent of grab sampling events for which the concentration returned below detection. %D/T is the percent of the total concentration that was found in the dissolved fraction, if applicable.

Parameter	Min	Mean	Max	StDev	% <MDL	%D/T
Routine Parameters (mg/L)						
TDS	60	93	160	30	0%	-
Hardness $CaCO_3$	51	81	150	30	0%	-
TSS	<1	80	240	64	7%	-
Alkalinity $CaCO_3$	45	62	97	17	0%	-
DOC	<0.5	1.0	1.3	0.3	79%	-
TOC	<0.5	0.6	0.6	-	86%	-
Major Ions (mg/L)						
CO_3^{2-}	54.0	75.3	120.0	20.5	0%	-
Ca^{2+}	14.0	19.7	32.0	5.1	0%	-
SO_4^{2-}	7.2	18.4	49.0	12.7	0%	-
Mg^{2+}	3.5	7.6	17.0	4.3	0%	-
Na^{+}	<0.5	0.7	0.9	0.2	71%	-
TCl	<0.03	0.4	0.8	0.2	29%	86%
K^{+}	<0.3	0.3	0.4	0.03	86%	-
Nutrients (mg/L)						
TN	<0.08	0.13	0.22	0.05	50%	-
TKN	<0.05	0.08	0.12	0.04	79%	-
NO_3 + NO_2	0.03	0.06	0.14	0.03	0%	-
TP	<0.003	0.02	0.03	0.01	7%	5%
Elements (µg/L)						
TFe	18	1018	2290	709	0%	<1%
TAl	31	638	1290	415	0%	1%
TSr	51	115	197	52	0%	80%
TZn	0.6	2.0	3.9	1.0	0%	10%
TCr	0.1	0.9	1.8	0.5	0%	0%
TCu	0.3	0.9	1.6	0.5	0%	13%
TPb	0.06	0.73	1.70	0.50	0%	<1%
TU	0.2	0.4	0.8	0.2	0%	90%
TAs	0.03	0.16	0.34	0.10	0%	16%
TCd	<0.001	0.005	0.007	0.003	86%	90%
TAg	<0.001	0.003	0.009	0.002	14%	<1%
THg	0.0002	0.0020	0.0032	0.0009	0%	10%

There were high concentrations of elements associated with carbonates, predominantly present in ionic form such as Ca, Sr, and U (e.g., Sr; Figure 2.2C). For example, typical concentrations of TSr were 50–200 µg/L, 59–100% of which was DSr (Figure 2.2C). TCa was 19–68 mg/L and TU was 0.20–0.75 µg/L. Potential contaminant concentrations were extremely low: <2 µg/L for each of total As, Cd, Cr, Pb, and <3.2 ng/L for THg (Figure 2.2B), with 85–100% of these occurring in the particulate phase. Concentrations of TAl were 31–1290 µg/L, ~1 % of which was DAl. The complete river chemistry dataset is included as an Extended Data Table A.1.

The PCA revealed that the chemical data split into two groups with distinct seasonal trends on opposite ends of the first principal component (PC1; Figure 2.4). The first group, with negative PC1 loadings, included: dissolved B, Ba, Ca, Li, Mg, Mn, Mo, Sr, Ti, U; total Sr, U, Sb, Mo; TDS, alkalinity and hardness; and the ions SO_4^{2-}, CO_3^{2-}, nitrate, and Ca^{2+}. These elements are strongly associated with the carbonate and shale lithologies that dominate local bedrock and surficial sediment cover (Arendt, Aciego and Hetland, 2015). The dissolved phase made up 60–100% of these parameters' total concentrations. These predominantly dissolved elements and ions were diluted during high-flow and most concentrated during low-flow. Elements and ions in this group covary strongly with electrical conductivity (e.g. Sr, Figure 2.2C), with Pearson correlation coefficients >0.7 ($p < 0.05$; Table A.4). The second group, with positive PC1 loadings, included: total Al, As, Be, Co, Cr, Cu, Fe, Hg, Li, Mn, P, Pb, Th, Tl, V, Zn; dissolved Hg (assumed to be colloidal); and TSS. This group contains potential legacy contaminants such as Hg, As, Cr, Cu, Pb, Zn. The particulate phase made up 85–100% of the second group's parameters' total concentrations. The concentrations of these predominantly particulate species

increased with high-flow conditions and covaried most closely with turbidity (e.g. Hg; Figure 2.2B; Figure 2.4), though the correlations were weak (Table A.3).

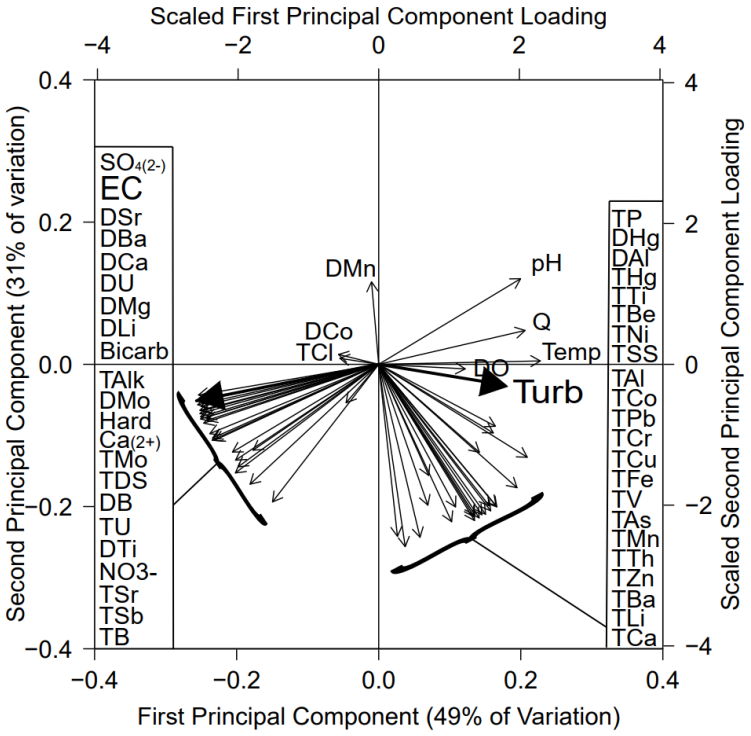

Figure 2.4. Biplot of variable loadings for PCA of select grab sample chemical data and down-sampled discharge and sonde data. Parameters grouped into a predominantly dissolved group with negative loadings on PC1 and a group of predominantly particulate parameters with positive loadings on PC1. Loadings for conductivity and turbidity, the continuous parameters which covary most strongly with the two chemical parameter groupings, have larger text and arrow size. Parameter labels are sorted top to bottom by decreasing order of their PC2 loading score Loading scores for PC1-4 are given in Table A.2.

2.4.3. Flux and Yield Calculations

Concentrations of select predominantly dissolved elements from the PCA were modeled using simple linear regression with conductivity (Table A.3). Mean annual fluxes of TDS, DCa, TSr, and TU were 3.4 Gg/yr (TDS), 0.69 Gg/yr (DCa), 3.9 Mg/yr (TSr), and 13 kg/yr (TU),

respectively, and the mean annual yields were 117 Mg/km^2/yr (TDS), 24 Mg/km^2/yr (DCa), 134 kg/km^2/yr (TSr), and 432 g/km^2/yr (TU), respectively (Table 2.2). Fluxes and yields of these parameters were ~20% higher in 2017 compared to 2018.

Concentration of select particulate elements and contaminants with positive PC1 loadings (Figure 2.4) were modeled using three methods (Appendix A; Table A.3; Table A.4; Table A.5). The results of the simple linear regression with turbidity follow. Mean annual fluxes were 4.5 Gg/yr (TSS), 35 Mg/yr (TAl), 46 kg/yr (TCr), 39 kg/yr (TPb), 7.5 kg/yr (TAs), and 0.10 kg/yr (THg), and the mean annual yields were 154 Mg/km^2/yr (TSS), 1.2 Mg/ km^2/yr (TAl), 1.6 kg/ km^2/yr (TCr), 1.3 kg/km^2/yr (TPb), 255 g/km^2/yr (TAs), and 3.2 g/km^2/yr (THg) (Table 2.2). Fluxes and yields of these parameters were ~60% higher in 2017 compared to 2018.

Table 2.2. Annual mean fluxes and yields of select chemical parameters modeled using simple linear regression with turbidity or conductivity from 1-hour sonde data.

Chemical Parameter	Modeling Parameter	R-value	Flux 2017	Yield 2017	Flux 2018	Yield 2018
			(Gg/yr)	**(Mg/km^2/yr)**	**(Gg/yr)**	**(Mg/km^2/yr)**
TSS	Turbidity	0.24	5.8	198	3.2	111
TDS	Conductivity	0.96	3.8	129	3.1	105
DCa	Conductivity	0.97	0.8	28	0.7	22
			(Mg/yr)	**(kg/km^2/yr)**	**(Mg/yr)**	**(kg/km^2/yr)**
TAl	Turbidity	0.39	46.3	1580	23.9	817
TSr	Conductivity	0.88	4.3	147	3.6	123
			(kg/yr)	**(g/km^2/yr)**	**(kg/yr)**	**(g/km^2/yr)**
TCr	Turbidity	0.34	59.4	2028	32.1	1095
TPb	Turbidity	0.14	48.4	1652	29.0	988
TU	Conductivity	0.96	13.5	462	11.5	394
TAs	Turbidity	0.09	9.0	307	6.0	204
THg	Turbidity	0.29	0.12	4.0	0.07	2.4

2.5. Discussion

2.5.1. Meltwater Chemistry in the Sunwapta River

Early-season meltwater was characterized by high conductivity, neutral pH, dilute particulate species, and high concentrations of major ions and dissolved trace elements (e.g. Sr, Figure 2.2) associated with the lithology of local bedrock and surficial sediment (ie. endogenous sources) (Arendt, Aciego and Hetland, 2015). This chemistry is best explained by early season re-establishment of the subglacial drainage network with the proglacial environment, and associated release of subglacial chemical weathering products (negative PC1 loadings, Figure 2.4). Clear diurnal fluctuations in Sunwapta River's conductivity were likely due to daily flushing of subglacial weathering products, a pattern also observed in distinct diurnal fluctuations of Sr isotope composition, pH, and conductivity of Athabasca Glacier meltwater (Clinger et al., 2016). As flow increased into the summer months, the water chemistry load of Sunwapta River, expressed as flux, continued to be primarily composed of total dissolved solids, even as dissolved species became more dilute and concentrations of total suspended sediment and particulate-associated species increased (Figure 2.2; Figure A.2). The chemical profile of these particulate species, including the potential legacy contaminants As, Cr, Hg, P, Pb, Tl, and Zn (positive PC1 loadings, Figure 2.4), suggests a primarily exogenous source: wet- and dry-deposition to the glacier surface. This decrease in conductivity and dilution of dissolved species reflects the increasing contribution of supra- and englacial melt—and associated legacy contaminant release from Athabasca Glacier and other glaciers in the watershed—during the peak of the ablation season. This finding is supported by noble gas tracer studies of Athabasca Glacier meltwater, which showed that July meltwater is dominated by surface melt, as opposed

to basal melt (Niu et al., 2017). Similarly, Sunwapta River $\delta^{18}O$ and $\delta^{2}H$ is least depleted in July-September and is similar to the Athabasca Glacier ice-melt isotopic endmember composition (Arendt, Aciego and Hetland, 2015), indicating a general shift from snow- to ice-melt throughout the Sunwapta River open-water season. Cooler late-season air temperatures diminished the contribution of supraglacial and englacial melt while subglacial channel network continued to contribute meltwater to Sunwapta River, as indicated by higher conductivity and endogenous dissolved element concentrations (negative PC1 loadings, Figure 2.4), and lower pH and exogenous particulate element concentrations (positive PC1 loadings, Figure 2.4).

Nutrient and contaminant trace element concentrations (e.g. N, P, Hg, Pb, Cu, Zn, Cr, Cd, As) were low and below CCME water quality guidelines for the protection of aquatic life (Canadian Council of Ministers of the Environment, 2019) throughout the 2017–2018 meltwater season. To further investigate the source of metals including Pb, Cr, Cu, Zn, and As, we compared Sunwapta River metal/Al ratios to mean metal/Al ratios from a compilation of glacial sediment geochemistry samples from nearby southeast British Columbia (Canil and Lacourse, 2011). We assume that anthropogenic contamination of Sunwapta River meltwater would raise the metal/Al ratio above that of the regional lithology (i.e., above what would be expected due to the physical and chemical weathering of bedrock). Water samples collected from the Sunwapta River have low enrichment factors of Pb_{EF} ~4; Cr_{EF} ~1; Ni_{EF} ~5; Cu_{EF} ~3; Zn_{EF} ~6; and As_{EF} ~3, representing ~1 – 6-fold enrichment. This suggests that legacy anthropogenic heavy metal contaminants, likely deposited over the industrial era, are present but limited (EF < 10) in 2017 – 2018 melt from the Athabasca Glacier. Moreover, the concentrations of heavy metals are low relative to contaminated ecosystems and predominantly present in non-bioavailable particulate phases with low potential for organometallic complexation, including methylation.

Sunwapta River contaminant concentrations were comparable to other small proglacial streams in alpine North America, the circum-Arctic, and Antarctica, where Hg concentrations are typically less than 8 ng/L (Sheppard, Deely and Edgerley, 1997; Søndergaard et al., 2012; Carling, Tingey and Fernandez, 2013; Carling et al., 2017; Vermilyea et al., 2017; Zdanowicz et al., 2018; St. Pierre et al., 2019). Potential contaminant trace element concentrations are also low in Wyoming proglacial streams (As < MDL; Cr < MDL; Cu < 6 µg/L; Pb < 7 µg/L; Zn < 20 µg/L) (Carling et al., 2017; VanLooy and Vandeberg, 2019). In contrast, small proglacial system in central east Asia have a greater range of THg concentrations (<MDL to 230 ng/L) (Paudyal et al., 2017; Sun et al., 2017; S. Sun et al., 2018; X. Sun et al., 2018; Lone et al., 2019).

Phosphorus (Neff et al., 2008; Brahney et al., 2015; VanLooy and Vandeberg, 2019) and nitrogen (Baron, Schmidt and Hartman, 2009; Holtgrieve et al., 2011; Barnes et al., 2014; VanLooy and Vandeberg, 2019) can also be delivered atmospherically to icefields and then released to downstream ecosystems. Very low nutrient concentrations in the Sunwapta River contrast somewhat with previous work on glacier meltwater contributions to downstream nutrient budgets in the Rockies (e.g. Baron, Schmidt and Hartman, 2009; Hobbs, Vinebrooke and Wolfe, 2011; Holtgrieve et al., 2011; Barnes et al., 2014; VanLooy and Vandeberg, 2019). There is paleolimnological and long-term monitoring evidence for increased delivery of anthropogenic N from retreating glaciers in, respectively, the Canadian (Hobbs, Vinebrooke and Wolfe, 2011) and Colorado (Baron, Schmidt and Hartman, 2009; Barnes et al., 2014) Rockies, though persistent drought may be partially responsible for the increased nitrate load in the Colorado Rockies (Mast et al., 2014).

2.5.2. Pairing Sonde and Grab Sample Results for Flux and Yield Modeling

Sampling of physiochemical parameters at high temporal resolution is useful for modeling trace element concentrations and fluxes that are typically only measured at low temporal resolution (e.g., monthly sampling) (Mast et al., 2014; Clinger et al., 2016; Kerr and Cooke, 2017; Vermilyea et al., 2017). Sonde-modeled temporal patterns of water chemistry at Sunwapta River reflect the evolution, connectivity, and contribution of two sources of melt and associated physiochemical inputs: (1) subglacial melt and local bedrock chemical weathering products, and (2) surface and englacial melt, and predominantly particulate, atmospherically deposited chemical constituents including potential contaminants (Figure 2.4). Compared to conductivity, turbidity was a less robust sonde parameter for modeling element concentrations at high resolution because the grab samples used for regression analysis had low concentrations of the elements of interest, low dynamic range, and are subject to higher sampling bias and replicate variability (Laceby et al., 2019). Sondes were placed along the river bed, while grab samples were collected higher in the water column; this may introduce a sampling bias because of vertical variability in suspended sediment transport. Nevertheless, two alternative flux estimate methods returned consistent results (Table A.5). Thus, the continuous turbidity sonde data were as effective as traditional grab sample linear interpolation and concentration averaging methods for modeling the flux of predominantly particulate species and potential contaminants in meltwater from Athabasca Glacier (Table A.5) (Kerr, Eimers and Yao, 2016). The modest correlation between turbidity and particulate species in Sunwapta River contrasts with the strong correlation of turbidity and mercury concentration at Lemon Creek (Alaska) (Vermilyea et al., 2017). Although average mercury concentrations in Lemon Creek are comparable to Sunwapta River, our study captured a smaller range of mercury concentrations, and two samples from

Lemon Creek with the highest mercury concentration strongly control the slope and strength of the regression between turbidity and mercury at Lemon Creek (Figure A.4). Suspended sediment settling in Sunwapta Lake may also have contributed to the lower effectiveness of turbidity-based modeling. The difference between Lemon Creek and Sunwapta River turbidity-mercury modeling suggests this relation is system dependent and subject to the limitations inherent to small sample sizes.

2.5.3. Sunwapta River Mercury Yield Compared to Other Watersheds

The annual THg yield for the Sunwapta River headwaters (2.4 – 4.0 g/km^2/yr; Table 2.2) is comparable to other small glaciated catchments globally, and comparable to small North American catchments in forested, wetland, urban, and agricultural settings, but is approximately an order of magnitude higher than THg yields for major Canadian watersheds (Table A.6). THg yields of small glaciated catchments are up to 19.9 g/km^2/yr (Vermilyea et al., 2017), and as low as 0.2 – 0.5 g/km^2/yr (Søndergaard et al., 2012; St. Pierre et al., 2019). Few studies have calculated yields of other trace element contaminants in glaciated catchments; this hinders comparison of trace element yields between glaciated catchments and catchments in different geographic or physiographic settings. Typical THg yields of forested, wetland, urban, and agricultural catchments under 3000 km^2 are less than 5.5 g/km^2/yr (Table A.6) (Hurley et al., 1995; Brigham et al., 2009).

Unlike watersheds with significant forest, wetland, urban, or agricultural cover, Hg and other contaminant trace elements in Sunwapta and other glaciated watersheds were largely present in the less bioaccessible particulate phase (Hurley et al., 1995; X. Sun et al., 2018). Yields of THg for major Canadian watersheds (>~20,000 km^2) are very low (0.1 – 0.4 g/km^2/yr;

e.g. Churchill, Nelson, North Saskatchewan rivers) (Kirk and St. Louis, 2009) and typically an order of magnitude lower than for small glaciated catchments. However, yields are higher for large northern rivers with substantial glacial and/or permafrost cover (e.g. Mackenzie River: 1.3 – 1.6 g/km^2/yr (Emmerton et al., 2013; Zolkos et al., 2020); Yukon River: 4.0 – 5.2 g/km^2/yr (Schuster et al., 2011; Zolkos et al., 2020)) (Table A.6). The positive correlation between THg and TSS, and predominance of particulate mercury at Sunwapta and other glacial rivers (Vermilyea et al., 2017), suggests that higher THg yields in glaciated catchments, as compared to large Canadian rivers, are likely driven primarily by the relatively high suspended load of proglacial rivers. The particle-bound contaminants released from glacierized catchments are not readily bioavailable (Gagnon and Fisher, 1997), and are transient in well-oxygenated river systems. However, the particle-bound contaminants likely sequester gradually in benthic sediments downstream of the proglacial setting, for example in lakes, fine-grained fluvial facies, and riparian zones. The ultimate bioavailability of particle-bound contaminants in these settings is controlled by settling location physiochemistry: pH, temperature, oxygen saturation, redox conditions, and organic matter availability (Ullrich, Tanton and Abdrashitova, 2001).

2.5.4. Conclusion

The increases in Sunwapta River annual water yield over the last ~70 years (Figure 2.3) coincide with a 2- to 5- fold increase in atmospheric deposition of nutrients (Green et al., 2004; Neff et al., 2008; Holtgrieve et al., 2011) and trace element contaminants (Phillips et al., 2011; Drevnick et al., 2016) in the Rocky Mountains over the past ~150 years. These changes have occurred in the context of accelerated glacial retreat driven by anthropogenic warming (Stocker et al., 2013; Zemp et al., 2019), the consequences of which include the recent detachment of

Columbia Glacier from its Columbia Icefield source (Rippin et al., 2020). Our data from Sunwapta River, together with projected patterns of regional glacier mass loss (Marshall et al., 2011; Clarke et al., 2015), suggest that the flux and yield of trace elements formerly sequestered in ice from Athabasca Glacier and other heavily glaciated basins in the Canadian Rockies will increase in coming years until peak water yield is reached (Milner et al., 2017).

Though significant concentrations of organochlorine compounds have been reported in glacial meltwaters in the Canadian Rocky Mountains (Blais et al., 2001; Lafrenière et al., 2006), priority pollutant trace elements concentrations have not previously been reported. The question of glacial meltwater release of legacy contaminants to downstream ecosystems rests on the assumption that glaciers contain a substantial stock of those legacy contaminants (Miner et al., 2017). Atmospheric transport models (Obrist et al., 2008) suggest that air masses originating in Asia—and carrying elevated mercury and lead loads—pass over the Columbia Icefield, where wet- and dry-deposition processes would presumably lead to accumulations of those contaminants in ice. However, we found that current concentrations, fluxes, and yields of these contaminants in Sunwapta River are low. Future work should directly measure concentrations and depositional fluxes of these trace elements in snowpacks, glaciers, and icefields of the Canadian Rocky Mountains.

2.6. References

Arendt, C. A., Aciego, S. M. and Hetland, E. A. (2015) 'An open source Bayesian Monte Carlo isotope mixing model with applications in Earth surface processes', *AGU*, 16, pp. 267–300. doi: 10.1002/2014GC005684.Key.

Arendt, C. A., Stevenson, E. I. and Aciego, S. M. (2016) 'Hydrologic controls on radiogenic Sr in meltwater from an alpine glacier system: Athabasca Glacier, Canada', *Applied Geochemistry*, 69, pp. 42–49. doi: 10.1016/j.apgeochem.2016.04.002.

Barnes, R. T. *et al.* (2014) 'Thawing glacial and permafrost features contribute to nitrogen export from Green Lakes Valley, Colorado Front Range, USA', *Biogeochemistry*, 117, pp. 413–430. doi: 10.1007/s10533-013-9886-5.

Baron, J. S., Schmidt, T. M. and Hartman, M. D. (2009) 'Climate-induced changes in high elevation stream nitrate dynamics', *Global Change Biology*, 15, pp. 1777–1789. doi: 10.1111/j.1365-2486.2009.01847.x.

Blais, J. M. *et al.* (2001) 'Melting Glaciers: A Major Source of Persistent Organochlorines to Subalpine Bow Lake in Banff National Park, Canada', *AMBIO: A Journal of the Human Environment*, 30, pp. 410–415. doi: 10.1579/0044-7447-30.7.410.

Bogdal, C. *et al.* (2010) 'Release of legacy pollutants from melting glaciers: Model evidence and conceptual understanding', *Environmental Science and Technology*, 44, pp. 4063–4069. doi: 10.1021/es903007h.

Bolch, T., Menounos, B. and Wheate, R. (2010) 'Landsat-based inventory of glaciers in western Canada, 1985-2005', *Remote Sensing of Environment*, 114, pp. 127–137. doi: 10.1016/j.rse.2009.08.015.

Brahney, J., N. *et al.* (2015) 'Global Biogeochemical Cycles: The nitrogen cycle', *Global Biogeochemical Cycles*, 29, pp. 1369–1383. doi: 10.1002/2015GB005137.

Brahney, J. *et al.* (2017) 'Evidence for a climate-driven hydrologic regime shift in the Canadian Columbia Basin', *Canadian Water Resources Journal*, 42, pp. 179–192. doi: 10.1080/07011784.2016.1268933.

Brigham, M. E. *et al.* (2009) 'Mercury cycling in stream ecosystems. 1. Water column chemistry and transport', *Environmental Science and Technology*, 43, pp. 2720–2725. doi: 10.1021/es802694n.

Brighenti, S. *et al.* (2019) 'Ecosystem shifts in Alpine streams under glacier retreat and rock glacier thaw: A review', *Science of the Total Environment*, 675, pp. 542–559. doi: 10.1016/j.scitotenv.2019.04.221.

Canadian Council of Ministers of the Environment (2019) 'Canadian Environmental Quality Guidelines for the Protection of Aquatic Life', pp. 1–26.

Canil, D. and Lacourse, T. (2011) 'An estimate for the bulk composition of juvenile upper continental crust derived from glacial till in the North American Cordillera', *Chemical Geology*,

284, pp. 229–239. doi: 10.1016/j.chemgeo.2011.02.024.

Carling, G. T. *et al.* (2017) 'Effect of Atmospheric Deposition and Weathering on Trace Element Concentrations in Glacial Meltwater at Grand Teton National Park, Wyoming, U.S.A.', *Arctic, Antarctic, and Alpine Research*, 49, pp. 427–440. doi: 10.1657/AAAR0016.071.

Carling, G. T., Tingey, D. G. and Fernandez, D. P. (2013) 'Mercury and Other Trace Elements in Glacial Wyoming', *University of Wyoming National Park Service Research Center Annual Report*, 36, pp. 1–9.

Clarke, G. K. C. C. *et al.* (2015) 'Projected deglaciation of western Canada in the twenty-first century', *Nature Geoscience*, 8, pp. 372–377. doi: 10.1038/ngeo2407.

Clinger, A. E. *et al.* (2016) 'Implications for post-comminution processes in subglacial suspended sediment using coupled radiogenic strontium and neodymium isotopes', *Geomorphology*, 259, pp. 134–144. doi: 10.1016/j.geomorph.2016.02.006.

Drevnick, P. E. *et al.* (2016) 'Spatiotemporal patterns of mercury accumulation in lake sediments of western North America', *Science of the Total Environment*, 568, pp. 1157–1170. doi: 10.1016/j.scitotenv.2016.03.167.

Ednie, M., Demuth, M. N. and Shepherd, B. (2017) *The mass balance of the Athabasca and Saskatchewan sectors of the Columbia Icefield, Alberta for 2015 and 2016*, *Geological Survey of Canada Open File 8228*. doi: doi.org/10.4095/302705.

Emmerton, C. A. *et al.* (2013) 'Mercury export to the Arctic Ocean from the Mackenzie River, Canada', *Environmental Science and Technology*, 47, pp. 7644–7654. doi: 10.1021/es400715r.

Environment and Climate Change Canada (2020) *Hourly Data Report - Climate*. Available at: https://climate.weather.gc.ca/historical_data/search_historic_data_e.html (Accessed: 28 April 2020).

Gagnon, C. and Fisher, N. S. (1997) 'Bioavailability of sediment-bound methyl and inorganic mercury to a marine bivalve', *Environmental Science and Technology*, 31, pp. 993–998. doi: 10.1021/es960364k.

Geisz, H. N. *et al.* (2008) 'Melting glaciers: A probable source of DDT to the Antarctic marine ecosystem', *Environmental Science and Technology*, 42, pp. 3958–3962. doi: 10.1021/es702919n.

Gilbert, R. and Shaw, J. (1981) 'Sedimentation in proglacial Sunwapta Lake, Alberta', *Canadian Journal of Earth Sciences*, 18, pp. 81–93. doi: 10.1139/e81-007.

González-Alonso, S. *et al.* (2017) 'Occurrence of pharmaceutical, recreational and psychotropic drug residues in surface water on the northern Antarctic Peninsula region', *Environmental Pollution*, 229, pp. 241–254. doi: 10.1016/j.envpol.2017.05.060.

Green, P. A. *et al.* (2004) 'Pre-industrial and contemporary fluxes of nitrogen through rivers: A global assessment based on typology', *Biogeochemistry*, 68, pp. 71–105. doi: 10.1023/B:BIOG.0000025742.82155.92.

Hart, J. K. (2006) 'Athabasca Glacier, Canada - A field example of subglacial ice and till

erosion?', *Earth Surface Processes and Landforms*, 31, pp. 65–80. doi: 10.1002/esp.1233.

Hobbs, W. O., Vinebrooke, R. D. and Wolfe, A. P. (2011) 'Biogeochemical responses of two alpine lakes to climate change and atmospheric deposition, Jasper and Banff national parks, Canadian rocky mountains', *Canadian Journal of Fisheries and Aquatic Sciences*, 68, pp. 1480–1494. doi: 10.1139/f2011-058.

Holtgrieve, G. W. *et al.* (2011) 'A coherent signature of anthropogenic nitrogen deposition to remote watersheds of the Northern Hemisphere', *Science*, 334, pp. 1545–1548. doi: 10.1126/science.1212267.

Huang, J. *et al.* (2015) 'Characterizations of wet mercury deposition on a remote high-elevation site in the southeastern Tibetan Plateau', *Environmental Pollution*, 206, pp. 518–526. doi: 10.1016/j.envpol.2015.07.024.

Hurley, J. P. *et al.* (1995) 'Influences of Watershed Characteristics on Mercury Levels in Wisconsin Rivers', *Environmental Science and Technology*, 29, pp. 1867–1875. doi: 10.1021/es00007a026.

Huss, M. and Hock, R. (2018) 'Global-scale hydrological response to future glacier mass loss', *Nature Climate Change*, 8, pp. 135–140. doi: 10.1038/s41558-017-0049-x.

Kerr, J. G. and Cooke, C. A. (2017) 'Erosion of the Alberta badlands produces highly variable and elevated heavy metal concentrations in the Red Deer River, Alberta', *Science of the Total Environment*, 596–597, pp. 427–436. doi: 10.1016/j.scitotenv.2017.04.037.

Kerr, J. G., Eimers, M. C. and Yao, H. (2016) 'Estimating stream solute loads from fixed frequency sampling regimes: The importance of considering multiple solutes and seasonal fluxes in the design of long-term stream monitoring networks', *Hydrological Processes*, 30, pp. 1521–1535. doi: 10.1002/hyp.10733.

Kirk, J. L. and St. Louis, V. L. (2009) 'Multiyear total and methyl mercury exports from two major sub-arctic rivers draining into Hudson Bay, Canada', *Environmental Science and Technology*, 43, pp. 2254–2261. doi: 10.1021/es803138z.

Laceby, J. P. *et al.* (2019) *Investigation of quality control data from Alberta's lotic water monitoring program, 2016-18.*, *In Press*.

Lafrenière, M. J. *et al.* (2006) 'Organochlorine pesticide and polychlorinated biphenyl concentrations in snow, snowmelt, and runoff at Bow Lake, Alberta', *Environmental Science and Technology*, 40, pp. 4909–4915. doi: 10.1021/es060237g.

Li, J. *et al.* (2017) 'Evidence for persistent organic pollutants released from melting glacier in the central Tibetan Plateau, China', *Environmental Pollution*, 220, pp. 178–185. doi: 10.1016/j.envpol.2016.09.037.

Li, X. *et al.* (2019) 'Seasonal controls of meltwater runoff chemistry and chemical weathering at Urumqi Glacier No.1 in central Asia', *Hydrological Processes*, 33, pp. 3258–3281. doi: 10.1002/hyp.13555.

Lone, A. *et al.* (2019) 'Hydrochemical assessment (major ions and Hg) of meltwater in high altitude glacierized Himalayan catchment', *Environmental Monitoring and Assessment*, 191–

213, p. 19. doi: 10.1007/s10661-019-7338-y.

Marshall, S. J. *et al.* (2011) 'Glacier water resources on the eastern slopes of the Canadian Rocky Mountains', *Canadian Water Resources Journal*, 36, pp. 109–134. doi: 10.4296/cwrj3602823.

Mast, M. A. *et al.* (2014) 'Links between N deposition and nitrate export from a high-elevation watershed in the Colorado front range', *Environmental Science and Technology*, 48, pp. 14258–14265. doi: 10.1021/es502461k.

Milner, A. M. *et al.* (2017) 'Glacier shrinkage driving global changes in downstream systems', *Proceedings of the National Academy of Sciences of the United States of America*, 114, pp. 9770–9778. doi: 10.1073/pnas.1619807114.

Miner, K. R. *et al.* (2017) 'Legacy organochlorine pollutants in glacial watersheds: A review', *Environmental Science: Processes and Impacts*, 19, pp. 1474–1483. doi: 10.1039/c7em00393e.

Neff, J. C. *et al.* (2008) 'Increasing eolian dust deposition in the western United States linked to human activity', *Nature Geoscience*, 1, pp. 189–195. doi: 10.1038/ngeo133.

Niu, Y. *et al.* (2017) 'Characterizing glacial meltwater sources in the Athabasca Glacier, Canada, using noble gases as tracers', *Applied Geochemistry*, 76, pp. 136–147. doi: 10.1016/j.apgeochem.2016.11.015.

Obrist, D. *et al.* (2008) 'Atmospheric mercury concentrations at Storm Peak Laboratory in the Rocky Mountains: Evidence for long-range transport from Asia, boundary layer contributions, and plant mercury uptake', *Atmospheric Environment*, 42, pp. 7579–7589. doi: 10.1016/j.atmosenv.2008.06.051.

OTT Hydromet (2020) *Hydrolab HL4 Multiparameter Sonde*. Available at: https://www.ott.com/products/water-quality-2/hydrolab-hl4-multiparameter-sonde-54/ (Accessed: 28 April 2020).

Paudyal, R. *et al.* (2017) 'Insights into mercury deposition and spatiotemporal variation in the glacier and melt water from the central Tibetan Plateau', *Science of the Total Environment*, 599–600, pp. 2046–2053. doi: 10.1016/j.scitotenv.2017.05.145.

Phillips, V. J. A. *et al.* (2011) 'Increased mercury loadings to Western Canadian Alpine Lakes over the past 150 years', *Environmental Science and Technology*, 45, pp. 2042–2047. doi: 10.1021/es1031135.

Rippin, D. M. *et al.* (2020) '"Detachment" of icefield outlet glaciers: catastrophic thinning and retreat of the Columbia Glacier (Canada)', *Earth Surface Processes and Landforms*, 45, pp. 459–472. doi: 10.1002/esp.4746.

Schindler, D. W. and Donahue, W. F. (2006) 'An impending water crisis in Canada's western prairie provinces', *Proceedings of the National Academy of Sciences of the United States of America*, 103, pp. 7210–7216. doi: 10.1073/pnas.0601568103.

Schuster, P. F. *et al.* (2011) 'Mercury export from the Yukon River Basin and potential response to a changing climate', *Environmental Science and Technology*, 45, pp. 9262–9267. doi: 10.1021/es202068b.

Sharma, B. M. *et al.* (2015) 'Melting Himalayan glaciers contaminated by legacy atmospheric depositions are important sources of PCBs and high-molecular-weight PAHs for the Ganges floodplain during dry periods', *Environmental Pollution*, 206, pp. 588–596. doi: 10.1016/j.envpol.2015.08.012.

Sheppard, D. S., Deely, J. M. and Edgerley, W. H. L. (1997) 'Heavy metal content of meltwaters from the Ross Dependency, Antarctica', *New Zealand Journal of Marine and Freshwater Research*, 31, pp. 313–325. doi: 10.1080/00288330.1997.9516769.

Søndergaard, J. *et al.* (2012) 'Mercury transport in a low-arctic river in Kobbefjord, West Greenland (64° N)', *Water, Air, and Soil Pollution*, 223, pp. 4333–4342. doi: 10.1007/s11270-012-1198-1.

St Pierre, K. A. *et al.* (2019) 'Drivers of Mercury Cycling in the Rapidly Changing Glacierized Watershed of the High Arctic's Largest Lake by Volume (Lake Hazen, Nunavut, Canada)', *Environmental Science and Technology*, 53, pp. 1175–1185. doi: 10.1021/acs.est.8b05926.

Steinlin, C. *et al.* (2016) 'A Temperate Alpine Glacier as a Reservoir of Polychlorinated Biphenyls: Model Results of Incorporation, Transport, and Release', *Environmental Science and Technology*, 50, pp. 5572–5579. doi: 10.1021/acs.est.5b05886.

Stern, G. A. *et al.* (2012) 'How does climate change influence arctic mercury?', *Science of The Total Environment*, 414, pp. 22–42. doi: 10.1016/j.scitotenv.2011.10.039.

Stocker, T. F. *et al.* (2013) 'Climate Change 2013: The Physical Science Basis. Contribution of Working Group I to the Fifth Assess- ment Report of the Intergovernmental Panel on Climate Change', in Stocker, T. F. et al. (eds). Cambridge University Press, p. 115.

Sun, S. *et al.* (2018) 'Insights into mercury in glacier snow and its incorporation into meltwater runoff based on observations in the southern Tibetan Plateau', *Journal of Environmental Sciences (China)*, 68, pp. 130–142. doi: 10.1016/j.jes.2018.03.033.

Sun, X. *et al.* (2017) 'The role of melting alpine glaciers in mercury export and transport: An intensive sampling campaign in the Qugaqie Basin, inland Tibetan Plateau', *Environmental Pollution*, 220, pp. 936–945. doi: 10.1016/j.envpol.2016.10.079.

Sun, X. *et al.* (2018) 'Mercury speciation and distribution in a glacierized mountain environment and their relevance to environmental risks in the inland Tibetan Plateau', *Science of the Total Environment*, 631–632, pp. 270–278. doi: 10.1016/j.scitotenv.2018.03.012.

Swennen, R. and Vandeginste, V. (2003) 'Genesis of zebra dolomites (Cathedral Formation : Canadian Cordillera Fold and Thrust Belt , British Columbia)', *Journal of Geochemical Exploration*, 78–79, pp. 571–577. doi: 10.1016/S0375-6742(03)00065-7.

Tennant, C. and Menounos, B. (2013) 'Glacier change of the Columbia Icefield, Canadian Rocky Mountains, 1919-2009', *Journal of Glaciology*, 59, pp. 671–686. doi: 10.3189/2013JoG12J135.

U.S. Environmental Protection Agency (1996) *Method 1669 Sampling Ambient Water for Trace Metals at EPA Water Quality Criteria Levels 20460*. Washington, D. C.

U.S. Environmental Protection Agency (2002) *Method 1631, Revision E: Mercury in water by oxidation, purge and trap, and cold vapor atomic fluorescence spectrometry*, *Epa 821-R-96-012*.

Ullrich, S. M., Tanton, T. W. and Abdrashitova, S. A. (2001) 'Mercury in the Aquatic Environment : A Review of Factors Affecting Methylation', *Environmental Science and Technology*, 31. doi: 10.1080/20016491089226.

US Environmental Protection Agency (2009) 'Environmental Chemistry, Transport and Fate', *Guidance for Reporting on the Environmental Fate and Transport of the Stressors of Concern in Problem Formulations*, p. 30.

VanLooy, J. A. and Vandeberg, G. S. (2019) 'Late summer glacial meltwater contributions to Bull Lake Creek stream flow and water quality, Wind River Range, Wyoming, USA', *Physical Geography*, 40, pp. 461–480. doi: 10.1080/02723646.2019.1565215.

Vermilyea, A. W. *et al.* (2017) 'Continuous proxy measurements reveal large mercury fluxes from glacial and forested watersheds in Alaska', *Science of the Total Environment*, 599–600, pp. 145–155. doi: 10.1016/j.scitotenv.2017.03.297.

Villa, S. *et al.* (2006) 'Organochlorine compounds in ice melt water from Italian Alpine rivers', *Ecotoxicology and Environmental Safety*, 63, pp. 84–90. doi: 10.1016/j.ecoenv.2005.05.010.

Water Survey of Canada (2020) *Daily Discharge Graph for SUNWAPTA RIVER AT ATHABASCA GLACIER (07AA007) [AB] - Water Level and Flow - Environment Canada*. Available at: https://wateroffice.ec.gc.ca/report/historical_e.html (Accessed: 28 April 2020).

YSI Inc. (2020) *Multiparameter water quality instrument - YSI EXO - EXO2 Sonde*. Available at: https://www.ysi.com/exo2 (Accessed: 28 April 2020).

Zdanowicz, C. *et al.* (2018) 'Snowmelt, glacial and atmospheric sources of mercury to a subarctic mountain lake catchment, Yukon, Canada', *Geochimica et Cosmochimica Acta*, 238, pp. 374–393. doi: 10.1016/j.gca.2018.06.003.

Zemp, M. *et al.* (2019) 'Global glacier mass changes and their contributions to sea-level rise from 1961 to 2016', *Nature*, 568, pp. 382–386. doi: 10.1038/s41586-019-1071-0.

Zhang, L., Wright, L. P. and Blanchard, P. (2009) 'A review of current knowledge concerning dry deposition of atmospheric mercury', *Atmospheric Environment*, 43, pp. 5853–5864. doi: 10.1016/j.atmosenv.2009.08.019.

Zolkos, S. *et al.* (2020) 'Mercury Export from Arctic Great Rivers', *Environmental Science & Technology*, 54, pp. 4140–4148. doi: 10.1021/acs.est.9b07145.

CHAPTER 3. Thaw features in continuous permafrost contribute minor amounts of mercury and other trace elements to downstream environments in the Old Crow River, Yukon

3.1. Introduction

Global warming poses numerous risks to Arctic landscapes and ecosystems. These risks include geomorphic risks such as accelerated coastal erosion (Lantuit and Pollard, 2008; Douglas et al., 2012; Frederick et al., 2016), and hydrological risks such as changes to the timing and magnitude of freshet and associated flooding of lowland communities (Schindler and Smol, 2006; Janowicz, 2017). Notably, warming in the Arctic is leading to biogeochemical changes to river water chemistry associated with inputs of legacy contaminants from degrading glaciers (e.g., Bogdal et al., 2010; Carling, Tingey and Fernandez, 2013; Miner et al., 2017; Vermilyea et al., 2017; VanLooy and Vandeberg, 2019) and permafrost (e.g., Baron, Schmidt and Hartman, 2009; Schuster et al., 2011; Stern et al., 2012; Barnes et al., 2014; Brighenti et al., 2019).

Permafrost, which is ground that has remained ≤ 0 °C for ≥ 2 years (Van Everdingen, 1998), is predicted to degrade by 30 to 99 % by 2100 (Koven, Riley and Stern, 2013) as a result of local ground warming. Permafrost soils, especially organic rich soils (Halbach et al., 2017), contain high stocks of legacy carbon (Schuur et al., 2009, 2015; Tarnocai, 2009) and contaminants, including mercury (Klaminder et al., 2008; Stern et al., 2012; Burke et al., 2018; Olson et al., 2018; Schuster et al., 2018) and nutrients (Gao et al., 2018; Brighenti et al., 2019). The rapid warming of arctic regions, driven by polar amplification (Screen and Simmonds, 2010), has initiated concern that thawing permafrost will mobilize high stocks of legacy contaminants to aquatic systems (Brighenti et al., 2019).

Permafrost degradation has two forms: thermal and physical. Thermal degradation involves the deepening of the active layer, increase of groundwater flow path depths and flow rates, and increased rates of chemical weathering (Toohey et al., 2016; Lafrenière and Lamoureux, 2019; Connolly et al., 2020). Physical degradation involves changes in geomorphology and sediment transport, for example due to increased sediment mass wasting, formation of thaw slumps and thermokarst lakes, and permafrost-peatland collapse (Colombo et al., 2018; Lafrenière and Lamoureux, 2019). The combined impact of thermal and physical permafrost degradation on downstream aquatic systems includes increased solute and suspended sediment loads, stream temperature increases, and even physical blockade by mass wasting (Colombo et al., 2018, 2019; St. Pierre et al., 2018; Brighenti et al., 2019; Lafrenière and Lamoureux, 2019).

Thaw slumps have been implicated as a significant pathway for organic carbon and trace elements, such as mercury and other legacy contaminants, to enter aquatic environments (Kokelj et al., 2013; St. Pierre et al., 2018; Lafrenière and Lamoureux, 2019; Mu et al., 2020). Thaw slumps form where ice-rich ground thaw on a slope leads to retrogressive slope collapse and mass wastage of sediment. Thaw slumps commonly form along river cut banks, where channel migration promotes exposure of ice-rich materials. The rate of thaw slump formation has increased by as much as 60-fold between 1985 and 2015 in a high arctic watershed on Banks Island (Lewkowicz and Way, 2019), with slump incidence and cover area increases also observed in the Western Canadian Arctic (Segal, Lantz and Kokelj, 2016) and on Herschel Island (Lantuit and Pollard, 2008). Thaw slumps can mobilize large fluxes of sediments to downstream environments (Kokelj et al., 2013).

Previous research into the effect of permafrost thaw on river water chemistry has often focused on mercury. Mercury is of concern due to its potential to methylate to methylmercury, which is toxic at low concentrations, bioaccumulates in biotic-species, and biomagnifies through food webs. Northern First Peoples communities who consume country foods are therefore at increased risk of mercury exposure (Donaldson et al., 2010). Indeed, mercury and other persistent pollutant concentrations are elevated in Eastern Arctic ecosystems (Brown et al., 2018), and northern First Peoples, especially Inuit and eastern-Canada First Nations communities, are exposed to heightened levels of mercury and other persistent pollutants (Donaldson et al., 2010; Kirk et al., 2012). Although concentrations of mercury in the atmosphere have been decreasing globally over the past 20 years (Zhang et al. 2016), arctic regions have experienced relatively smaller decreases in atmospheric mercury concentrations (Cole et al., 2013). One reason for this may be the year-round uptake of gaseous elemental mercury (GEM) by arctic plants, which leads to high soil mercury concentrations that greatly exceed the mercury concentrations of temperate soils (Obrist et al. 2017). Thus, arctic soils may contain disproportionately high stocks of mercury (Olson et al., 2018; Schuster et al., 2018). Put together, permafrost degradation has been implicated as a significant source of legacy mercury to the Arctic Ocean (e.g., Douglas et al., 2012; Fisher et al., 2012; Kirk et al., 2012; Stern et al., 2012; AMAP/UNEP, 2013; Sonke et al., 2018; Lim et al., 2019s). These implications are especially concerning because mercury methylation in organic soils increases 10-fold at the temperature gradient experienced by thawing soils: between –2 °C and +8 °C (Yang et al., 2016). This research is motivated by the limited evidence of legacy contaminant release within moderately sized rivers with near complete organic-rich permafrost cover. Few studies have characterized a broad hydrochemical parameter suite, and simultaneously examined seasonal

variability at a high temporal-resolution and within-watershed variability in a permafrost-dominated river.

Here we characterize the concentrations, fluxes, and yields of contaminants, including nutrients, mercury, and other trace elements in the Old Crow River, Yukon, Canada. The Old Crow River watershed is underlain completely by continuous permafrost, which is actively thawing. To quantify the impact of this thaw on water quality within the Old Crow River, water chemistry was sampled ~weekly at the river mouth over the 2019 open-water season. Furthermore, grab samples were collected at eight, physiographically varied major tributary creeks, and upstream and downstream of four thaw slumps during the period of peak-thaw in late-July to further assess point sources and downstream transport of potential contaminants. We show that mercury and other contaminant trace element and nutrient concentrations peaked during the spring freshet, which mobilized sediment during high flow, and were lowest during the late summer interval of peak permafrost thaw. The annual flux and yield of mercury for Old Crow River was significantly lower than at comparable permafrost-influenced watersheds. Our results highlight the need to reassess the simple paradigm that permafrost thaw is releasing significant concentrations of nutrients (Baron, Schmidt and Hartman, 2009; Holmes et al., 2012; Barnes et al., 2014), mercury (Schuster et al., 2011, 2018; St. Pierre et al., 2018), and other trace elements (Pokrovsky et al., 2016, 2018) to downstream ecosystems, and underscore the need to assess other potential sources of elevated trace element and nutrient contaminants in the arctic environment.

3.2. Site Description

The Old Crow River is a 13,900 km^2 undeveloped arctic watershed underlain entirely by continuous permafrost (Yukon Ecoregion Working Group, 2004) (Figure 3.1). The river's mainstem meanders through the Old Crow Flats, a continentally situated region with significant thermokarst lake and pond cover (~35%), glaciolacustrine sediments, and ice-rich, peatland permafrost (Yukon Ecoregions Working Group, 2004). Notable permafrost thaw features along the river include thermokarst lakes, retrogressive thaw slumps, active layer detachment slides, and debris flows of thawed material (Yukon Ecoregion Working Group, 2004), all with variable connectivity to the Old Crow River. Significant portions of the Old Crow Flats have remained frozen since the draining of glacial lake Old Crow ~15 ka (Zazula et al., 2004; Kennedy et al., 2010). Due to the high heat capacity of water, the river itself is underlain by talik (Yukon Ecoregions Working Group, 2004).

The Old Crow watershed is contained within the traditional territory of the Vuntut Gwitchin First Nation and has remained undeveloped due to the 1993 Vuntut Gwitchin First Nation Final Agreement (The Government of Canada, The Vuntut Gwitchin First Nation and The Government of the Yukon, 1993). Thus, land use along the Old Crow River is limited to hunting, trapping, and fishing; there are no agricultural, urban, or industrial land-uses along the river's entire reach and no point sources of mercury, other heavy metals, or nutrients such as ore-mining, oil-sands development, or fossil-fuel burning. As such, the Old Crow River represents an ideal system to quantify the impact of permafrost thaw on lotic systems.

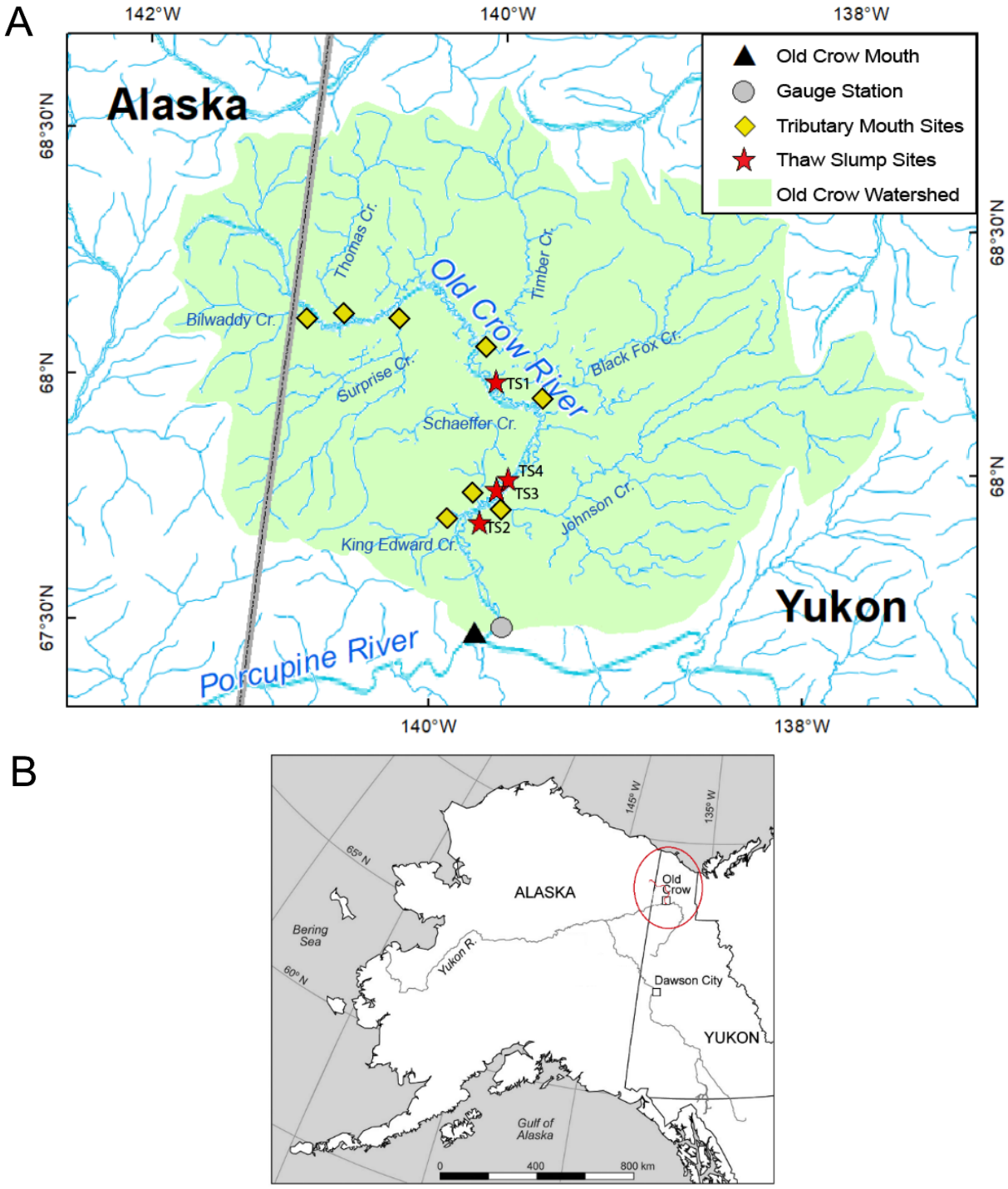

Figure 3.1. (A) Map of Old Crow River watershed, with locations of thaw slump (red star), tributary (yellow diamond), gauging station (grey circle) and sampling site at mouth (black triangle) sampling locations. (B) Inset map of Alaska and Yukon, showing the mainstem of the Old Crow River within the Yukon River basin (modified from Reyes, Froese and Jensen, 2010).

The Old Crow River is ice free from mid-May to mid-October (Yukon Ecoregion Working Group, 2004; Janowicz, 2017). The catchment has a nival hydrological regime: break-up has occurred historically in mid-May, followed by a strong spring (late-May to early-June) freshet driven by snowmelt and a second, lower magnitude, high flow period in late summer. Freeze-up has occurred historically in mid-October. Historically, Old Crow River discharge at its confluence with the larger Porcupine River averages ~50 m^3/s annually and ~100 m^3/s during the open water season (May 1 – November 1), with a mean peak discharge of ~770 m^3/s between 1977 and 2019. The 1980 – 2010 mean annual temperature at the village of Old Crow, at the southern end of the watershed, is –8 °C and mean July temperatures are between 12 °C and 15 °C (Environment and Climate Change Canada, 2020). Mean annual precipitation in this region is ~280 mm, approximately half of which falls as snow (Environment and Climate Change Canada, 2020).

3.3. Methods

3.3.1. Water and Sediment Sampling

Water grab samples were collected ~weekly (total and routine parameters; n=16) and ~monthly (dissolved parameters; n=5) at the west bank of the Old Crow River mouth from May 28 – October 8, 2019 (Figure 3.1). The sampling location is 14 km downstream (7 km linear distance) of the Water Survey of Canada gauge station (09FC001; 67°35'20" N, 139°47'30" W). Between July 21 and 28, 2019, we also collected samples for total, dissolved, and routine parameters from eight tributary creeks that drain into the Old Crow River and a suite of samples associated with thaw slumps (Old Crow River samples upstream and downstream of four thaw

slumps, as well as thaw slump meltwater and sediment samples). Detailed descriptions of sampling locations are contained in Appendix B.

Water samples were collected in precleaned polypropylene bottles (for routine parameters, trace elements, and nutrients) or Teflon capped amber borosilicate glass double-bagged in polypropylene (for mercury and methylmercury) following EPA Method 1669 (U.S. Environmental Protection Agency, 1996). Bottles were triple rinsed with river water and then filled at a depth of 15 cm, in continuous flow. Samples intended for total analysis were immediately acidified with trace metal grade HNO_3 (for trace elements and nutrients (0.1% v/v)) and HCl (for mercury (0.2% v/v) and methyl mercury (0.4% v/v)) for the purpose of sample preservation. Samples intended for dissolved parameters were kept at 4 °C and returned to the laboratory within 48 hours, then filtered through 0.45 μm HCl-washed cellulose nitrite filters, and acidified. Clean, powder-free nitrile gloves were worn during sampling. Field blanks were rinsed and filled at the shore of the river, and filtered in the field laboratory on a monthly basis. Duplicates were collected for the first month of weekly grab-sampling events at the river mouth (Appendix B; Table B.2).

Active retrogressive thaw slumps along the Old Crow River typically form in tall (~30 m) bluffs on the cutbank side of river meanders, which are capped by 2 – 10 m of silty clay deposited when Glacial Lake Old Crow covered much of the study region during the last glaciation (Zazula et al., 2004) and ~1 m of peat. The four active retrogressive thaw slumps sampled for this study were representative of other active and inactive slumps observed in the catchment in terms of basin width, headwall height, and organic-poor-sediment. Retrogressive thaw slump activity was qualitatively assessed from the air on the basis moisture (sediment colour) and vegetation cover of slump basin. Thaw slumps were ~30 – 40 m wide with headwalls

~2 – 5 m tall. River water samples up- and downstream of thaw slump were collected, when possible, 30 m upstream and downstream of the slump feature, between July 21 – 28, 2019. Where this was not logistically possible, a sampling location was chosen which visually sampled water before the rill entered the mainstem, and after the rill entered the mainstem. An additional water sample was collected along the actively flowing rill of the thaw slump debris tongue's slope (Figure 3.2). Additional sampling location details can be found in Appendix B.

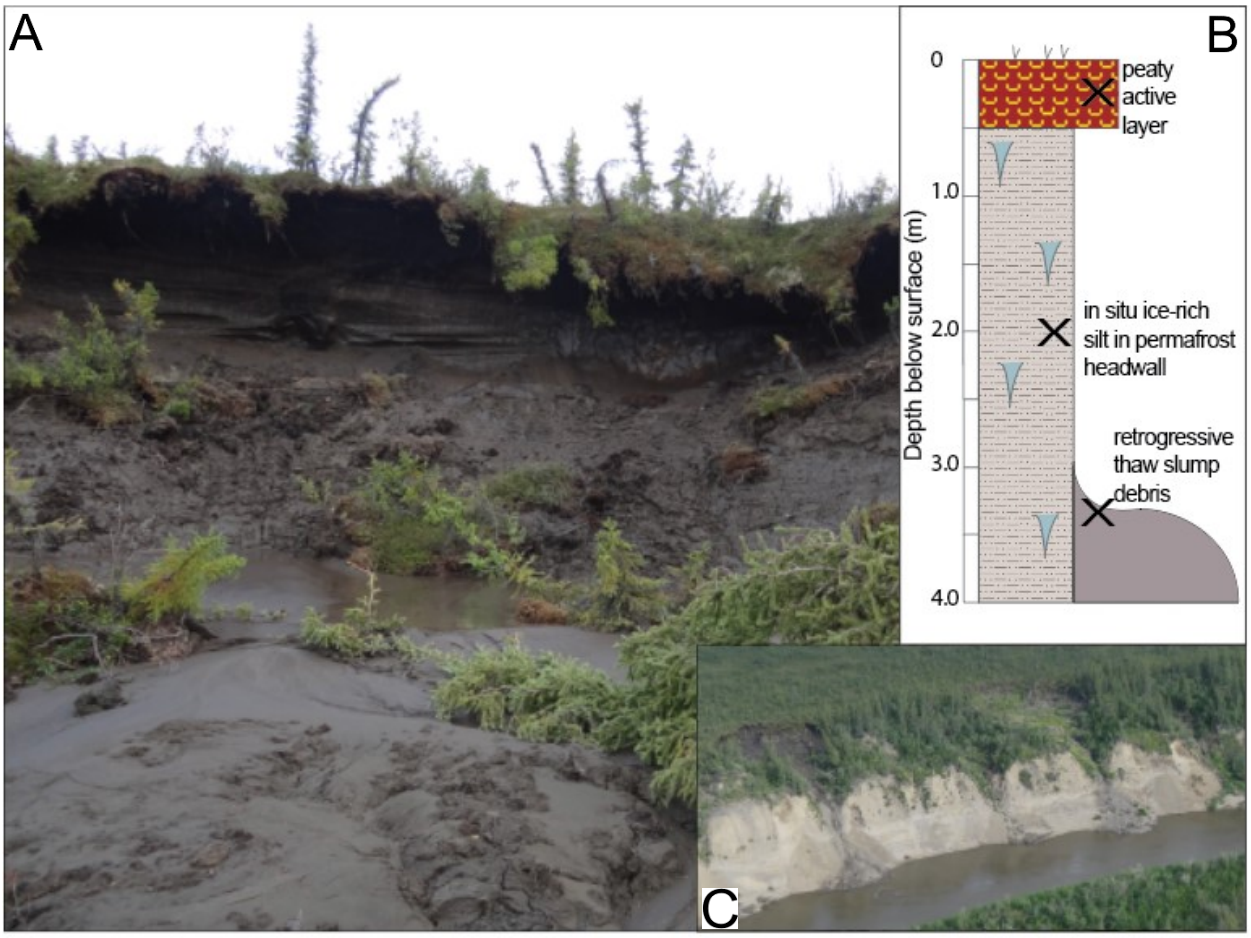

Figure 3.2. (A) Photograph of an active retrogressive thaw slump basin and headwall. The overhanging organic-rich active layer, headwall (typically 2 – 5 meters) with in-situ silt- and ice-rich sediment, and basin floor (typically 30 – 40 meters across) with thawed debris can be observed. (B) Composite stratigraphic log of a typical retrogressive thaw slump, with sediment sampling locations marked with "X". (C) Two adjacent retrogressive thaw slumps along the Old Crow River.

Thaw slump sediments were collected from the organic-rich peaty active layer at the top of the headwall, from in-situ ice rich sediment exposed in the headwall, and from re-transported thawed material along the thaw slump basin and debris tongue (Figure 3.2B). Samples were collected into doubled polypropylene bags, stored on ice in the field, and frozen until analysis.

3.3.2. Analytical Methods

River water samples were analyzed for a broad suite of parameters. The analyses included: turbidity, pH, conductivity, alkalinity, total dissolved solids, total suspended solids, organic and inorganic carbon, and major ions (Al, Ca, K, Mg, Na, SO_4, Cl). The element analyses included: total and dissolved nitrogen and phosphorus species, 31 total and dissolved trace elements, as well as total and dissolved mercury and methylmercury by standard methods (additional information is provided in Appendix B). Stable hydrogen and oxygen isotopes were determined by cavity ring-down spectroscopy on a Picarro L2130-I isotope analyzer, and presented in standard δ-notation relative to Vienna Standard Mean Ocean Water (VSMOW).

Sediment samples were freeze dried, homogenized on an agate mill, and subsampled. One set of subsamples was analyzed on a Direct Mercury Analyzer-80 (DMA) for total mercury concentration (EPA Method 7473). A second set of subsamples was analyzed for organic matter by Loss on Ignition (LOI) performed at 550 ºC (4 hours) in a muffle furnace. A third set of ~0.5 g sediment subsamples was analyzed for both labile and residual trace element concentrations (Graney et al. 1995; Gobeil et al. 2013). Labile fractions were extracted in ~6 mL of Optima-grade 10% v/v HNO_3, agitated for 24 hours at room temperature, then centrifuged at 4000 rpm for 30 minutes. The supernatant was decanted into fresh containers and analyzed by inductively-

coupled mass spectrometry. The residual sediment was rinsed with deionized water, centrifuged 3 times, and re-freeze-dried before being digested using HF-HNO_3 at 110ºC and then analyzed by inductively-coupled mass spectrometry. Duplicates were analyzed for every 10^{th} sediment sample from the slumps (Appendix B). Marine Isotope Standard Reference Material (MESS-4) was analyzed in duplicate for ICP-MS analysis, and in quadruplicate for DMA analysis (Table B.3; Table B.4). For DMA analysis, the MESS-4 mean Hg concentration was 77.2 ± 2.9 µg/kg (n=4), within the accepted 20% range of the accepted value of 90 ± 40 µg Hg/kg. The relative percent difference between two sets of unknown duplicates was 0.6 % and 2.5 %. For ICP-MS analysis, the reference material results were 22.6 ± 0.1 mg/kg, within the 1σ range for Pb in MESS-4 of 21.5 ± 1.2 mg/kg, and the relative percent difference between four sets of duplicates was 20%, 0.6%, 2.2%, and 0.6%.

3.3.3. Statistical Methods

3.3.3.1. Simple Linear Regression and Principal Component Analysis

Simple linear regression (SLR) and principal component analysis (PCA) were used to examine relations among two subsets of the data: (1) weekly total, routine, and mean-daily discharge data from the river mouth (n=16), and (2) total, dissolved, and routine data from across the basin (tributaries, up- and downstream of slumps, and at the mouth) sampled in late-July (n=18). Simple linear regression models were calculated for all the parameters with the following suite of predictor variables: mean-daily discharge, total suspended solids, dissolved organic carbon, $\delta^{18}O$, and deuterium-excess (calculated as d-excess = $\delta^{2}H - 8 \times \delta^{18}O$). These parameters are representative of water flow, sediment load, organic matter input, snow/rain contribution, and

evaporation, respectively. For simple linear regression, data below detection and missing observations were left blank. For PCA, data were centered and standardized after substituting zero values for data below method detection limits (MDL). Chemical parameters for which >25% of analyses were below the MDL or missing were not included in the PCA.

3.3.3.2. Flux and Yield Calculations

Total trace element and total nutrient concentrations that correlated positively ($r > 0.7$) with mean-daily discharge were modelled at daily time-steps using simple linear regression equations with mean-daily discharge. Daily mercury, methylmercury, and dissolved organic carbon concentrations were additionally modeled using a natural logarithm regression with mean-daily discharge. These modelled daily concentrations were then multiplied by the associated mean-daily discharge to obtain a timeseries of daily flux (mass/day) for 2019 and summed to obtain annual flux (mass/year). Annual flux was divided by the watershed area (13900 km^2) to obtain annual watershed yield (mass/year/km^2). The simple linear regression relation for mercury was also applied to historic discharge data between 1977 and 2018 to model historic mercury flux and yield.

3.3.3.3. Enrichment Factors

Enrichment factors (EF) were calculated by normalizing element concentrations to aluminum relative to the corresponding ratios for upper continental crust compiled by Wedepohl (1995) as $EF = ([TE]_{sample}/[Al]_{sample}) / ([TE]_{UCC}/[Al]_{UCC})$, where TE is the element concentration of interest.

3.4. Results

3.4.1. Historic Climate and Discharge

Air temperatures in 2019 ranged from –45 ºC to +29 ºC, with an average of –5.5 ºC and maximum of +29 ºC on July 24. Cumulative annual precipitation was 182 mm, less than the 1980–2010 climate normal average of 280 mm. In 2019, break-up began on May 15 and discharge peaked on May 26 at ~1140 m^3/s (Figure 3.3). Discharge increased to ~380 m^3/s on August 18 during a period of intense rainfall between August 3 and August 20. River ice began to form on October 7, and freeze-up occurred around October 12. Discharge in 2019, compared to the 42-year record, had a high peak discharge magnitude, early peak-freshet date, and high annual water yield (Figure 3.3A). Overall, over the past 42 years (1977 – 2019), annual water yield increased by ~120% and peak freshet date has moved earlier by eight days; peak discharge magnitude has not changed significantly (Figure 3.4; Figure B.1). There is a roughly decadal oscillation apparent in water yield which correlates moderately ($r = 0.42$) with Pacific Decadal Oscillation (June index), and with March (same year; $r = –0.51$), and September (prior year; $r = –0.48$) sea ice extent (all correlations had p-value <0.05). The increase in water yield volume are spread over the spring and autumn (Figure 3.5).

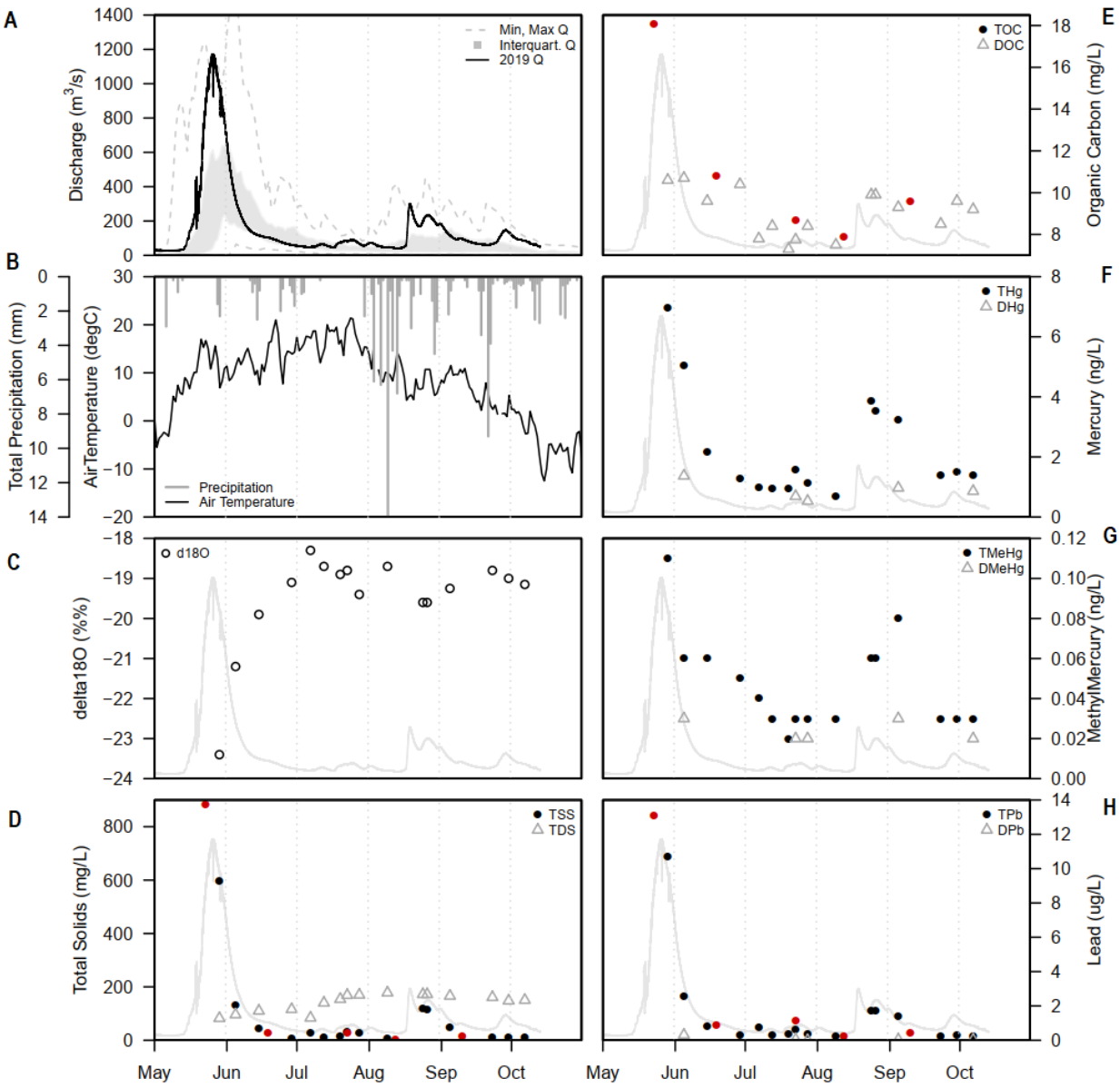

Figure 3.3. Timeseries of Old Crow River hydrometeorological and water sample data. (A) 2019 discharge with minimum, maximum, and interquartile range of 1977 – 2019 discharge, (B) air temperature and precipitation, (C) $\delta^{18}O$, (D-H) concentrations of chemical parameters collected by our study (black and grey) and Environment and Climate Change Canada (red) for: (D) total suspended and dissolved solids, (E) total and dissolved carbon, (F) total and dissolved mercury, (G) total and dissolved methylmercury, (H) and total and dissolved lead. Grey line in C-H is 2019 Old Crow River discharge for reference.

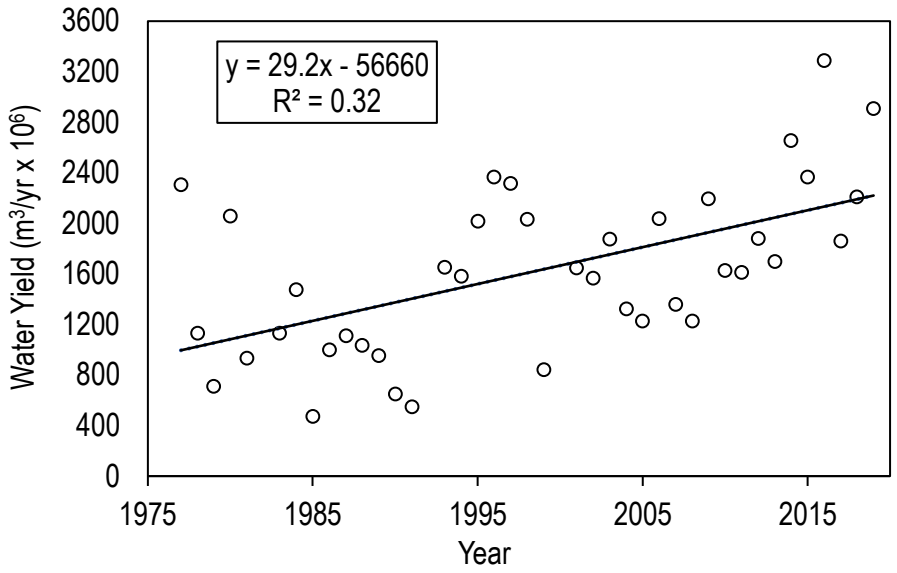

Figure 3.4. Annual water yield at the mouth of Old Crow River.

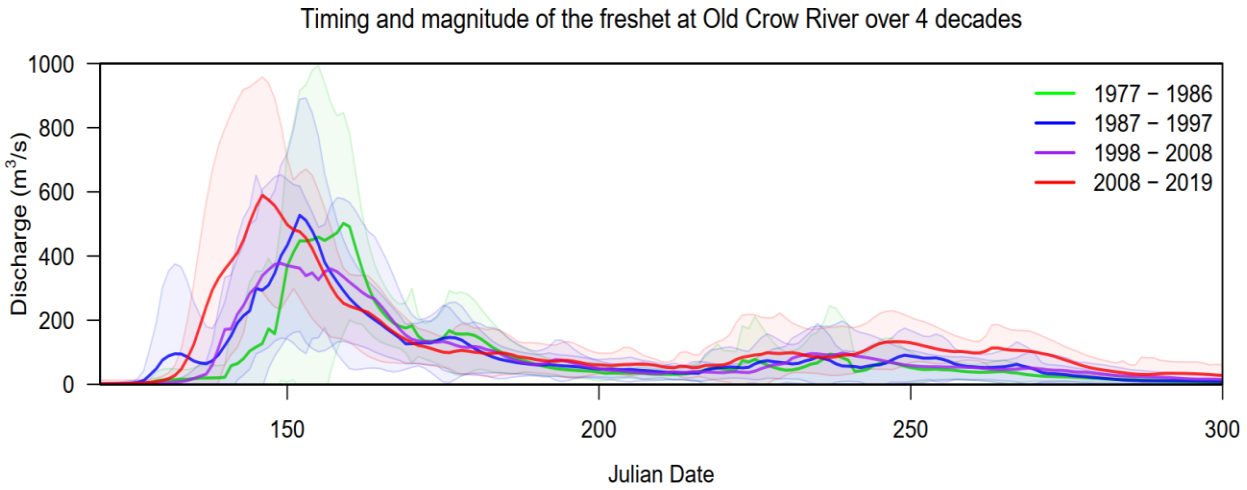

Figure 3.5. Times series of decadal-mean mean-daily Old Crow River discharge (solid lines) and one standard deviation (translucent polygons).

3.4.2. Seasonal Record of Water Chemistry from the Old Crow River Mouth

Old Crow River is a highly turbid and rich in carbonate, iron, organic material, and solutes (Table 3.1). Alkalinity ranged from 46 – 124 mg/L, and the pH was neutral to somewhat alkaline at 7.4 – 8.8. Trace element and nutrient concentrations displayed strong seasonal variability. Concentrations of total trace elements (As, Cd, Cr, Co, Cu, Fe, Pb, Ni, Se, Ag, Tl, U, V), total nitrogen, and total phosphorus, were highest during the spring freshet and very low throughout the rest of the year, with the exception of a small increase in mid-August (Figure 3.3). Concentrations of total nitrogen were low (~0.5 mg/L). Nitrogen was predominantly present in the dissolved form (TDN/TN: 85%). NO_2+NO_3 was primarily nitrate; nitrite (~3 µg/L) and ammonia (~23 µg/L) concentrations were low. In contrast, total phosphorus concentrations were high (~84 µg/L) but predominantly (79%) particulate in form; the concentration of TP ranged between meso-eutrophic and hyper-eutrophic concentrations, as qualified by CCME guidelines. Soluble reactive phosphorus only ranged between 5 and 9 µg/L.

Total concentrations of several trace elements (As, Cd, Cr, Cu, Fe, Pb, and Zn) exceeded the CCME chronic guideline during the peak-freshet sampling event on May 28, 2019, but mean open-water-season concentrations were below CCME guidelines. CCME guidelines were also exceeded during early-June and mid-August for total Cr and Cu. The CCME guideline for total Fe was exceeded during all grab-sampling events. Total Hg and MeHg did not exceed CCME guidelines but 42 % and 53 % of mercury species, respectively, were present in the more readily bioavailable dissolved forms.

Table 3.1. Summary of grab sample chemistry results (n=16 total; n=5 dissolved) from the mouth of Old Crow River. %<MDL is the fraction of total parameter results which returned below the parameter's detection limit; %D/T is the average percentage of the total sample which was present in the dissolved phase. *% NO_2^- / (NO_2^- + NO_3^-); DON = TKN – NH_3; n/a: total or dissolved parameter were below detection.

Parameter	Min	Mean	Max	%<MDL	%D/T
Routine Parameters (mg/L)					
DOC	7.3	9.1	10.9		
DIC	9.9	18.2	27.9		
TSS	11	111	178		
TDS	6	107	598		
Alkalinity	46	84	124		
Cond (µS/cm)	103	202	270		
Turb (NTU)	3	38	253		
pH	7.4	8.1	8.8		
δ18O (‰)	-23.4	-19.6	-18.3		
Nutrients (µg/L)					
TP	21	84	500	0%	21%
SRP	5	6.5	9		
TN	354	478	907	0%	85%
DON	344	423	802		
NO2+NO3	3	39	95	19%	7%
NH3	4	23	37		
Major Ions (mg/L)					
Ca	18	35.2	51.84	0%	
SO4	5.3	23.74	45.5	0%	
Na	1.0	3.3	5.8	0%	
Mg	0.3	2.4	7.2	0%	
Cl	0.3	0.9	2.3	0%	
K	<0.02	0.49	0.99	6%	
Al	0.004	0.012	0.034		
Elements (µg/L)					
Fe	370	1870	12500	0%	11%
Al	66	507	3930	0%	8%
Sr	51	92	127	0%	~99%
Zn	0.7	6.1	34.3	0%	<15%
Ni	0.8	3.6	18.2	0%	66%
Ti	0.4	3.0	10.4	0%	26%
Cu	1.3	3.0	14.9	0%	59%
V	0.5	2.3	15.6	0%	29%
Pb	0.2	1.4	10.7	0%	<8%
As	0.6	1.3	5.3	0%	59%
Cr	0.2	1.0	6.7	0%	n/a
U	0.3	0.6	1.3	0%	93%
Se	<0.2	0.3	0.5	25%	~99%
Th	0.02	0.18	1.35	0%	36%
Sb	0.07	0.11	0.18	0%	n/a
Cd	<0.01	0.05	0.30	19%	16%
Tl	<0.003	0.01	0.07	19%	<1%
Ag	<0.001	0.01	0.05	13%	<1%
Hg	0.0007	0.0023	0.0070	0%	42%
MeHg	0.00002	0.00005	0.00010	0%	53%

The distribution of dissolved versus particulate species varied between contaminants. Mercury, MeHg, Ni, Cu, As, and Cr were commonly present in dissolved phases (D/T: 41 – 66 %), while Fe, Al, Zn, Cd, and Pb were commonly present in the particulate phase (D/T: <15 %). Enrichment factors (EFs) relative to mean upper continental crust (Wedepohl, 1995) suggest that the Old Crow River is enriched with respect to numerous chalcophile elements. River mouth sample mean EFs were in excess of 10 for the trace elements Sb, As, Ba, Bi, B, Cd, Co, Cu, Fe, Pb, Li, Mn, Hg, Mo, Ni, Se, Ag, Sr, U, and Zn. Mean EFs were below 10 for Be, Ca, Cl, Cr, Tl, Th, Ti, and V.

In general, total river mouth nutrient and contaminant trace element (N, P, Hg, MeHg, As, Cd, Cr, Co, Cu, Fe, Pb, Ni, Se, Ag, Tl, V, Zn) concentrations closely track discharge ($r > 0.8$) and total suspended solids ($r > 0.85$), but only moderately track DOC ($r = 0.3 – 0.7$) (Table B.5). This general rule does not apply strictly to mercury and methylmercury, which although strongly correlated with discharge and total suspended solids ($r = 0.8 – 0.9$), were also strongly correlated with $\delta^{18}O$ ($r = –0.8 – –0.95$) and DOC ($r = 0.7 – 0.8$) (Figure 3.6).

The overall covariance between the multiple parameters is viewed more holistically in the PCA (Figure 3.7). Total contaminant trace element concentration, total nutrients (N and P), TSS, discharge, DOC, and $\delta^{18}O$ covary, and control the largest proportion of variation and the distribution of loadings along the first principal component axis (PC1) (Figure 3.7A). DOC had a weaker loading than TSS, discharge, or $\delta^{18}O$ indicating a lower degree of covariance with the parameters with strong negative PC1 loadings. Dissolved and ionic phases control the distribution of parameters along the second principal component axis (PC2), indicating that their concentrations vary independently to total-element concentrations.

From break-up to freeze-up, the Old Crow River water chemistry evolved from being highly controlled by discharge and sediment supply, manifested by high total-trace element concentrations (negative PC1 scores), towards being represented most strongly by groundwater dilution, manifested by high ionic species from late-June through freeze-up (positive PC1 scores) (Figure 3.7B). Specifically, the samples collected during high discharge—during the spring freshet and less so following an interval of high August rainfall—have negative PC1 species scores (Figure 3.7B) which covary with the negative PC1 loadings of total-contaminant parameters (Figure 3.7A). In contrast, samples collected during low discharge have positive PC1 species scores (Figure 3.7B) which covary with the ionic parameters with positive PC1 loadings (Figure 3.7A). Unsurprisingly, given the strong correlation coefficients with numerous total trace element and nutrient parameters, we found that mean-daily discharge correlates strongly with PC1 ($R^2 = 0.97$), while PC1 reflects 66% of variation in the dataset. As such, mean-daily discharge may be considered as a robust modeling parameter, especially for the total trace elements and total nutrients (inset, Figure 3.7A).

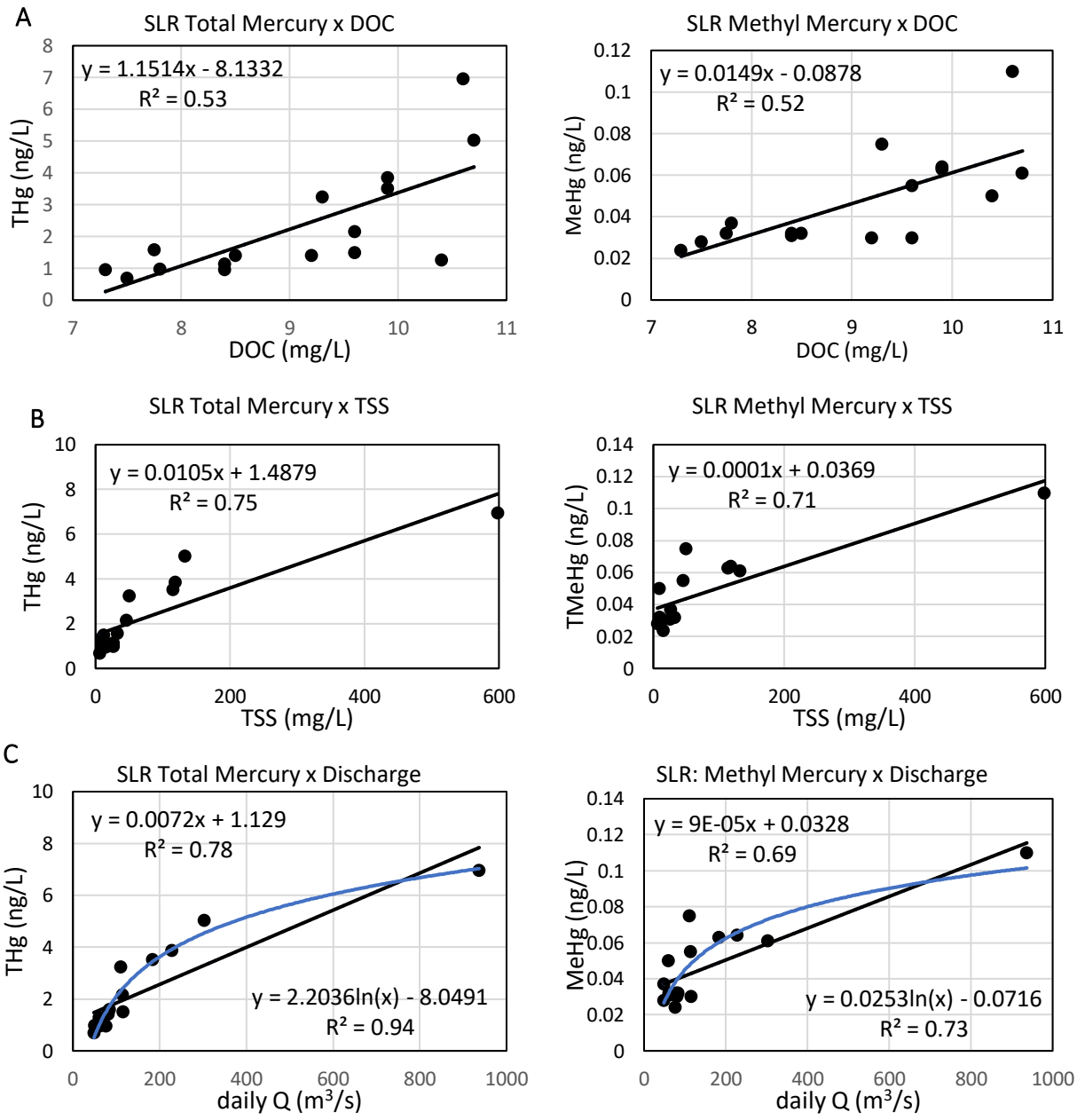

Figure 3.6. Simple linear regression (black trend line) and natural logarithmic regression (blue trend line) of THg and TMeHg as of function of (A) DOC, (B) TSS, or (C) mean-daily discharge.

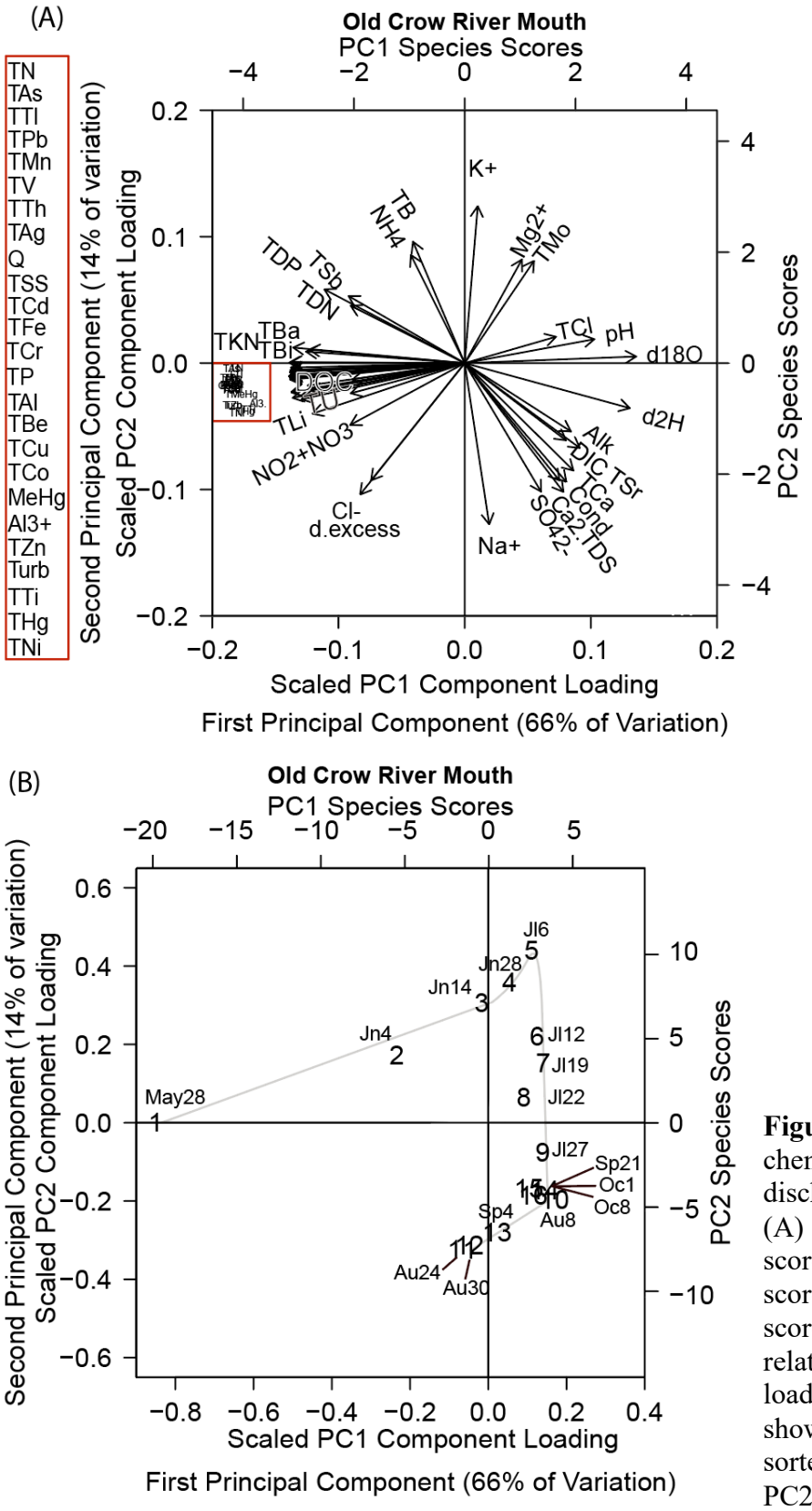

Figure 3.7. PCA of water chemistry parameters and discharge at the River Mouth. (A) Scaled parameter loading scores and (B) scaled sample scores. Note that the sample scores plot (B) is zoomed out relative to the parameter loadings plot (A). Red box inset shows the parameter loadings, sorted from top to bottom by PC2 loading.

3.4.3. Annual Flux and Yield

The 2019 annual fluxes of sediment, dissolved organic carbon, and major elements were 682 Gg, (TSS), 29 Gg, (DOC), 16 Gg (TFe), and 5 Gg (TAl) (Table 3.2). The 2019 watershed yields of potential trace element contaminants for the Old Crow River were 0.014 g/km^2/yr (MeHg), 0.8 g/km^2/yr (THg), 5 g/km2/yr (TAg), 6 g/km^2/yr (TTl), 26 g/ km^2/yr (TCd), 0.5 – 1.0 kg/km^2/yr (TAs, TCo, TCr, and TPb), and 1 – 3 kg/km^2/yr (TCu, TV, TNi, TZn). Nutrient yields were: 44 kg/km^2/yr (TN) and 130 kg/km^2/yr (TP).

Approximately 44 % of the water yield occurred during the mid-May through mid-June freshet, 12 % occurred during mid-June and mid-August, 23 % occurred between mid-August and mid-October, and the remaining 22 % of water yield occurred during the ~seven months of ice-cover. This temporal pattern of water yield is exaggerated in the modeled mercury flux data; approximately 74 % of the mercury flux occurred during the mid-May through mid-June freshet; 5 % occurred mid-June – mid-August, 13 % occurred mid-August – mid-October, and the remaining 9 % of mercury flux is transported during the ice-covered winter. Historical annual flux and yield of mercury, estimated using the 2019 discharge-Hg SLR model, may have approximately doubled over the past 42 years (Figure 3.8).

Table 3.2. Annual flux and yield estimated using a discharge-SLR equation model, or *annual flux and yield estimated using a discharge-natural-logarithm-regression equation model.

Parameter	Flux	Yield
	Gg/yr	**Mg/yr/km^2**
TSS	681.7	49.0
DOC	28.9	2.1
DOC*	29.0	2.1
Fe	16.5	1.2
Al	4.5	0.3
N	1.8	0.1
	Mg/yr	**kg/yr/km^2**
P	616.9	44.4
Zn	43.9	3.2
Ni	23.7	1.7
V	18.5	1.3
Cu	18.1	1.3
Pb	12.3	0.9
Cr	7.9	0.6
As	7.4	0.5
Co	6.8	0.5
	kg/yr	**g/yr/km^2**
Cd	366.6	26.4
Tl	83.5	6.0
Ag	62.2	4.5
Hg	11.8	0.9
Hg*	11.4	0.8
MeHg	0.20	0.01
MeHg*	0.19	0.01

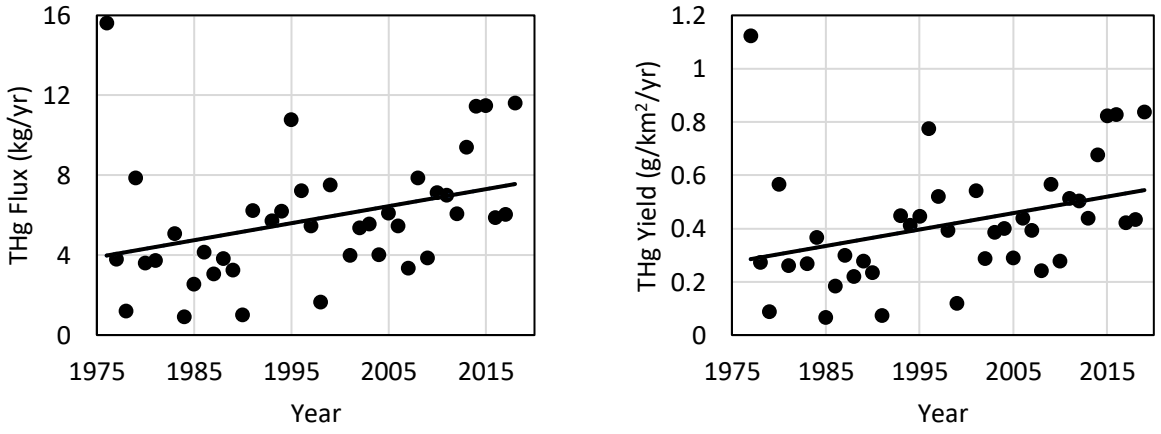

Figure 3.8. Total mercury flux (left) and yield (right), modeled using SLR applied to mean-daily discharge from 1977 – 2019 for Old Crow River.

3.4.4. Water Chemistry Record from across the Old Crow River Basin

Samples were collected across the basin's eight tributaries, upstream and downstream of four thaw slumps along the river's mainstem, and twice the river mouth over seven consecutive days in late-July, 2019. Overall, contaminant trace element concentrations, apart from TFe, were low, below CCME guidelines for the protection of aquatic life, and have low dynamic range (Figure 3.9). This was despite the differences in sampling location, sub-catchment size, bank vegetation, water-clarity, substrate/benthic zone cover, or flow obstructions (Appendix B; Table B.1). However, multiple elements had enrichment factors of >10, including: Sb, As, Ba, B, Cd, Cu, Fe, Pb, Li, Mn, Mo, N, Se, Ag, Sr, U, Zn, Hg.

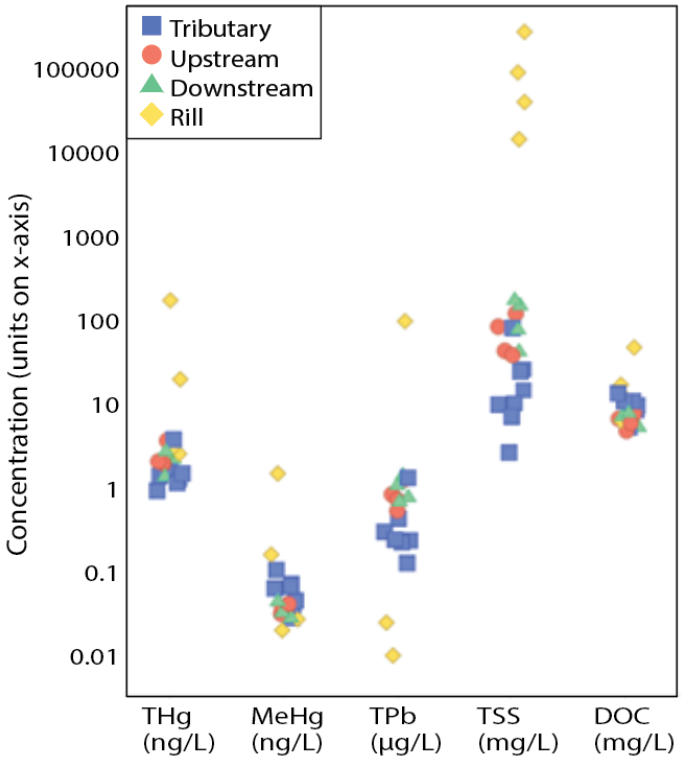

Figure 3.9. Jitter plot of chemical parameter concentrations across the river basin in July 2019.

Total suspended sediment (TSS), like at the mouth, was most strongly correlated with total trace element concentrations across the basin, and DOC strongly correlated with most dissolved trace element concentrations (Table B.6).

Though the explanatory power of the river basin chemistry PCA is relatively weak, with PC1 and PC2 respectively explaining only 32% and 27% of variation in the dataset, the PCA reveals some differences in hydrochemistry of the mainstem and tributary samples (Figure 3.10). On the whole, mainstem water chemistry (negative PC1 and PC2 scores; Figure 3.10B) is more driven by carbonate parameters including: calcium, TDS, Sr, U, alkalinity (negative PC1 loadings; Figure 3.10A). Compared to the tributaries, mainstem samples also have higher total trace element contaminant concentrations (negative PC2 loadings; Figure 3.10A); lower dissolved mercury, dissolved methylmercury, and dissolved organic carbon concentrations (negative PC1 loadings; Figure 3.10A); and low methylmercury/total-mercury ratios (1 – 4 %) (Figure 3.11). The tributaries (positive PC2 scores; Figure 3.10B), conversely, have a higher proportion of dissolved mercury and methylmercury, and higher methylmercury/mercury ratios (2 – 7 %; Figure 3.11) (positive PC2 loadings; Figure 3.10A) and lower concentrations of trace element contaminants.

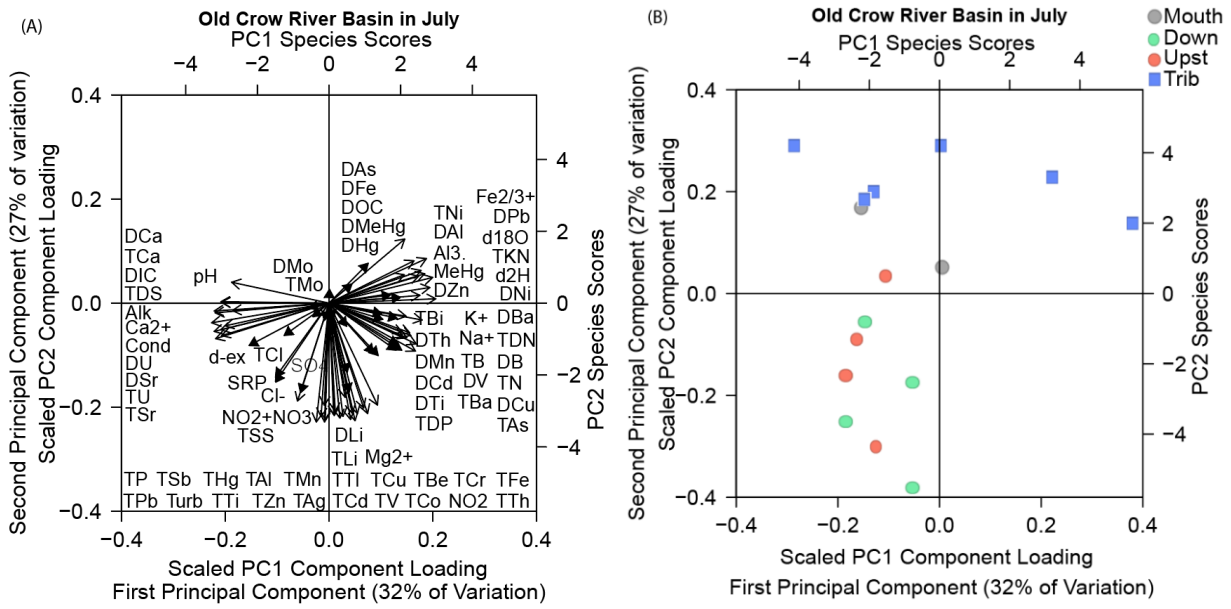

Figure 3.10. PCA of chemical parameters grab sampled at the eight tributaries, upstream and downstream of four thaw slumps, and at the river mouth in late-July of 2019. (A) Parameter loadings and (B) sample scores.

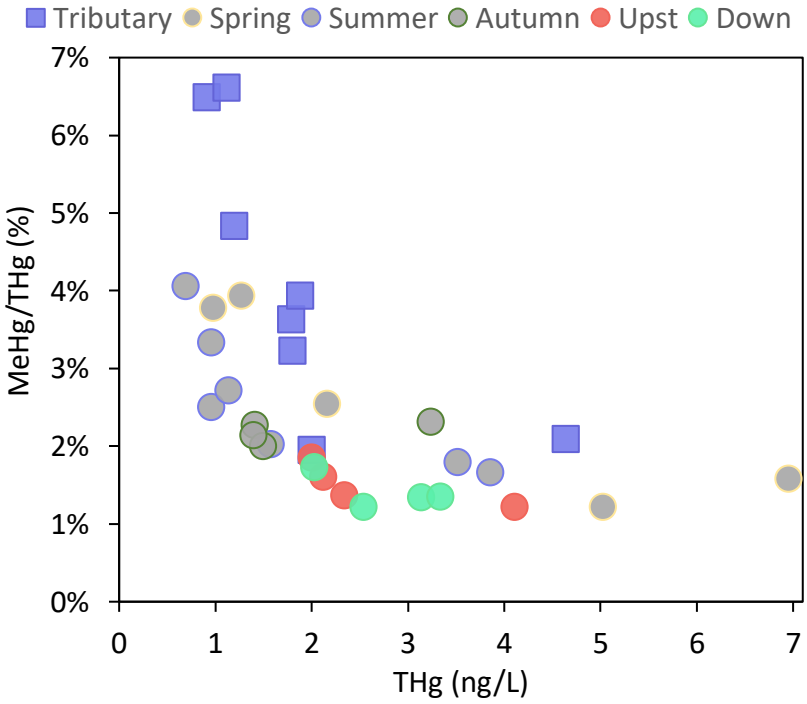

Figure 3.11. Methylmercury to total mercury ratio Old Crow River tributaries (blue squares; n=8), upstream (red circle; n=4) and downstream (green circle; n=4) of four thaw slumps on Old Crow River, and across the open-water season at the river mouth (grey circle, subdivided with yellow outline for spring, blue outline for summer, and green outline for autumn; n=16).

3.4.5. Water and Sediment Chemistry of Active Retrogressive Thaw Slumps

Meltwater draining from the debris tongues of active retrogressive thaw slumps, which we term rill water, had estimated discharge of < 1 L/s (ie. < 0.001 m3/s). Contaminant trace element concentrations in two rill water samples were at or exceeded the 26 ng/L CCME guideline for total mercury (Figure 3.12). Rill samples were extremely sediment rich (14 – 315 g/L). Concentrations of trace elements upstream and downstream of active retrogressive thaw slumps, however, did not differ significantly (Figure 3.9; Figure 3.12).

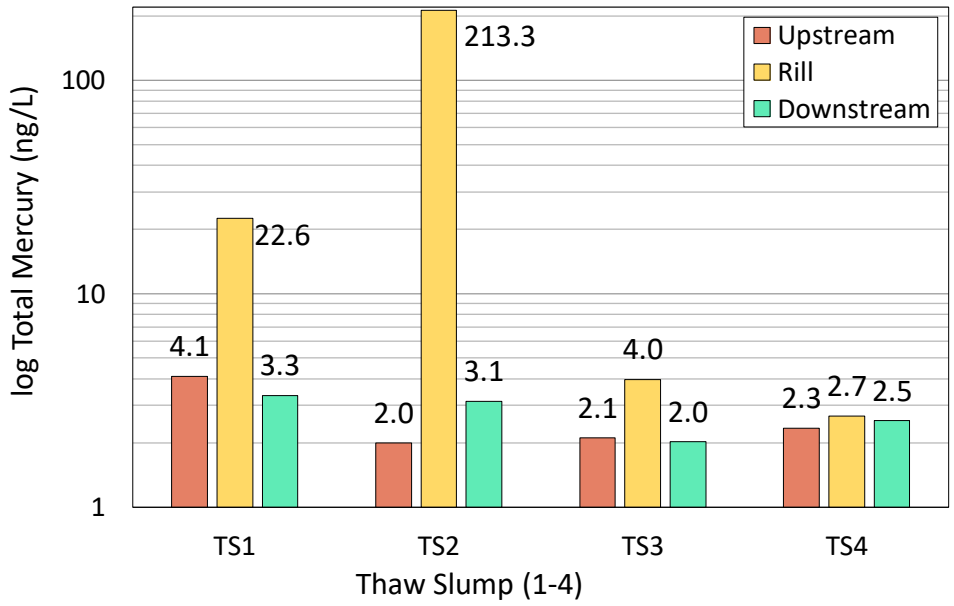

Figure 3.12. Total mercury concentration for thaw slump rill water and Old Crow River samples upstream and downstream of the sampled thaw slumps.

Active retrogressive thaw slump sediments were not enriched relative to aluminum concentrations in average upper continental crust (Wedepohl, 1995) (Table 3.3). For example, sediment mercury concentrations ranged from 45 – 115 µg/kg and were on average 1.6x and up

to ~3x enriched relative to upper continental crust (Wedepohl, 1995). We found negative correlations between organic content and contaminant concentration (THg vs LOI: r = –0.16; TPb vs LOI: r = –0.65) (Figure 3.13).

Table 3.3. Retrogressive Thaw Slump Sediment (active layer, in-situ ice rich sediment in the headwall, and thawed debris) mean concentration of elements, standard deviation, % lability in acid extracts, average concentration in the upper continental crust (Wedepohl, 1995), and enrichment factors calculated relative to Aluminum.

Parameter	Mean Concentration (ppm)	Stdev (ppm)	%Labile	%Labile Stdev	[UCC] Wedepohl (ppm)	Enrichment Factor (Al)
Hg	0.07	0.02	n/a	n/a	0.056	1.6
Na	3889.2	1895.0	2%	3%	25670	0.2
Mg	9143.1	3095.3	36%	17%	13510	0.9
Al	59408.7	24485.8	5%	3%	77440	1.0
P	985.1	200.3	49%	12%	665	1.9
K	17195.2	7899.6	2%	1%	28650	0.8
Ca	13153.8	5051.8	89%	13%	29450	0.6
Ti	3346.6	1391.2	0%	0%	3117	1.4
V	175.3	82.5	7%	3%	53	4.3
Cr	80.4	35.6	6%	2%	35	3.0
Fe	48833.2	16975.7	30%	9%	30890	2.1
Mn	362.1	71.5	67%	11%	527	0.9
Co	11.3	3.3	42%	14%	11.6	1.3
Ni	33.6	10.1	37%	12%	18.6	2.4
Cu	29.0	9.7	45%	10%	14.3	2.6
Ga	15.3	6.5	6%	2%	14	1.4
As	7.1	2.5	20%	9%	2	4.6
Se	1.6	0.4	23%	6%	0.083	24.3
Rb	96.2	39.1	2%	1%	110	1.1
Sr	122.6	21.5	33%	18%	316	0.5
Ag	0.6	0.2	8%	3%	0.055	14.8
Sn	1.9	0.8	1%	0%	2.5	1.0
Sb	0.9	0.3	4%	4%	0.31	4.0
Cs	6.0	2.8	1%	1%	5.8	1.4
Tl	0.7	0.3	6%	4%	0.75	1.2
Pb	16.3	5.6	55%	5%	17	1.3
Th	9.4	3.6	21%	12%	10.3	1.2
U	3.2	0.9	25%	6%	2.5	1.7

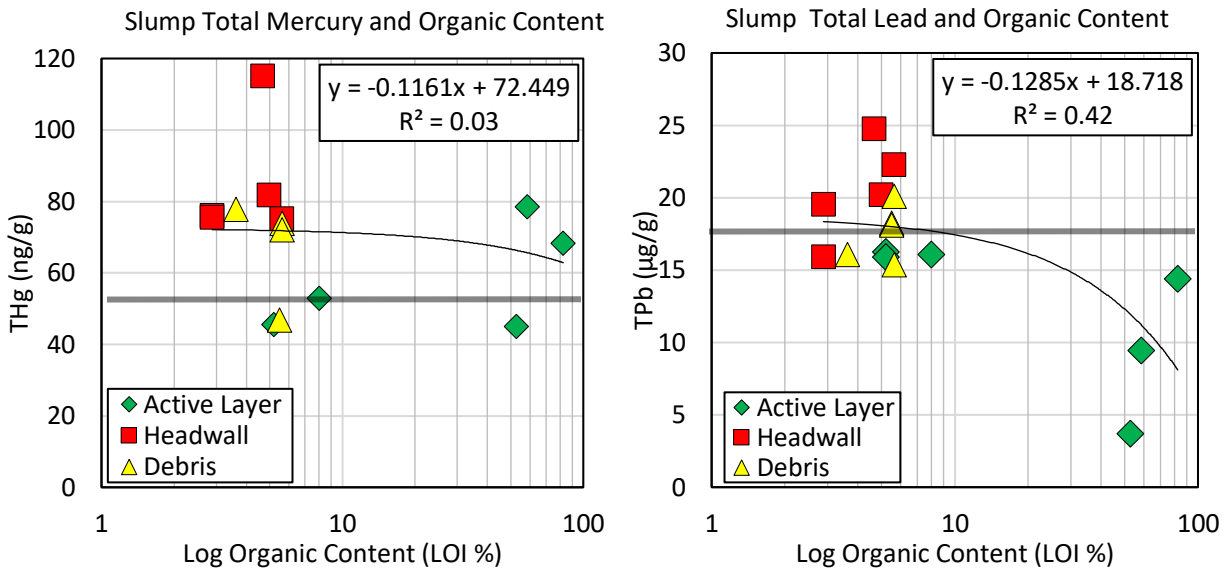

Figure 3.13. Active retrogressive thaw slump mercury and lead concentrations versus loss on ignition (black linear trendlines). Average upper continental crust composition (horizontal grey lines) (Wedepohl, 1995) for Hg and Pb.

3.5. Discussion

3.5.1. Contaminant Temporality

High contaminant concentrations and fluxes in the Old Crow River were seasonally linked to the spring snowmelt and autumn rainfall. These two seasons are characterized by increases in total suspended sediment concentrations during high and turbid discharge due to increased channel scouring and inputs associated with the flushing of the landscape. Open water season contaminant concentrations and fluxes were lowest during the period of peak-permafrost thaw (Figure 3.3) at the river mouth and tributaries, and active retrogressive thaw slumps did not substantially raise downstream contaminant concentrations (Figure 3.9). Overall, the annual flux and yield of contaminants was low and comparable to non-permafrost influenced watersheds (Table 3.4). The low contaminant concentrations during the period of peak-thaw, and low annual

contaminant fluxes and yields contrast work which implicates thawing permafrost as a crucial source of legacy contaminant trace elements (Schuster et al., 2011; Emmerton et al., 2013; Sonke et al., 2018; St. Pierre et al., 2018; Lim et al., 2019), and nutrients (Baron, Schmidt and Hartman, 2009; Barnes et al., 2014; Colombo et al., 2018, 2019; Brighenti et al., 2019) to downstream aquatic systems.

Old Crow River discharge is a strong predictor of total nutrient and trace element contaminant concentrations and yields (Figure 3.6; Figure 3.7; Table B.5). Measuring discharge and total contaminant concentrations during the spring freshet is critical for characterizing contaminant budgets in the Old Crow River and other arctic drainages. The one-month spring freshet (mid-May – mid-June) carried 44 % of the water yield for 2019 over 8.5 % of the year and an estimated 74 % of the total mercury yield. These results compare well with other arctic rivers where the freshet also controlled a large proportion (> 35 %) of contaminant flux (Holemann, Schirmacher and Prange, 2005; Schuster et al., 2011; Sonke et al., 2018; Zolkos et al., 2020). Rapid increases in discharge as snow melts lead to especially pronounced spring freshet in regions underlain by continuous permafrost due to the limited depth to which precipitation can infiltrate (Lafrenière and Lamoureux, 2019). This leads to a high proportion of overland flow compared to non-permafrost regions. As such, there is an increase in the hydrological connectivity of the land surface with the river system, in addition to increased channel scouring, which lead to high suspended sediment concentrations in the river.

Our observations are corroborated at the large watershed scale by Zolkos et al. (2020) who document that TSS and runoff (annual water volume normalized to watershed area) together explain a large proportion of variation ($R^2 = 0.97$) in arctic river mercury yields. Old Crow River water yield has roughly doubled over the last ~half century (Figure 3.4), with pronounced

increases in water yield during the spring freshet (Figure 3.5). Given the strong relation between total contaminant concentrations and mean-daily discharge, it is also likely that mercury and other contaminant fluxes and yields increased over that interval (Figure 3.8). The driving mechanism behind this increase in water yield and consequent contaminant yield is yet to be explored. Increases in moisture transport to northern regions (McClelland et al., 2004), and increased winter time precipitation are likely driving mechanisms. The Pacific Decadal Oscillation and sea-ice cover in the arctic are further drivers which are moderately correlated to the temporal patterns in Old Crow River water yield. Given that there were exceedances of CCME guidelines during the 2019 freshet, this foreshadows negative consequences for future water quality.

As climate warming leads to higher moisture transport to northern regions (McClelland et al., 2004; Douglas, Turetsky and Koven, 2020), freshet contaminant fluxes and yields may increase along with discharge and water yields. However, as permafrost degradation continues to deepen active layers (Lafrenière and Lamoureux, 2019), the strong correlation between discharge and contaminant concentration may decrease for the freshet interval, on account of the decreased overland flow. Simultaneously, the annual release of solutes through groundwater will increase as active layers deepen (Barnes et al., 2014; Toohey et al., 2016; Brighenti et al., 2019; Lafrenière and Lamoureux, 2019; Shogren et al., 2019). No research project has yet quantified the magnitude of these two inversely correlated factors on stream water chemistry contaminant concentrations.

3.5.2. Retrogressive Thaw Slump Impact on River Chemistry

Retrogressive thaw slumps and thermokarst have previously been implicated as significant input sources of labile mercury and nutrients to lake and river systems (Kokelj et al., 2013; Burke et al., 2018; St. Pierre et al., 2018). In the Peel River watershed in NWT, concentrations of mercury were as high as 1.2 µg/L in waters draining retrogressive thaw slumps, with high mercury concentrations persisting downstream for up to a kilometer (St. Pierre et al., 2018). In contrast, although total mercury concentrations were high (213 ng/L) in the debris flow rills at one of the thaw slumps along the Old Crow River, rill discharge was low (<0.001 m^3/s), and our study found no difference in mercury concentration upstream and downstream of thaw slumps. The difference in the downstream impact of thaw slumps in the Peel and Old Crow rivers is likely due to the difference in proportion between river discharge and thaw slump size at the two study locations. The St. Pierre et al. (2018) study was conducted along small headwater creek tributaries to the Peel River (instantaneous-discharge of 0.01 – 0.12 m^3/s); in some cases, the headwater creeks' retrogressive thaw slump debris even dammed the tributary flow. Old Crow River Mouth discharge during July was ~90 m^3/s, and thus rill input (< 0.001 m^3/s) was diluted by a factor of ~10^5. This suggests that the direct contribution of thawed material from the active retrogressive thaw slumps to the Old Crow River was much lower. Additionally, rill inputs were predominantly in the particulate phase, suggesting slump sediments have limited bioavailability, depending on turbulence and particle size, may settle out downstream.

Rather than being uniformly distributed across permafrost landscapes, thaw slumps in the Canadian Arctic are influenced strongly by Quaternary geology and are present at relatively high density in ice-rich terrain near former ice-sheet margins (Segal, Lantz and Kokelj, 2016).

Notably, in the Peel River watershed, retrogressive thaw slumps grow in size to "mega-slump" size (up to 10^6 m^3 volume of mobilized material, up to 0.4 km^2 basin area, and up to 25 m headwall height), and mobilize vast volumes of sediment (Kokelj et al., 2013). Thaw slumps along the Old Crow River are small in proportion to the river, there is no current evidence of mega-slumping, and retrogressive thaw slumps formed predominantly along cut banks in Pleistocene glaciolacustrine sediments (Zazula et al., 2004).

We hypothesized that the active layer peats at the thaw slump sample sites (Figure 3.2; Figure 3.13) would have higher concentrations of mercury than the thaw slump headwall ice-rich silts and thawed debris sediments, because arctic plants strongly uptake gaseous elemental mercury (Obrist et al., 2017). Recent work has used soil organic matter proxies to estimate mercury stocks in the northern hemisphere (Schuster et al., 2018; Lim et al., 2020). However, organic matter was not a strong predictor of contaminant concentration (e.g., mercury and lead; Figure 3.13). In fact, retrogressive thaw slump active layer peats, headwall ice-rich silt, and thawed debris sediment mercury concentrations (70.0 ± 20.0 µg/kg) were higher than peats from infilled thermokarst lake basins across the Old Crow Flats of 20.7 ± 9.8 µg/kg (Bandara, 2017).

3.5.3. Contaminant Source and Enrichment Factors

There are three competing explanations for the high enrichment factors observed in Old Crow River water samples: (a) high concentrations of legacy contaminants from organic-rich permafrost thaw are entering the waterway during via overland and active layer groundwater flow, (b) thermokarst lakes and wetlands, which cover 35% of the Old Crow Flats, contribute high proportions of dissolved and methylated contaminants to the river, or, (c) sediments derived

from naturally chalcophile-enriched shale bedrock in the northern reaches of the watershed and/or from shale-sourced glaciolacustrine deposits across the south and center of the watershed are entering the waterway via channel scouring.

In the Northwest Territories, hydrologically connected fens were shown to contain 4.5 – 14.5 times more dissolved methylmercury than hydrologically disconnected bogs (Gordon et al., 2016). Additionally, Burke et al. (2018) show that depositional fluxes of total mercury are higher in thermokarst lakes than in nearby lakes that are not affected by thermokarst processes. It has yet to be explored if snowmelt and precipitation facilitate direct hydrological linkage from thermokarst lakes and wetlands to the Old Crow River; such linkage would probably result in a contaminant load with methylated mercury and a substantial dissolved fraction. However, the strong association of contaminant concentration to total suspended sediment, and the low MeHg/THg ratio during high discharge seasons, suggest that thermokarst lake spillage does not contribute significantly to contaminant concentrations in the Old Crow River. Additionally, water sampled from Schaeffer and Surprise Creeks, which drain the central Old Crow Flats and have substantial thermokarst lake terrain (Table B.1), did not have elevated contaminant concentrations relative to other tributaries that were less affected by thermokarst processes.

The high concentrations of TFe in the Old Crow River throughout the year suggests that the Old Crow River source sediments are iron rich and therefore possibly sulphide rich. Sulphide-rich bedrock is typically rich in chalcophile elements, including the contaminants Sb, As, Cd, Cu, Hg, Pb, Se, and Zn. For example, in the Badlands along the Red Deer River in southwest Canada, concentrations of total Cd, Cu, Hg and Pb covaried closely with high suspended sediment concentrations (Kerr and Cooke, 2017). Additionally, suspended sediment explained a greater proportion of variance in contaminant concentrations than dissolved organic

carbon did; this suggests that flushing of the organic-rich land surface exerts a weaker control on contaminant concentration than channel scouring.

The likely source of contaminant trace elements in the Old Crow River Basin is the loose bluff materials lining the banks of this river, or the shale-source rocks in northern watershed. However, sediments at the four sampled active retrogressive thaw slumps did not have high enrichment factors. A close examination of sediment and peat trace element composition across the watershed may be conducted in the future to investigate this further.

3.5.4. Mercury Yield

Many researchers have suggested that permafrost-dominated river basins contribute substantial yields of mercury to the Arctic Ocean (e.g. Douglas et al., 2012; Fisher et al., 2012; Kirk et al., 2012; Stern et al., 2012; AMAP/UNEP, 2013; Sonke et al., 2018; Lim et al., 2019). Mercury yield (0.8 g/km^2/yr) from the Old Crow River basin, a pristine watershed entirely underlain by continuous permafrost, was substantially lower than the Yukon River (~75% permafrost cover (Schuster et al., 2011; Zolkos, et al., 2020)), and somewhat lower than the Mackenzie, Yenisey, Lena, and Kolyma rivers (respectively, 67%, 33-66%, 78-94%, and 100% permafrost cover (Emmerton et al., 2013; Sonke et al., 2018; Zolkos et al., 2020) (Table 3.4). Old Crow River's mercury yields are most comparable to watersheds with minimal permafrost cover including: Ob River which drains westernmost Russia (Sonke et al., 2018; Zolkos et al., 2020), and the North Saskatchewan, Churchill, and Nelson rivers in Canada (Kirk and St. Louis, 2009). A paucity of data prevents comparisons of other trace element yields in the Old Crow River to rivers in permafrost, glaciated, agricultural, or urbanized catchments.

Table 3.4. Total Mercury Yields at a range of physiographic and geographic locations

Watershed Identifier	Perma-frost Cover	Glacial Cover	Watershed Area (km^2)	Water Yield (km^3/yr)	Average Discharge (m^3/s)	Average THg concentration	THg-Yield ($g/km^2/yr$)	Source	Watershed Physiographic Description	Geographic Location
Old Crow	100%	-	13900	2.91	81	2.5	0.9	This Study	small arctic	Arctic, Canada
Kolyma	100%	-	530000	116*	3,500	9.7	2.1	Zolkos et al., 2020	large arctic	Arctic, Russia
Lena	78 – 94%	-	2430000	534*	16,500	10.6	2.7	Zolkos et al., 2020	large arctic	Arctic, Russia
Yukon	75%	1.1%	850000 830000	203*	6,500	10.6 14.9	5.17 4	Schuster et al., 2011 Zolkos et al., 2020	large arctic large arctic	Alaska, USA Arctic, USA
Mackenzie	67%	-	1680000 1780000	285*	9,000	9.0	1.6 1.3 – 2.4	Zolkos et al., 2020 Emmerton et al., 2013	large arctic	Arctic, Canada
Yenisey	33 – 66%	-	2400000	606*	19,500	6.5	1.5	Zolkos et al., 2020	large arctic	Arctic, Russia
Ob	4 – 18%	-	2990000	411*	12,500	5.6	0.8	Zolkos et al., 2020	large arctic	Arctic, Russia
Churchill	15 – 31%	-	281000	51	1,620	1.96	0.13	Kirk & St. Louis, 2009	large prairie	Arctic, Canada
Nelson	4 – 11%	-	892000	80	2,500	0.88	0.13	Kirk & St. Louis, 2009	large prairie	Arctic, Canada
N. Sask. At Edmonton	-	-	28100	7.5	238	1.5	0.4	Kirk & St. Louis, 2009	large prairie	Canadian Prairie
Peterson Creek	0%	-	25			5.6	3.0 – 6.0	Vermilyea et al., 2017	forested/ wetland	Coastal Alaska
various forested	0%	-	62 – 2630		-		0.87 – 4.36	Brigham, et al., 2009	forested	Ore., Wis., Fla., U.S.A.
various urban	0%	-	64 – 115		-		1.60 – 3.63	Brigham, et al., 2009	urban	Ore., Wis., Fla., U.S.A.
Sunwapta	-	70%	29.3	0.05	3.2	2.0	3.5 2.6 – 4.5	Staniszewska et al., this thesis	proglacial	Rockies, Canada
Lemon Creek	-	55%	32			2.3	19.9	Vermilyea et al., 2017	proglacial	Coastal Alaska
L. Hazen tributaries	100%	41%	7156	0.3 – 1.0	-	0.4	1.7 0.57 – 3.88	St. Pierre et al., 2019	proglacial	Arctic, Canada

Permafrost cover from Schuster et al., 2011, and Heslop et al., 2017; Yukon River Glacial coverage from Wada et al., 2011
*Water Yields from Sonke et al., 2018

The Yukon River has significantly higher mercury yields (Schuster et al., 2011; Zolkos et al., 2020) than the Old Crow River and five other large permafrost-influenced rivers draining into the Arctic Ocean (Ob, Yenisey, Lena, Kolyma, Mackenzie). The Old Crow River, a tributary to the Yukon River, had ~2.5 times lower mercury concentrations, ~6 times lower annual mercury yield, and a higher proportion of dissolved mercury (Schuster et al., 2011). Although Schuster et al. (2011) implicated thawing permafrost as a key driver of elevated mercury concentrations and yields in the Yukon River, our results suggest that thermokarst along the river course does not contribute significantly to mercury concentration or yield at a basin scale.

Numerous other physiographic and anthropogenic factors distinguish the Yukon River from these rivers. The Yukon River watershed is extensively glaciated, particularly in its headwater region of southwest Yukon (Brabets, Wang and Meade, 2000). Surficial sediments associated with glaciation are readily erodible, and thus currently and formerly glaciated basins have high sediment yields (Church and Ryder, 1972; Dornblaser and Striegl, 2009; Wada et al., 2011). For example, sediment yield is 670 times higher in glacierized tributaries than in forested and wetland tributaries to Tanana River, itself a tributary to the Yukon River (Wada et al., 2011) (Figure 3.14). The Porcupine River—which the Old Crow River is a direct tributary to—has a much lower suspended sediment yield relative to water yield, compared to both the glacier-influenced Tanana River and the lower Yukon River (Dornblaser and Striegl, 2009). Currently and previously glaciated catchments may therefore have higher contaminant yields primarily due to their high suspended sediment yields. Furthermore, while mercury concentration, flux and yield decrease during the summer months at the Old Crow River, they remain high at the Yukon River estuary, which suggests that glacial discharge drives the sediment (Chikita, Kemnitz and Kumai, 2002) and contaminant yield in the Yukon River basin. The total sediment yield of the

Yukon River (72.2 t/km^2/yr), however, cannot fully explain the difference in contaminant yield compared to, for example, the Mackenzie River (66.5 t/km^2/yr sediment yield) (Wada et al., 2011), unless glacier mobilized sediments in the Yukon River basin are more mercury rich than in the Mackenzie River basin where mercury yield is ~less than half that of the Yukon River (Zolkos et al., 2020).

The Upper Yukon River watershed also incorporates the Klondike Placer Gold Mining region where sediment yields are unnaturally elevated (Yukon Placer Secretariat, 2016), and where mercury was used during early placer gold mining (Willis, 1997). There are also several cinnabar (mercury-sulfide) deposits along the lower Yukon River (Malone, 1962). The Mackenzie River, likewise, is downstream of mining activities, namely the Athabasca Oil Sands Region upstream of Great Slave Lake. Watersheds in the Athabasca Oil Sands Region are accumulating mercury and may be an important source for downstream regions (Wasiuta et al., 2019). A further alternative mercury source for the Yukon River at its estuary may be related to wet- and dry-deposition of gaseous elemental mercury-rich air masses from across the Pacific Ocean (Dastoor et al., 2015). Near Juneau in southern Alaska, a small non-glaciated, non-permafrost, forested catchment also has high (3 – 6 g/km^2/yr) total mercury yield; and an adjacent glaciated catchment has a mercury yield of 19.9 g/km^2/yr (Vermilyea et al., 2017). These yields are extremely high relative to average mercury yields from rivers globally of < 3 g/km^2/yr (Domagalski et al., 2016). The downstream transport of mercury mobilized by mining activity and the impact of airmasses transported across the Pacific are yet to be quantified in the Yukon River.

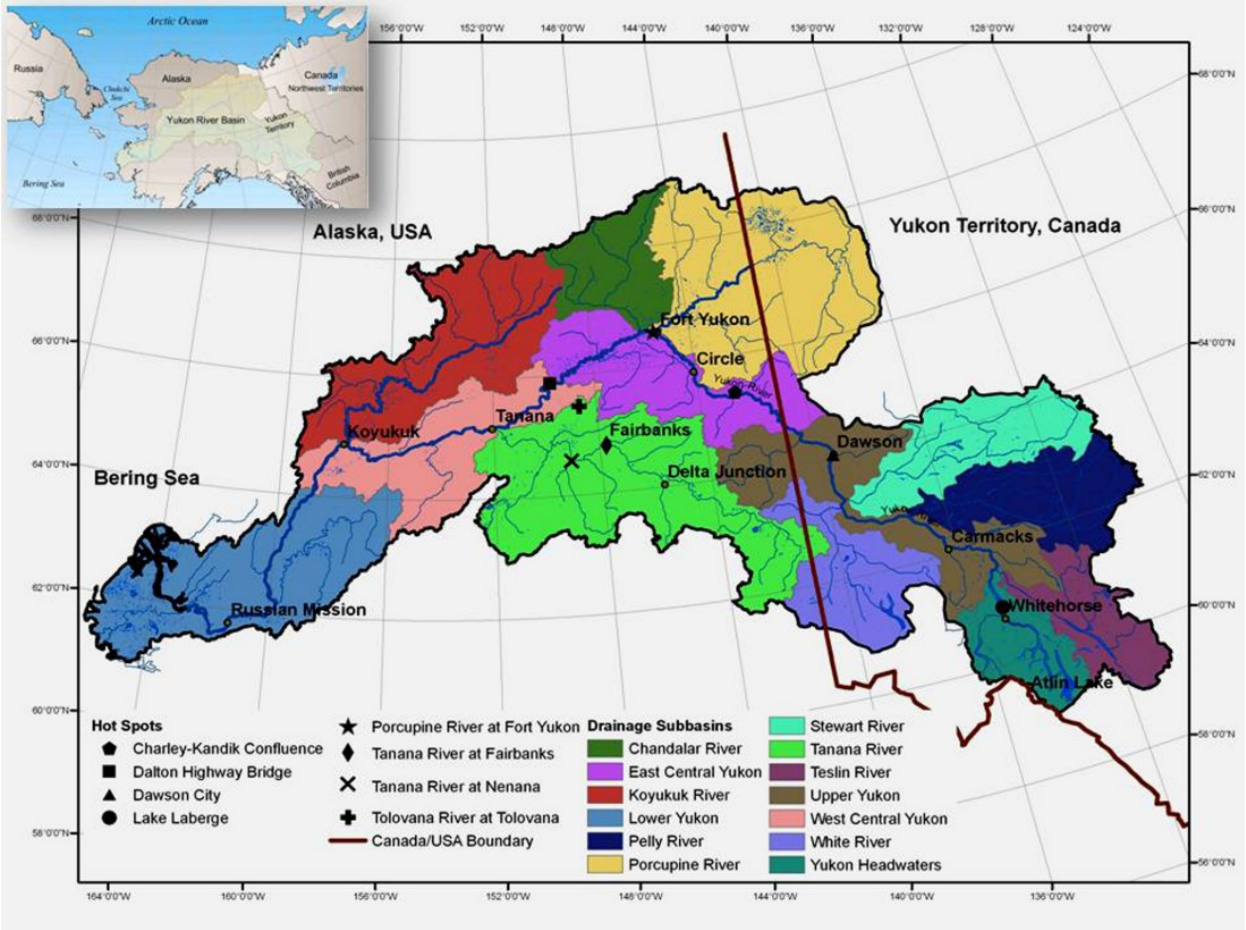

Figure 3.14. Sub-catchments of the Yukon River, from Dubé et al. (2013).

3.5.5. Conclusion

High temporal-resolution water chemistry records are seldom collected in remote arctic watersheds due to logistical considerations. We collected a high temporal-resolution (~weekly) record of a broad suite of water chemistry parameters in a pristine arctic watershed underlain by continuous permafrost. This high temporal-resolution record of water chemistry across the open water season reduces flux estimation uncertainty inherent to sampling parameters with a high degree of concentration variation (Kerr, Eimers and Yao, 2016), and reduces the potential to

miss short duration events such as the freshet (Holmes et al., 2012; Sonke et al., 2018) or high-flow events related to precipitation (Vermilyea et al., 2017). Additionally, the moderate sized watershed allowed the exclusion of certain confounding factors such as the influence of human land uses (Shogren et al., 2019).

We infer that suspended sediment mobilization by channel scouring during high discharge periods dominates contaminant fluxes in the Old Crow River. Thus, the principal factors to consider in the assessment of future contaminant fluxes in permafrost landscapes are those which contribute to strong freshet: the magnitudes of winter precipitation and spring air temperatures. The magnitude of annual precipitation is the next most important factor to consider as it drives high annual water yield. Freshet and baseflow measurements paired with long term discharge data records and climate-precipitation models should be investigated as tools for predicting future contaminant release from Arctic drainages.

3.6 References

AMAP/UNEP (2013) *Technical Background Report for the Global Mercury Assessment*, *Arctic Monitoring and Assessment Programme*. Oslo, Norway/UNEP Chemicals Branch, Geneva, Switzerland. doi: 10.1088/1751-8113/45/44/444010.

Anderton, I. (2004) *Porcupine River Watershed Fisheries Information Summary Report*. Whitehorse, YT.

Bandara, S. (2017) *Records of atmospheric mercury deposition and post-depositional mobility in peat permafrost archives from central and northern Yukon, Canada*, University of Alberta.

Barnes, R. T. *et al.* (2014) 'Thawing glacial and permafrost features contribute to nitrogen export from Green Lakes Valley, Colorado Front Range, USA', *Biogeochemistry*, 117, pp. 413–430. doi: 10.1007/s10533-013-9886-5.

Baron, J. S., Schmidt, T. M. and Hartman, M. D. (2009) 'Climate-induced changes in high elevation stream nitrate dynamics', *Global Change Biology*, 15, pp. 1777–1789. doi: 10.1111/j.1365-2486.2009.01847.x.

Bogdal, C. *et al.* (2010) 'Release of legacy pollutants from melting glaciers: Model evidence and conceptual understanding', *Environmental Science and Technology*, 44, pp. 4063–4069. doi: 10.1021/es903007h.

Brabets, T. P., Wang, B. and Meade, R. H. (2000) *Environmental and hydrologic overview of the Yukon River basin, Alaska and Canada*, *Water resources Investigations*. Anchorage, Alaska. doi: 10.3133/wri994204.

Brigham, M. E. *et al.* (2009) 'Mercury cycling in stream ecosystems. 1. Water column chemistry and transport', *Environmental Science and Technology*, 43, pp. 2720–2725. doi: 10.1021/es802694n.

Brighenti, S. *et al.* (2019) 'Ecosystem shifts in Alpine streams under glacier retreat and rock glacier thaw: A review', *Science of the Total Environment*, 675, pp. 542–559. doi: 10.1016/j.scitotenv.2019.04.221.

Brown, T. M. *et al.* (2018) 'The distribution and trends of persistent organic pollutants and mercury in marine mammals from Canada's Eastern Arctic', *Science of the Total Environment*, 618, pp. 500–517. doi: 10.1016/j.scitotenv.2017.11.052.

Burke, S. M. *et al.* (2018) 'Patterns and controls of mercury accumulation in sediments from three thermokarst lakes on the Arctic Coastal Plain of Alaska', *Aquatic Sciences*, 80, pp. 1–15. doi: 10.1007/s00027-017-0553-0.

Carling, G. T., Tingey, D. G. and Fernandez, D. P. (2013) 'Mercury and Other Trace Elements in Glacial Wyoming', *University of Wyoming National Park Service Research Center Annual Report*, 36, pp. 1–9.

Chikita, K. A., Kemnitz, R. and Kumai, R. (2002) 'Characteristics of sediment discharge in the subarctic Yukon River, Alaska', *Catena*, 48, pp. 235–253. doi:

10.1016/S0341-8162(02)00032-2.

Church, M. and Ryder, J. M. (1972) 'Paraglacial sedimentation: A consideration of fluvial processes conditioned by glaciation', *Bulletin of the Geological Society of America*, 83, pp. 3059–3072. doi: 10.1130/0016-7606.

Cole, A. S. *et al.* (2013) 'Ten-year trends of atmospheric mercury in the high Arctic compared to Canadian sub-Arctic and mid-latitude sites', *Atmospheric Chemistry and Physics*, 13, pp. 1535–1545. doi: 10.5194/acp-13-1535-2013.

Colombo, N. *et al.* (2018) 'Review : Impacts of permafrost degradation on inorganic chemistry of surface fresh water', *Global and Planetary Change*, 162, pp. 69–83. doi: 10.1016/j.gloplacha.2017.11.017.

Colombo, N. *et al.* (2019) 'Influence of permafrost, rock and ice glaciers on chemistry of high-elevation ponds (NW Italian Alps)', *Science of the Total Environment*, 685, pp. 886–901. doi: 10.1016/j.scitotenv.2019.06.233.

Connolly, C. T. *et al.* (2020) 'Groundwater as a major source of dissolved organic matter to Arctic coastal waters', *Nature communications*, 11, p. 1479. doi: 10.1038/s41467-020-15250-8.

Dastoor, A. *et al.* (2015) 'Atmospheric mercury in the Canadian Arctic. Part II : Insight from modeling', *Science of the Total Environment*, 509–510, pp. 16–27. doi: 10.1016/j.scitotenv.2014.10.112.

Domagalski, J. *et al.* (2016) 'Comparison of mercury mass loading in streams to atmospheric deposition in watersheds of Western North America: Evidence for non-atmospheric mercury sources', *Science of The Total Environment*, 568, pp. 638–650. doi: 10.1016/j.scitotenv.2016.02.112.

Donaldson, S. G. G. *et al.* (2010) 'Environmental contaminants and human health in the Canadian Arctic', *Science of The Total Environment*, 408, pp. 5165–5234. doi: 10.1016/j.scitotenv.2010.04.059.

Dornblaser, M. M. and Striegl, R. G. (2009) 'Suspended sediment and carbonate transport in the Yukon River Basin, Alaska: Fluxes and potential future responses to climate change', *Water Resources Research*, 45. doi: 10.1029/2008WR007546.

Douglas, T. A. *et al.* (2012) 'The fate of mercury in Arctic terrestrial and aquatic ecosystems, a review', *Environmental Chemistry*, 9, pp. 321–355. doi: 10.1071/EN11140.

Douglas, T. A., Turetsky, M. R. and Koven, C. D. (2020) 'Increased rainfall stimulates permafrost thaw across a variety of Interior Alaskan boreal ecosystems', *npj Climate and Atmospheric Science*, 3, pp. 1–7. doi: 10.1038/s41612-020-0130-4.

Dubé, M. G. *et al.* (2013) 'Accumulated state of the Yukon River watershed: Part I critical review of literature', *Integrated Environmental Assessment and Management*, 9, pp. 426–438. doi: 10.1002/ieam.1360.

Emmerton, C. A. *et al.* (2013) 'Mercury export to the Arctic Ocean from the Mackenzie River, Canada', *Environmental Science and Technology*, 47, pp. 7644–7654. doi: 10.1021/es400715r.

Environment and Climate Change Canada (2020) *Old Crow A - Canadian Climate Normals 1981-2010 Station Data - Climate - Environment and Climate Change Canada*. Available at: https://climate.weather.gc.ca/climate_normals/index_e.html (Accessed: 11 June 2020).

Van Everdingen, R. O. (1998) 'Glossary of Permafrost and Related Ground-Ice Terms', *Arctic and Alpine Research*, 21, p. 213. doi: 10.2307/1551636.

Fisher, J. A. *et al.* (2012) 'Riverine source of Arctic Ocean mercury inferred from atmospheric observations', *Nature Geoscience*, 5, pp. 499–504. doi: 10.1038/ngeo1478.

Frederick, J. M. *et al.* (2016) 'The Arctic Coastal Erosion Problem', *Sandia Report*. Albuquerque, New Mexico, SAND2016-9, p. 122.

Gao, L. *et al.* (2018) 'Yields and Characterization of Dissolved Organic Matter From Different Aged Soils in Northern Alaska', *Journal of Geophysical Research: Biogeosciences*, 123, pp. 2035–2052. doi: 10.1029/2018JG004408.

Gobeil, C., Tessier, A. and Couture, R. M. (2013) 'Upper Mississippi pb as a mid-1800s chronostratigraphic marker in sediments from seasonally anoxic lakes in eastern Canada', *Geochimica et Cosmochimica Acta*, 113, pp. 125–135. doi: 10.1016/j.gca.2013.02.023.

Gordon, J. *et al.* (2016) 'Mercury and methylmercury biogeochemistry in a thawing permafrost wetland complex, Northwest Territories, Canada', *Hydrological Processes*, 30, pp. 3627–3638. doi: 10.1002/hyp.10911.

Graney, J. R. *et al.* (1995) 'Long-term changes of mercury, lead and persistent organic pollutants in arctic environments', *Geochimica et Cosmochimica Acta*, 59, pp. 1715–1728. doi: 10.1007/s11270-006-3009-z.

Halbach, K. *et al.* (2017) 'The presence of mercury and other trace metals in surface soils in the Norwegian Arctic', *Chemosphere*, 188, pp. 567–574. doi: 10.1016/j.chemosphere.2017.09.012.

Holemann, J. A., Schirmacher, M. and Prange, A. (2005) 'Seasonal variability of trace metals in the Lena River and the southeastern Laptev Sea : Impact of the spring freshet', *Global and Planetary Change*, 48, pp. 112–125. doi: 10.1016/j.gloplacha.2004.12.008.

Holmes, R. M. *et al.* (2012) 'Seasonal and Annual Fluxes of Nutrients and Organic Matter from Large Rivers to the Arctic Ocean and Surrounding Seas', *Estuaries and Coasts*, 35, pp. 369–382. doi: 10.1007/s12237-011-9386-6.

Janowicz, J. R. (2017) 'Impacts of Climate Warming on River Ice Break-up and Snowmelt Freshet Processes on the Porcupine River in Northern Yukon', *CGU HS Committee on River Ice Processes and the Environment: 19th Workshop on the Hydraulics of Ice Covered Rivers*.

Kennedy, K. E. *et al.* (2010) 'Last Glacial Maximum age for the northwest Laurentide maximum from the Eagle River spillway and delta complex, northern Yukon', *Quaternary Science Reviews*, 29, pp. 1288–1300. doi: 10.1016/j.quascirev.2010.02.015.

Kerr, J. G. and Cooke, C. A. (2017) 'Erosion of the Alberta badlands produces highly variable and elevated heavy metal concentrations in the Red Deer River, Alberta', *Science of the Total Environment*, 596–597, pp. 427–436. doi: 10.1016/j.scitotenv.2017.04.037.

Kerr, J. G., Eimers, M. C. and Yao, H. (2016) 'Estimating stream solute loads from fixed frequency sampling regimes: The importance of considering multiple solutes and seasonal fluxes in the design of long-term stream monitoring networks', *Hydrological Processes*, 30, pp. 1521–1535. doi: 10.1002/hyp.10733.

Kirk, J. L. *et al.* (2012) 'Mercury in Arctic marine ecosystems: Sources, pathways and exposure', *Environmental Research*. Elsevier, 119, pp. 64–87. doi: 10.1016/j.envres.2012.08.012.

Kirk, J. L. and St. Louis, V. L. (2009) 'Multiyear total and methyl mercury exports from two major sub-arctic rivers draining into Hudson Bay, Canada', *Environmental Science and Technology*, 43, pp. 2254–2261. doi: 10.1021/es803138z.

Klaminder, J. *et al.* (2008) 'An explorative study of mercury export from a thawing palsa mire', *Journal of Geophysical Research: Biogeosciences*, 113, pp. 1–9. doi: 10.1029/2008JG000776.

Kokelj, S. V. *et al.* (2013) 'Thawing of massive ground ice in mega slumps drives increases in stream sediment and solute flux across a range of watershed scales', *Journal of Geophysical Research: Earth Surface*, 118, pp. 681–692. doi: 10.1002/jgrf.20063.

Koven, C. D., Riley, W. J. and Stern, A. (2013) 'Analysis of permafrost thermal dynamics and response to climate change in the CMIP5 earth system models', *Journal of Climate*, 26, pp. 1877–1900. doi: 10.1175/JCLI-D-12-00228.1.

Lafrenière, M. J. and Lamoureux, S. F. (2019) 'Effects of changing permafrost conditions on hydrological processes and fluvial fluxe', *Earth-Science Reviews*, 191, pp. 212–223. doi: 10.1016/j.earscirev.2019.02.018.

Lantuit, H. and Pollard, W. H. (2008) 'Fifty years of coastal erosion and retrogressive thaw slump activity on Herschel Island, southern Beaufort Sea, Yukon Territory, Canada', *Geomorphology*, 95, pp. 84–102. doi: 10.1016/j.geomorph.2006.07.040.

Lewkowicz, A. G. and Way, R. G. (2019) 'Extremes of summer climate trigger thousands of thermokarst landslides in a High Arctic environment', *Nature Communications*, 10, pp. 1–11. doi: 10.1038/s41467-019-09314-7.

Lim, A. G. *et al.* (2019) 'Enhanced particulate Hg export at the permafrost boundary, western Siberia', *Environmental Pollution*, 254, pp. 1–12. doi: 10.1016/j.envpol.2019.113083.

Lim, A. G. *et al.* (2020) 'A revised pan-Arctic permafrost soil Hg pool based on Western Siberian peat Hg and carbon observations', *Biogeosciences*, 17, pp. 3083–3097. doi: 10.5194/bg-17-3083-2020.

Malone, K. (1962) *Mercury Occurrences in Alaska*, *United States Department of the Interior Bureau of Mines*.

McClelland, J. W. *et al.* (2004) 'Increasing river discharge in the Eurasian Arctic: Consideration of dams, permafrost thaw, and fires as potential agents of change', *Journal of Geophysical Research Atmospheres*, 109, pp. 1–12. doi: 10.1029/2004JD004583.

Miner, K. R. *et al.* (2017) 'Legacy organochlorine pollutants in glacial watersheds: A review', *Environmental Science: Processes and Impacts*, 19, pp. 1474–1483. doi: 10.1039/c7em00393e.

Mu, C. *et al.* (2020) 'Permafrost degradation enhances the risk of mercury release on Qinghai-Tibetan Plateau', *Science of the Total Environment*, 708, pp. 1–8. doi: 10.1016/j.scitotenv.2019.135127.

Obrist, D. *et al.* (2017) 'Tundra uptake of atmospheric elemental mercury drives Arctic mercury pollution', *Nature*, 547, pp. 201–204. doi: 10.1038/nature22997.

Olson, C. *et al.* (2018) 'Mercury in Active-Layer Tundra Soils of Alaska: Concentrations, Pools, Origins, and Spatial Distribution', *Global Biogeochemical Cycles*, 32, pp. 1058–1073. doi: 10.1029/2017GB005840.

St. Pierre, K. A. *et al.* (2018) 'Unprecedented Increases in Total and Methyl Mercury Concentrations Downstream of Retrogressive Thaw Slumps in the Western Canadian Arctic', *Environmental Science and Technology*, 52, pp. 14099–14109. doi: 10.1021/acs.est.8b05348.

St. Pierre, K. A. *et al.* (2019) 'Drivers of Mercury Cycling in the Rapidly Changing Glacierized Watershed of the High Arctic's Largest Lake by Volume (Lake Hazen, Nunavut, Canada)', *Environmental Science and Technology*, 53, pp. 1175–1185. doi: 10.1021/acs.est.8b05926.

Pokrovsky, O. S. *et al.* (2016) 'Trace element transport in western Siberian rivers across a permafrost gradient', *Biogeosciences*, 13, pp. 1877–1900. doi: 10.5194/bg-13-1877-2016.

Pokrovsky, O. S. *et al.* (2018) 'Dissolved Organic Matter Controls Seasonal and Spatial Selenium Concentration Variability in Thaw Lakes across a Permafrost Gradient', *Environmental Science & Technology*, 52, pp. 10254–10262. doi: 10.1021/acs.est.8b00918.

Reyes, A. V., Froese, D. G. and Jensen, B. J. L. (2010) 'Permafrost response to last interglacial warming: Field evidence from non-glaciated Yukon and Alaska', *Quaternary Science Reviews*, 29, pp. 3256–3274. doi: 10.1016/j.quascirev.2010.07.013.

Schindler, D. W. and Smol, J. P. (2006) 'Cumulative effects of climate warming and other human activities on freshwaters of Arctic and subarctic North America', *Ambio*, 35, pp. 160–168. doi: 10.1579/0044-7447(2006)35.

Schuster, P. F. *et al.* (2011) 'Mercury export from the Yukon River Basin and potential response to a changing climate', *Environmental Science and Technology*, 45, pp. 9262–9267. doi: 10.1021/es202068b.

Schuster, P. F. *et al.* (2018) 'Permafrost Stores a Globally Significant Amount of Mercury', *Geophysical Research Letters*, 45, pp. 1463–1471. doi: 10.1002/2017GL075571.

Schuur, E. A. G. *et al.* (2009) 'The effect of permafrost thaw on old carbon release and net carbon exchange from tundra', *Nature Letters*, 459, pp. 556–559. doi: doi:10.1038/nature08031.

Schuur, E. A. G. *et al.* (2015) 'Climate change and the permafrost carbon feedback', *Nature Review*, 520, pp. 171–179. doi: 10.1038/nature14338.

Screen, J. A. and Simmonds, I. (2010) 'The central role of diminishing sea ice in recent Arctic temperature amplification', *Nature*, 464, pp. 1334–1337. doi: 10.1038/nature09051.

Segal, R. A., Lantz, T. C. and Kokelj, S. V (2016) 'Acceleration of thaw slump activity in glaciated landscapes of the Western Canadian Arctic', *Environmental Research Letters*, 11, p.

12. doi: 10.1088/1748-9326/11/3/034025.

Shogren, A. J. *et al.* (2019) 'Revealing biogeochemical signatures of Arctic landscapes with river chemistry', *Scientific Reports*, 9, pp. 1–11. doi: 10.1038/s41598-019-49296-6.

Sonke, J. E. *et al.* (2018) 'Eurasian river spring flood observations support net Arctic Ocean mercury export to the atmosphere and Atlantic Ocean', *Proceedings of the National Academy of Sciences of the United States of America*, 115, pp. E11586–E11594. doi: 10.1073/pnas.1811957115.

Stern, G. A. *et al.* (2012) 'How does climate change influence arctic mercury?', *Science of The Total Environment*, 414, pp. 22–42. doi: 10.1016/j.scitotenv.2011.10.039.

Tarnocai, C. (2009) 'The Impact of Climate Change on Canadian Peatlands', *Canadian Water Resources Journal*, 34, pp. 453–466. doi: 10.4296/cwrj3404453.

The Government of Canada, The Vuntut Gwitchin First Nation and The Government of the Yukon (1993) *Vuntut Gwitchin First Nation Final Agreement*. doi: 10.1017/CBO9781107415324.004.

Toohey, R. C. *et al.* (2016) 'Multidecadal increases in the Yukon River Basin of chemical fluxes as indicators of changing flowpaths, groundwater, and permafrost', *Geophysical Research Letters*, 43, pp. 12,120-12,130. doi: 10.1002/2016GL070817.

U.S. Environmental Protection Agency (1996) *Method 1669 Sampling Ambient Water for Trace Metals at EPA Water Quality Criteria Levels 20460*. Washington, D. C.

VanLooy, J. A. and Vandeberg, G. S. (2019) 'Late summer glacial meltwater contributions to Bull Lake Creek stream flow and water quality, Wind River Range, Wyoming, USA', *Physical Geography*, 40, pp. 461–480. doi: 10.1080/02723646.2019.1565215.

Vermilyea, A. W. *et al.* (2017) 'Continuous proxy measurements reveal large mercury fluxes from glacial and forested watersheds in Alaska', *Science of the Total Environment*, 599–600, pp. 145–155. doi: 10.1016/j.scitotenv.2017.03.297.

Wada, T. *et al.* (2011) 'Glacial effects on discharge and sediment load in the subarctic Tanana River Basin, Alaska', *Arctic, Antarctic, and Alpine Research*, 43, pp. 632–648. doi: 10.1657/1938-4246-43.4.632.

Wasiuta, V. *et al.* (2019) 'Accumulating Mercury and Methylmercury Burdens in Watersheds Impacted by Oil Sands Pollution', *Environmental Science and Technology*, 53, pp. 12856–12864. doi: 10.1021/acs.est.9b02373.

Wedepohl, H. K. (1995) 'The composition of the continental crust', *Geochimica et Cosmochimica Acta*, 59, pp. 1217–1232. doi: 10.1016/0016-7037(95)00038-2.

Willis, B. L. (1997) *The environmental effects of the Yukon Gold Rush, 1896-1906: Alterations to land, destruction of wildlife, and disease*. University of Western Ontario.

Yang, Z. *et al.* (2016) 'Warming increases methylmercury production in an Arctic soil', *Environmental Pollution*, 214, pp. 504–509. doi: 10.1016/j.envpol.2016.04.069.

Yukon Ecoregion Working Group (2004) 'Old Crow Flats', in Smith, C. A. S., Meikle, J. C., and

Roots, C. F. (eds) *Ecoregions of the Yukon Territory: Biophysical Properties of Yukon Landscapes*. Summerland, British Columbia: Minister of Supply and Services Canada, pp. 115–122.

Yukon Placer Secretariat (2016) *Water Quality Monitoring Annual Report Klondike Watershed 2016*.

Zazula, G. D. *et al.* (2004) 'Late Pleistocene chronology of glacial Lake Old Crow and the north west margin of the Laurentide Ice Sheet', *Quaternary Glaciations - Extent and Chronology, Part II*. Edited by J. Ehlers and P. L. Gibbard, pp. 347–362. doi: 10.1016/S1571-0866(04)80207-0..

Zhang, Y. *et al.* (2016) 'Observed decrease in atmospheric mercury explained by global decline in anthropogenic emissions', *Proceedings of the National Academy of Sciences of the United States of America*, 113, pp. 526–531. doi: 10.1073/pnas.1516312113.

Zolkos, S. *et al.* (2020) 'Mercury Export from Arctic Great Rivers', *Environmental Science and Technology*, 54, pp. 4140–4148. doi: 10.1021/acs.est.9b07145.

CHAPTER 4. Thesis Discussion

4.1. Conclusion

The primary goal of this thesis was to quantify the release of legacy contaminants from the cryosphere to downstream environments. I monitored and modeled nutrients and trace element hydrochemistry in proglacial Sunwapta River in the Rocky Mountains of Alberta, and along the Old Crow River in arctic Yukon. The results suggest these systems, and by extension other glaciers in the Canadian Rocky Mountains and other moderately sized Canadian Arctic watersheds underlain by continuous permafrost, release low concentrations and low annual fluxes (mass) and yields (mass normalized to watershed area) of legacy contaminants to downstream environments. An important contribution of this thesis research is a high temporal-resolution suite of nutrient, trace element, and major ion chemistry for two previously unstudied and remote watersheds. These datasets contributed to new understanding of the seasonality of glacial ice-melt and permafrost river hydrochemistry, and within-watershed variability of permafrost-dominated river hydrochemistry.

4.2. Summary

Nutrient and trace element priority pollutant concentrations have not previously been reported for glacier-fed streams in the Canadian Rocky Mountains. In Chapter Two I presented the first multi-year trace element and nutrient hydrochemistry profile from proglacial Sunwapta River in the Canadian Rocky Mountains. I found that contaminant concentrations were highest during peak melt (<2 ug/L (Pb, Cr, As) and <3.5 ng/L (Hg)) and more dilute during low flow.

Overall, contaminant concentrations and annual yields were low (<2.5 kg/km^2/yr (TCr); <1.7 kg/km^2/yr (TPb); <0.3 kg/km^2/yr (TAs); <4 g/km^2/yr (THg)), had low dynamic range, and were predominantly particle bound (>85% of total concentration). These results imply that the released contaminants are not bioavailable, are transient in river systems, and ultimately augment downstream sedimentary contaminant stocks. I tested if turbidity, recorded at high temporal resolution by sondes, could reliably model trace element concentrations. Although the modeled contaminant flux results were consistent with two flux estimates based on lower-resolution grab sample data, the regression models relating contaminant concentration to sonde turbidity did not meet tests for statistical significance and the consistency between flux estimates is likely due to the low contaminant concentrations. In contrast, weathering components derived from local geology were most dilute during peak melt, and most concentrated during low flow. We inferred that their source was subglacial melt. We were able to robustly model subglacial melt hydrochemistry at a high temporal resolution using conductivity recorded by sonde.

In Chapter Three I presented nutrient and trace element concentration data for the Old Crow River basin, a 13,900 km^2 watershed in arctic Yukon underlain by organic-rich continuous permafrost. I collected a uniquely high resolution (~weekly) and chemically broad grab-sample record at the outlet of this remote and undeveloped arctic watershed. I also collected water samples at eight tributary streams as well as up- and downstream of four active retrogressive thaw slumps across the watershed during the period of peak permafrost thaw. Concentrations of nutrient and trace element contaminants were high but particle-bound during the spring freshet, when snowmelt contributed to high water levels and high flow mobilized bank sediments. In contrast, contaminant concentrations and fluxes were lowest during the late summer during the period of peak permafrost thaw. Overall, contaminant concentrations were low and below

chronic water quality guidelines over the course of the year. I modeled the annual flux and yield of contaminants from river mouth using simple linear regression with daily discharge. Contaminant fluxes and yields are low. For example, the annual mercury yield was 0.8 g/km^2/yr, which is low and comparable to temperate natural streams (Shanley and Bishop, 2012; Domagalski et al., 2016; Vermilyea et al., 2017). Water chemistry was not contaminated downstream of four thaw slumps, and contaminant concentrations were low in all eight tributaries to the Old Crow River. Overall, the results suggest that thaw features, including thaw slumps and thermokarst lakes, do not significantly augment contaminant concentrations at the watershed scale, and that overall legacy contaminant concentrations may be low in fluvial systems located in continuous permafrost landscapes.

4.3. Future Work

Records of trace element contaminant fluxes and yields from rivers are rare, with the exception of mercury which has garnered substantial attention. Future studies of glacier and permafrost hydrochemistry should consider collecting more broad-parameter datasets to further characterize different anthropogenic impacts on the environment. This will allow comparison of cryosphere and non-cryosphere fluvial fluxes in future studies.

Future work should investigate and quantify the effect of climate perturbations on the release of legacy contaminants in glacier and permafrost connected watersheds. Climate change perturbations include: the timing and magnitude of precipitation and discharge, water source shifts, and increased flood risk, erosion, chemical weathering, permafrost thaw, and groundwater flow-path depths and magnitudes. For example, future work should quantify how thermal

permafrost degradation contributes solutes and contaminants through groundwater discharge to lotic and lentic aquatic ecosystems. In general, future research should focus further on the impact of cryosphere degradation to lentic aquatic systems which are more sensitive to long term and cumulative change, and where physical and chemical conditions promote methylation and eutrophication.

The strong control of discharge on trace element and nutrient concentrations and fluxes at the Sunwapta and Old Crow rivers allowed the use of long-term historic discharge data sets to model past, and predict future contaminant release. Precipitation and water yield trends do, however, vary regionally. Long term discharge records and models of precipitation should nevertheless be investigated for their potential to model contaminant release from other glacier and permafrost regions. Increases in moisture transport to northern regions (McClelland et al., 2004), and increased winter time precipitation are likely driving mechanisms behind increased water yield in permafrost regions, although sea ice cover, the Pacific Decadal Oscillation, and snow-land cover are further factors which should be considered. In glacierized catchments, peak water should be taken into consideration for modeling contaminant release.

The low yield of mercury in the Old Crow River, which is a tributary to the high-mercury-yield Yukon River (Schuster et al., 2011; Zolkos et al., 2020), highlights the need to investigate alternative—with respect to permafrost—point and regional sources of mercury input into the Yukon River. I recommend a project targeted at monitoring water quality downstream of alternative point sources of mercury input to the Yukon River. For example, downstream of the Klondike placer gold mining region in Yukon, downstream of non-placer ore mining operations in Alaska, downstream of Fairbanks, and along Tanana and White rivers which incorporate significant suspended sediment fluxes from glacial sediments. If the source is localized then

water quality management practices may be applied to reduce the mercury export documented at the Yukon River estuary (Schuster et al., 2011; Zolkos et al., 2020), and consequently reduce mercury supply to the Arctic Ocean (Fisher et al., 2012; Sonke et al., 2018).

4.4. References

Domagalski, J. *et al.* (2016) 'Comparison of mercury mass loading in streams to atmospheric deposition in watersheds of Western North America: Evidence for non-atmospheric mercury sources', *Science of The Total Environment*, 568, pp. 638–650. doi: 10.1016/j.scitotenv.2016.02.112.

Fisher, J. A. *et al.* (2012) 'Riverine source of Arctic Ocean mercury inferred from atmospheric observations', *Nature Geoscience*, 5, pp. 499–504. doi: 10.1038/ngeo1478.

McClelland, J. W. *et al.* (2004) 'Increasing river discharge in the Eurasian Arctic: Consideration of dams, permafrost thaw, and fires as potential agents of change', *Journal of Geophysical Research Atmospheres*, 109, pp. 1–12. doi: 10.1029/2004JD004583.

Schuster, P. F. *et al.* (2011) 'Mercury export from the Yukon River Basin and potential response to a changing climate', *Environmental Science and Technology*, 45, pp. 9262–9267. doi: 10.1021/es202068b.

Shanley, J. B. and Bishop, K. (2012) 'Mercury in the Environment : Pattern and Process: Part 3', in Bank, M. S. (ed.) *Mercury in the Environment : Pattern and Process*. 1st edn. University of California Press, pp. 99–196. doi: 10.1525/california/9780520271630.001.0001.

Sonke, J. E. *et al.* (2018) 'Eurasian river spring flood observations support net Arctic Ocean mercury export to the atmosphere and Atlantic Ocean', *Proceedings of the National Academy of Sciences of the United States of America*, 115, pp. E11586–E11594. doi: 10.1073/pnas.1811957115.

Vermilyea, A. W. *et al.* (2017) 'Continuous proxy measurements reveal large mercury fluxes from glacial and forested watersheds in Alaska', *Science of the Total Environment*, 599–600, pp. 145–155. doi: 10.1016/j.scitotenv.2017.03.297.

Zolkos, S. *et al.* (2020) 'Mercury Export from Arctic Great Rivers', *Environmental Science & Technology*, 54, pp. 4140–4148. doi: 10.1021/acs.est.9b07145.

BIBLIOGRAPHY

AMAP/UNEP (2013) *Technical Background Report for the Global Mercury Assessment*, *Arctic Monitoring and Assessment Programme*. Oslo, Norway/UNEP Chemicals Branch, Geneva, Switzerland. doi: 10.1088/1751-8113/45/44/444010.

Amos, H. M. *et al.* (2014) 'Global Biogeochemical Implications of Mercury Discharges from Rivers and Sediment Burial', *Environmental Science and Technology*, 48, pp. 9514–9522. doi: 10.1021/es502134t.

Anderton, I. (2004) *Porcupine River Watershed Fisheries Information Summary Report*. Whitehorse, YT.

Andrews, T. D. *et al.* (2016) 'Permafrost Thaw and Aboriginal Cultural Landscapes in the Gwich'in Region, Canada', *Journal of Preservation Technology*, 47, 15–22. doi: 10.1017/CBO9781107415324.004.

Arendt, C. A., Aciego, S. M. and Hetland, E. A. (2015) 'An open source Bayesian Monte Carlo isotope mixing model with applications in Earth surface processes', *AGU*, 16, pp. 267–300. doi: 10.1002/2014GC005684.Key.

Arendt, C. A., Stevenson, E. I. and Aciego, S. M. (2016) 'Hydrologic controls on radiogenic Sr in meltwater from an alpine glacier system: Athabasca Glacier, Canada', *Applied Geochemistry*, 69, pp. 42–49. doi: 10.1016/j.apgeochem.2016.04.002.

Bandara, S. (2017) *Records of atmospheric mercury deposition and post-depositional mobility in peat permafrost archives from central and northern Yukon, Canada*, *University of Alberta*.

Barbante, C. *et al.* (2004) 'Historical record of European emissions of heavy metals to the atmosphere since the 1650s from alpine snow/ice cores drilled near Monte Rosa', *Environmental Science and Technology*, 38, pp. 4085–4090. doi: 10.1021/es049759r.

Barnes, R. T. *et al.* (2014) 'Thawing glacial and permafrost features contribute to nitrogen export from Green Lakes Valley, Colorado Front Range, USA', *Biogeochemistry*, 117, pp. 413–430. doi: 10.1007/s10533-013-9886-5.

Baron, J. S., Schmidt, T. M. and Hartman, M. D. (2009) 'Climate-induced changes in high elevation stream nitrate dynamics', *Global Change Biology*, 15, pp. 1777–1789. doi: 10.1111/j.1365-2486.2009.01847.x.

Beal, S. A. *et al.* (2015) 'Ice Core Perspective on Mercury Pollution during the Past 600 Years', *Environmental Science and Technology*, 49, pp. 7641–7647. doi: 10.1021/acs.est.5b01033.

Blais, J. M., Schindler, D. W., Muir, D. C. G., *et al.* (2001) 'Melting Glaciers: A Major Source of Persistent Organochlorines to Subalpine Bow Lake in Banff National Park, Canada', *AMBIO: A Journal of the Human Environment*, 30, pp. 410–415. doi: 10.1579/0044-7447-30.7.410.

Bogdal, C. *et al.* (2010) 'Release of legacy pollutants from melting glaciers: Model evidence and conceptual understanding', *Environmental Science and Technology*, 44, pp. 4063–4069. doi: 10.1021/es903007h.

Bolch, T., Menounos, B. and Wheate, R. (2010) 'Landsat-based inventory of glaciers in western Canada, 1985-2005', *Remote Sensing of Environment*, 114, pp. 127–137. doi: 10.1016/j.rse.2009.08.015.

Brabets, T. P., Wang, B. and Meade, R. H. (2000) *Environmental and hydrologic overview of the Yukon River basin, Alaska and Canada*, *Water resources Investigations*. Anchorage, Alaska. doi: 10.3133/wri994204.

Brahney, J., N. *et al.* (2015) 'Global Biogeochemical Cycles: The nitrogen cycle', *Global Biogeochemical Cycles*, 29, pp. 1369–1383. doi: 10.1002/2015GB005137.

Brahney, J., *et al.* (2017) 'Evidence for a climate-driven hydrologic regime shift in the Canadian Columbia Basin', *Canadian Water Resources Journal*, 42, pp. 179–192. doi: 10.1080/07011784.2016.1268933.

Brigham, M. E. *et al.* (2009) 'Mercury cycling in stream ecosystems. 1. Water column chemistry and transport', *Environmental Science and Technology*, 43, pp. 2720–2725. doi: 10.1021/es802694n.

Brighenti, S. *et al.* (2019) 'Ecosystem shifts in Alpine streams under glacier retreat and rock glacier thaw: A review', *Science of the Total Environment*, 675, pp. 542–559. doi: 10.1016/j.scitotenv.2019.04.221.

Brown, T. M. *et al.* (2018) 'The distribution and trends of persistent organic pollutants and mercury in marine mammals from Canada's Eastern Arctic', *Science of the Total Environment*, 618, pp. 500–517. doi: 10.1016/j.scitotenv.2017.11.052.

Burke, S. M. *et al.* (2018) 'Patterns and controls of mercury accumulation in sediments from three thermokarst lakes on the Arctic Coastal Plain of Alaska', *Aquatic Sciences*, 80, pp. 1–15. doi: 10.1007/s00027-017-0553-0.

Canadian Council of Ministers of the Environment (2019) 'Canadian Environmental Quality Guidelines for the Protection of Aquatic Life', pp. 1–26.

Canil, D. and Lacourse, T. (2011) 'An estimate for the bulk composition of juvenile upper continental crust derived from glacial till in the North American Cordillera', *Chemical Geology*, 284, pp. 229–239. doi: 10.1016/j.chemgeo.2011.02.024.

Carling, G. T. *et al.* (2017) 'Effect of Atmospheric Deposition and Weathering on Trace Element Concentrations in Glacial Meltwater at Grand Teton National Park, Wyoming, U.S.A.', *Arctic, Antarctic, and Alpine Research*, 49, pp. 427–440. doi: 10.1657/AAAR0016.071.

Carling, G. T., Tingey, D. G. and Fernandez, D. P. (2013) 'Mercury and Other Trace Elements in Glacial Wyoming', *University of Wyoming National Park Service Research Center Annual Report*, 36, pp. 1–9.

Chikita, K. A., Kemnitz, R. and Kumai, R. (2002) 'Characteristics of sediment discharge in the subarctic Yukon River, Alaska', *Catena*, 48, pp. 235–253. doi: 10.1016/S0341-8162(02)00032-2.

Church, M. and Ryder, J. M. (1972) 'Paraglacial sedimentation: A consideration of fluvial processes conditioned by glaciation', *Bulletin of the Geological Society of America*, 83, pp.

3059–3072. doi: 10.1130/0016-7606.

Clarke, G. K. C. C. *et al.* (2015) 'Projected deglaciation of western Canada in the twenty-first century', *Nature Geoscience*, 8, pp. 372–377. doi: 10.1038/ngeo2407.

Clinger, A. E. *et al.* (2016) 'Implications for post-comminution processes in subglacial suspended sediment using coupled radiogenic strontium and neodymium isotopes', *Geomorphology*, 259, pp. 134–144. doi: 10.1016/j.geomorph.2016.02.006.

Cole, A. S. *et al.* (2013) 'Ten-year trends of atmospheric mercury in the high Arctic compared to Canadian sub-Arctic and mid-latitude sites', *Atmospheric Chemistry and Physics*, 13, pp. 1535–1545. doi: 10.5194/acp-13-1535-2013.

Colombo, N. *et al.* (2018) 'Review : Impacts of permafrost degradation on inorganic chemistry of surface fresh water', *Global and Planetary Change*, 162, pp. 69–83. doi: 10.1016/j.gloplacha.2017.11.017.

Colombo, N. *et al.* (2019) 'Influence of permafrost, rock and ice glaciers on chemistry of high-elevation ponds (NW Italian Alps)', *Science of the Total Environment*, 685, pp. 886–901. doi: 10.1016/j.scitotenv.2019.06.233.

Connolly, C. T. *et al.* (2020) 'Groundwater as a major source of dissolved organic matter to Arctic coastal waters', *Nature communications*, 11, p. 1479. doi: 10.1038/s41467-020-15250-8.

Dastoor, A. *et al.* (2015) 'Atmospheric mercury in the Canadian Arctic. Part II : Insight from modeling', *Science of the Total Environment*, 509–510, pp. 16–27. doi: 10.1016/j.scitotenv.2014.10.112.

Domagalski, J., *et al.* (2016) 'Comparison of mercury mass loading in streams to atmospheric deposition in watersheds of Western North America: Evidence for non-atmospheric mercury sources', *Science of The Total Environment*, 568, pp. 638–650. doi: 10.1016/j.scitotenv.2016.02.112.

Donaldson, S. G. G. *et al.* (2010) 'Environmental contaminants and human health in the Canadian Arctic', *Science of The Total Environment*, 408, pp. 5165–5234. doi: 10.1016/j.scitotenv.2010.04.059.

Dornblaser, M. M. and Striegl, R. G. (2009) 'Suspended sediment and carbonate transport in the Yukon River Basin, Alaska: Fluxes and potential future responses to climate change', *Water Resources Research*, 45. doi: 10.1029/2008WR007546.

Douglas, T. A. *et al.* (2012) 'The fate of mercury in Arctic terrestrial and aquatic ecosystems, a review', *Environmental Chemistry*, 9, pp. 321–355. doi: 10.1071/EN11140.

Douglas, T. A., Turetsky, M. R. and Koven, C. D. (2020) 'Increased rainfall stimulates permafrost thaw across a variety of Interior Alaskan boreal ecosystems', *npj Climate and Atmospheric Science*, 3, pp. 1–7. doi: 10.1038/s41612-020-0130-4.

Drevnick, P. E. *et al.* (2016) 'Spatiotemporal patterns of mercury accumulation in lake sediments of western North America', *Science of the Total Environment*, 568, pp. 1157–1170. doi: 10.1016/j.scitotenv.2016.03.167.

Dubé, M. G. *et al.* (2013) 'Accumulated state of the Yukon River watershed: Part I critical review of literature', *Integrated Environmental Assessment and Management*, 9, pp. 426–438. doi: 10.1002/ieam.1360.

Dudka, S. and Adriano, D. C. (2010) 'Environmental Impacts of Metal Ore Mining and Processing: A Review', *Journal of Environment Quality*, 26, pp. 590–602. doi: 10.2134/jeq1997.00472425002600030003x.

Eagles-Smith, C. A. *et al.* (2016) 'Spatial and temporal patterns of mercury concentrations in freshwater fish across the Western United States and Canada', *Science of the Total Environment*, 568, pp. 1171–1184. doi: 10.1016/j.scitotenv.2016.03.229.

Ednie, M., Demuth, M. N. and Shepherd, B. (2017) *The mass balance of the Athabasca and Saskatchewan sectors of the Columbia Icefield, Alberta for 2015 and 2016*, *Geological Survey of Canada Open File 8228*. doi: doi.org/10.4095/302705.

Eichler, A. *et al.* (2012) 'Three centuries of Eastern European and Altai lead emissions recorded in a Belukha ice core', *Environmental Science and Technology*, 46, pp. 4323–4330. doi: 10.1021/es2039954.

Emmerton, C. A. *et al.* (2013) 'Mercury export to the Arctic Ocean from the Mackenzie River, Canada', *Environmental Science and Technology*, 47, pp. 7644–7654. doi: 10.1021/es400715r.

Environment and Climate Change Canada (2020) *Old Crow A - Canadian Climate Normals 1981-2010 Station Data - Climate - Environment and Climate Change Canada*. Available at: https://climate.weather.gc.ca/climate_normals/index_e.html (Accessed: 11 June 2020).

Environment and Climate Change Canada (2020) *Hourly Data Report - Climate*. Available at: https://climate.weather.gc.ca/historical_data/search_historic_data_e.html (Accessed: 28 April 2020).

Van Everdingen, R. O. (1998) 'Glossary of Permafrost and Related Ground-Ice Terms', *Arctic and Alpine Research*, 21, p. 213. doi: 10.2307/1551636.

Ferrario, C., Finizio, A. and Villa, S. (2017) 'Legacy and emerging contaminants in meltwater of three Alpine glaciers', *Science of the Total Environment*, 574, pp. 350–357. doi: 10.1016/j.scitotenv.2016.09.067.

Fisher, J. A. *et al.* (2012) 'Riverine source of Arctic Ocean mercury inferred from atmospheric observations', *Nature Geoscience*, 5, pp. 499–504. doi: 10.1038/ngeo1478.

Fitzgerald, W. F. *et al.* (2005) 'Modern and historic atmospheric mercury fluxes in northern Alaska: Global sources and arctic depletion', *Environmental Science and Technology*, 39, pp. 557–568. doi: 10.1021/es049128x.

Frederick, J. M. *et al.* (2016) 'The Arctic Coastal Erosion Problem', *Sandia Report*. Albuquerque, New Mexico, SAND2016-9, p. 122.

Gagnon, C. and Fisher, N. S. (1997) 'Bioavailability of sediment-bound methyl and inorganic mercury to a marine bivalve', *Environmental Science and Technology*, 31, pp. 993–998. doi: 10.1021/es960364k.

Gao, L. *et al.* (2018) 'Yields and Characterization of Dissolved Organic Matter From Different Aged Soils in Northern Alaska', *Journal of Geophysical Research: Biogeosciences*, 123, pp. 2035–2052. doi: 10.1029/2018JG004408.

Geisz, H. N. *et al.* (2008) 'Melting glaciers: A probable source of DDT to the Antarctic marine ecosystem', *Environmental Science and Technology*, 42, pp. 3958–3962. doi: 10.1021/es702919n.

Gilbert, R. and Shaw, J. (1981) 'Sedimentation in proglacial Sunwapta Lake, Alberta', *Canadian Journal of Earth Sciences*, 18, pp. 81–93. doi: 10.1139/e81-007.

Gobeil, C., Tessier, A. and Couture, R. M. (2013) 'Upper Mississippi pb as a mid-1800s chronostratigraphic marker in sediments from seasonally anoxic lakes in eastern Canada', *Geochimica et Cosmochimica Acta*, 113, pp. 125–135. doi: 10.1016/j.gca.2013.02.023.

González-Alonso, S. *et al.* (2017) 'Occurrence of pharmaceutical, recreational and psychotropic drug residues in surface water on the northern Antarctic Peninsula region', *Environmental Pollution*, 229, pp. 241–254. doi: 10.1016/j.envpol.2017.05.060.

Gordon, J. *et al.* (2016) 'Mercury and methylmercury biogeochemistry in a thawing permafrost wetland complex, Northwest Territories, Canada', *Hydrological Processes*, 30, pp. 3627–3638. doi: 10.1002/hyp.10911.

Graney, J. R. *et al.* (1995) 'Long-term changes of mercury, lead and persistent organic pollutants in arctic environments', *Geochimica et Cosmochimica Acta*, 59, pp. 1715–1728. doi: 10.1007/s11270-006-3009-z.

Green, P. A. *et al.* (2004) 'Pre-industrial and contemporary fluxes of nitrogen through rivers: A global assessment based on typology', *Biogeochemistry*, 68, pp. 71–105. doi: 10.1023/B:BIOG.0000025742.82155.92.

Halbach, K. *et al.* (2017) 'The presence of mercury and other trace metals in surface soils in the Norwegian Arctic', *Chemosphere*, 188, pp. 567–574. doi: 10.1016/j.chemosphere.2017.09.012.

Hammerschmidt, C. R. (2011) 'Mercury and carbon dioxide emissions: Uncoupling a toxic relationship', *Environmental Toxicology and Chemistry*, 30, pp. 2640–2646. doi: 10.1002/etc.702.

Hart, J. K. (2006) 'Athabasca Glacier, Canada - A field example of subglacial ice and till erosion?', *Earth Surface Processes and Landforms*, 31, pp. 65–80. doi: 10.1002/esp.1233.

Heath, J. and Baron, J. S. (2014) 'Climate, Not Atmospheric Deposition, Drives the Biogeochemical Mass-Balance of a Mountain Watershed', *Aquatic Geochemistry*, 20, pp. 167–181. doi: 10.1007/s10498-013-9199-2.

Hobbs, W. O., Vinebrooke, R. D. and Wolfe, A. P. (2011) 'Biogeochemical responses of two alpine lakes to climate change and atmospheric deposition, Jasper and Banff national parks, Canadian rocky mountains', *Canadian Journal of Fisheries and Aquatic Sciences*, 68, pp. 1480–1494. doi: 10.1139/f2011-058.

Holemann, J. A., Schirmacher, M. and Prange, A. (2005) 'Seasonal variability of trace metals in the Lena River and the southeastern Laptev Sea : Impact of the spring freshet', *Global and*

Planetary Change, 48, pp. 112–125. doi: 10.1016/j.gloplacha.2004.12.008.

Holmes, R. M. *et al.* (2012) 'Seasonal and Annual Fluxes of Nutrients and Organic Matter from Large Rivers to the Arctic Ocean and Surrounding Seas', *Estuaries and Coasts*, 35, pp. 369–382. doi: 10.1007/s12237-011-9386-6.

Holtgrieve, G. W. *et al.* (2011) 'A coherent signature of anthropogenic nitrogen deposition to remote watersheds of the Northern Hemisphere', *Science*, 334, pp. 1545–1548. doi: 10.1126/science.1212267.

Horowitz, H. M. *et al.* (2014) 'Historical Mercury Releases from Commercial Products: Global Environmental Implications', *Environmental Science & Technology*, 48, pp. 10242−10250. doi: dx.doi.org/10.1021/es501337j.

Huang, J. *et al.* (2015) 'Characterizations of wet mercury deposition on a remote high-elevation site in the southeastern Tibetan Plateau', *Environmental Pollution*, 206, pp. 518–526. doi: 10.1016/j.envpol.2015.07.024.

Hurley, J. P. *et al.* (1995) 'Influences of Watershed Characteristics on Mercury Levels in Wisconsin Rivers', *Environmental Science and Technology*, 29, pp. 1867–1875. doi: 10.1021/es00007a026.

Huss, M. and Hock, R. (2018) 'Global-scale hydrological response to future glacier mass loss', *Nature Climate Change*, 8, pp. 135–140. doi: 10.1038/s41558-017-0049-x.

IPCC (2013) *IPCC, 2013: Climate Change 2013: The Physical Science Basis. Contribution of Working Group I to the Fifth Assessment Report of the Intergovernmental Panel on Climate Change*, *the Fifth Assessment Report*. Stocker T.F. et al. (eds), Cambridge, United Kingdom and New York, NY, USA: Cambridge University Press.

Janowicz, J. R. (2017) 'Impacts of Climate Warming on River Ice Break-up and Snowmelt Freshet Processes on the Porcupine River in Northern Yukon', *CGU HS Committee on River Ice Processes and the Environment: 19th Workshop on the Hydraulics of Ice Covered Rivers*.

Järup, L. (2003) 'Hazards of heavy metal contamination', *British Medical Bulletin*, 68, pp. 167–182. doi: 10.1093/bmb/ldg032.

Kennedy, K. E. *et al.* (2010) 'Last Glacial Maximum age for the northwest Laurentide maximum from the Eagle River spillway and delta complex, northern Yukon', *Quaternary Science Reviews*, 29, pp. 1288–1300. doi: 10.1016/j.quascirev.2010.02.015.

Kerr, J. G. and Cooke, C. A. (2017) 'Erosion of the Alberta badlands produces highly variable and elevated heavy metal concentrations in the Red Deer River, Alberta', *Science of the Total Environment*, 596–597, pp. 427–436. doi: 10.1016/j.scitotenv.2017.04.037.

Kerr, J. G., Eimers, M. C. and Yao, H. (2016) 'Estimating stream solute loads from fixed frequency sampling regimes: The importance of considering multiple solutes and seasonal fluxes in the design of long-term stream monitoring networks', *Hydrological Processes*, 30, pp. 1521–1535. doi: 10.1002/hyp.10733.

Kidd, K., Clayden, M. and Jardine, T. (2012) 'Part IV Bioaccumulation, Toxicity, and Metallomics; Chapter 14. Bioaccumulation and Biomagnification of Mercury Through Food

Webs', in Liu, G., Cai, Y., and O'Driscoll, N. (eds) *Environmental Chemistry and Toxicology of Mercury*. 1st edn. John Wiley & Sons, Inc.

Kirk, J. L. *et al.* (2012) 'Mercury in Arctic marine ecosystems: Sources, pathways and exposure', *Environmental Research*. Elsevier, 119, pp. 64–87. doi: 10.1016/j.envres.2012.08.012.

Kirk, J. L. and St. Louis, V. L. (2009) 'Multiyear total and methyl mercury exports from two major sub-arctic rivers draining into Hudson Bay, Canada', *Environmental Science and Technology*, 43, pp. 2254–2261. doi: 10.1021/es803138z.

Klaminder, J. *et al.* (2008) 'An explorative study of mercury export from a thawing palsa mire', *Journal of Geophysical Research: Biogeosciences*, 113, pp. 1–9. doi: 10.1029/2008JG000776.

Kneib, M. *et al.* (2020) 'Glacier retreat changes diurnal variation intensity and frequency of hydrologic variables in Alpine and Andean streams', *Journal of Hydrology*, 583, pp. 1–11. doi: 10.1016/j.jhydrol.2020.124578.

Kokelj, S. V. *et al.* (2013) 'Thawing of massive ground ice in mega slumps drives increases in stream sediment and solute flux across a range of watershed scales', *Journal of Geophysical Research: Earth Surface*, 118, pp. 681–692. doi: 10.1002/jgrf.20063.

Koven, C. D., Riley, W. J. and Stern, A. (2013) 'Analysis of permafrost thermal dynamics and response to climate change in the CMIP5 earth system models', *Journal of Climate*, 26, pp. 1877–1900. doi: 10.1175/JCLI-D-12-00228.1.

Laceby, J. P. *et al.* (2019) *Investigation of quality control data from Alberta's lotic water monitoring program, 2016-18.*, *In Press*.

Lafrenière, M. J. *et al.* (2006) 'Organochlorine pesticide and polychlorinated biphenyl concentrations in snow, snowmelt, and runoff at Bow Lake, Alberta', *Environmental Science and Technology*, 40, pp. 4909–4915. doi: 10.1021/es060237g.

Lafrenière, M. J. and Lamoureux, S. F. (2019) 'Effects of changing permafrost conditions on hydrological processes and fluvial fluxes', *Earth-Science Reviews*, 191, pp. 212–223. doi: 10.1016/j.earscirev.2019.02.018.

Laird, M. J. *et al.* (2018) 'Mercury and omega-3 fatty acid profiles in freshwater fish of the Dehcho Region, Northwest Territories: Informing risk benefit assessments', *Science of the Total Environment*, 637–638, pp. 1508–1517. doi: 10.1016/j.scitotenv.2018.04.381.

Lantuit, H. and Pollard, W. H. (2008) 'Fifty years of coastal erosion and retrogressive thaw slump activity on Herschel Island, southern Beaufort Sea, Yukon Territory, Canada', *Geomorphology*, 95, pp. 84–102. doi: 10.1016/j.geomorph.2006.07.040.

Lehmann-Konera, S. *et al.* (2019) 'Concentrations and loads of DOC, phenols and aldehydes in a proglacial arctic river in relation to hydro-meteorological conditions. A case study from the southern margin of the Bellsund Fjord – SW Spitsbergen', *Catena*, 174, pp. 117–129. doi: 10.1016/j.catena.2018.10.049.

Lehnherr, I. *et al.* (2018) 'The world's largest High Arctic lake responds rapidly to climate warming', *Nature Communications*, 9, pp. 1–9. doi: 10.1038/s41467-018-03685-z.

Leitch, D. R. *et al.* (2007) 'The delivery of mercury to the Beaufort Sea of the Arctic Ocean by the Mackenzie River', *Science of the Total Environment*, 373, pp. 178–195. doi: 10.1016/j.scitotenv.2006.10.041.

Lewkowicz, A. G. and Way, R. G. (2019) 'Extremes of summer climate trigger thousands of thermokarst landslides in a High Arctic environment', *Nature Communications*, 10, pp. 1–11. doi: 10.1038/s41467-019-09314-7.

Li, J. *et al.* (2017) 'Evidence for persistent organic pollutants released from melting glacier in the central Tibetan Plateau, China', *Environmental Pollution*, 220, pp. 178–185. doi: 10.1016/j.envpol.2016.09.037.

Li, X. *et al.* (2019) 'Seasonal controls of meltwater runoff chemistry and chemical weathering at Urumqi Glacier No.1 in central Asia', *Hydrological Processes*, 33, pp. 3258–3281. doi: 10.1002/hyp.13555.

Lim, A. G. *et al.* (2019) 'Enhanced particulate Hg export at the permafrost boundary, western Siberia', *Environmental Pollution*, 254, pp. 1–12. doi: 10.1016/j.envpol.2019.113083.

Lim, A. G. *et al.* (2020) 'A revised pan-Arctic permafrost soil Hg pool based on Western Siberian peat Hg and carbon observations', *Biogeosciences*, 17, pp. 3083–3097. doi: 10.5194/bg-17-3083-2020.

Lone, A. *et al.* (2019) 'Hydrochemical assessment (major ions and Hg) of meltwater in high altitude glacierized Himalayan catchment', *Environmental Monitoring and Assessment*, 191–213, pp. 1–19. doi: 10.1007/s10661-019-7338-y.

Malone, K. (1962) *Mercury Occurrences in Alaska*, *United States Department of the Interior Bureau of Mines*.

Marshall, S. J. *et al.* (2011) 'Glacier water resources on the eastern slopes of the Canadian Rocky Mountains', *Canadian Water Resources Journal*, 36, pp. 109–134. doi: 10.4296/cwrj3602823.

Mast, M. A. *et al.* (2014) 'Links between N deposition and nitrate export from a high-elevation watershed in the Colorado front range', *Environmental Science and Technology*, 48, pp. 14258–14265. doi: 10.1021/es502461k.

McClelland, J. W. *et al.* (2004) 'Increasing river discharge in the Eurasian Arctic: Consideration of dams, permafrost thaw, and fires as potential agents of change', *Journal of Geophysical Research Atmospheres*, 109, pp. 1–12. doi: 10.1029/2004JD004583.

McConnell, J. R. and Edwards, R. (2008) 'Coal burning leaves toxic heavy metal legacy in the Arctic', *Proceedings of the National Academy of Sciences of the United States of America*, 105, pp. 12140–12144. doi: 10.1073/pnas.0803564105.

Milner, A. M. *et al.* (2017) 'Glacier shrinkage driving global changes in downstream systems', *Proceedings of the National Academy of Sciences of the United States of America*, 114, pp. 9770–9778. doi: 10.1073/pnas.1619807114.

Miner, K. R. *et al.* (2017) 'Legacy organochlorine pollutants in glacial watersheds: A review', *Environmental Science: Processes and Impacts*, 19, pp. 1474–1483. doi: 10.1039/c7em00393e.

Mu, C. *et al.* (2020) 'Permafrost degradation enhances the risk of mercury release on Qinghai-Tibetan Plateau', *Science of the Total Environment*, 708, pp. 1–8. doi: 10.1016/j.scitotenv.2019.135127.

Neff, J. C. *et al.* (2008) 'Increasing eolian dust deposition in the western United States linked to human activity', *Nature Geoscience*, 1, pp. 189–195. doi: 10.1038/ngeo133.

Niu, Y. *et al.* (2017) 'Characterizing glacial meltwater sources in the Athabasca Glacier, Canada, using noble gases as tracers', *Applied Geochemistry*, 76, pp. 136–147. doi: 10.1016/j.apgeochem.2016.11.015.

Nriagu, J. O. (1979) 'Global inventory of natural and anthropogenic emissions of trace metals to the atmosphere', *Nature*, 279, pp. 409–411. doi: 10.1038/279409a0.

Nriagu, J. O. (1990) 'Global Metal Pollution Poisoning the Biosphere', *Environment: Science and Policy for Sustainable Development*, 32, pp. 7–33. doi: doi: 10.1080/00139157.1990.9929037.

Obrist, D. *et al.* (2008) 'Atmospheric mercury concentrations at Storm Peak Laboratory in the Rocky Mountains: Evidence for long-range transport from Asia, boundary layer contributions, and plant mercury uptake', *Atmospheric Environment*, 42, pp. 7579–7589. doi: 10.1016/j.atmosenv.2008.06.051.

Obrist, D. *et al.* (2017) 'Tundra uptake of atmospheric elemental mercury drives Arctic mercury pollution', *Nature*, 547, pp. 201–204. doi: 10.1038/nature22997.

Olson, C. *et al.* (2018) 'Mercury in Active-Layer Tundra Soils of Alaska: Concentrations, Pools, Origins, and Spatial Distribution', *Global Biogeochemical Cycles*, 32, pp. 1058–1073. doi: 10.1029/2017GB005840.

OTT Hydromet (2020) *Hydrolab HL4 Multiparameter Sonde*. Available at: https://www.ott.com/products/water-quality-2/hydrolab-hl4-multiparameter-sonde-54/ (Accessed: 28 April 2020).

Paudyal, R. *et al.* (2017) 'Insights into mercury deposition and spatiotemporal variation in the glacier and melt water from the central Tibetan Plateau', *Science of the Total Environment*, 599–600, pp. 2046–2053. doi: 10.1016/j.scitotenv.2017.05.145.

Phillips, V. J. A. *et al.* (2011) 'Increased mercury loadings to Western Canadian Alpine Lakes over the past 150 years', *Environmental Science and Technology*, 45, pp. 2042–2047. doi: 10.1021/es1031135.

St. Pierre, K. A. *et al.* (2018) 'Unprecedented Increases in Total and Methyl Mercury Concentrations Downstream of Retrogressive Thaw Slumps in the Western Canadian Arctic', *Environmental Science and Technology*, 52, pp. 14099–14109. doi: 10.1021/acs.est.8b05348.

St. Pierre, K. A. *et al.* (2019) 'Drivers of Mercury Cycling in the Rapidly Changing Glacierized Watershed of the High Arctic's Largest Lake by Volume (Lake Hazen, Nunavut, Canada)', *Environmental Science and Technology*, 53, pp. 1175–1185. doi: 10.1021/acs.est.8b05926.

Pokrovsky, O. S. *et al.* (2016) 'Trace element transport in western Siberian rivers across a permafrost gradient', *Biogeosciences*, 13, pp. 1877–1900. doi: 10.5194/bg-13-1877-2016.

Pokrovsky, O. S. *et al.* (2018) 'Dissolved Organic Matter Controls Seasonal and Spatial Selenium Concentration Variability in Thaw Lakes across a Permafrost Gradient', *Environmental Science & Technology*, 52, pp. 10254–10262. doi: 10.1021/acs.est.8b00918.

Reyes, A. V., Froese, D. G. and Jensen, B. J. L. (2010) 'Permafrost response to last interglacial warming: Field evidence from non-glaciated Yukon and Alaska', *Quaternary Science Reviews*, 29, pp. 3256–3274. doi: 10.1016/j.quascirev.2010.07.013.

Rippin, D. M. *et al.* (2020) '"Detachment" of icefield outlet glaciers: catastrophic thinning and retreat of the Columbia Glacier (Canada)', *Earth Surface Processes and Landforms*, 45, pp. 459–472. doi: 10.1002/esp.4746.

Schindler, D. W. and Donahue, W. F. (2006) 'An impending water crisis in Canada's western prairie provinces', *Proceedings of the National Academy of Sciences of the United States of America*, 103, pp. 7210–7216. doi: 10.1073/pnas.0601568103.

Schindler, D. W. and Smol, J P (2006) 'Cumulative effects of climate warming and other human activities on freshwaters of Arctic and subarctic North America', *Ambio*, 35, pp. 160–168. doi: 10.1579/0044-7447(2006)35.

Schuster, P. F. *et al.* (2002) 'Atmospheric mercury deposition during the last 270 years: A glacial ice core record of natural and anthropogenic sources', *Environmental Science and Technology*, 36, pp. 2303–2310. doi: 10.1021/es0157503.

Schuster, P. F. *et al.* (2011) 'Mercury export from the Yukon River Basin and potential response to a changing climate', *Environmental Science and Technology*, 45, pp. 9262–9267. doi: 10.1021/es202068b.

Schuster, P. F., Schaefer, Kevin, M., *et al.* (2018) 'Permafrost Stores a Globally Significant Amount of Mercury', *Geophysical Research Letters*, 45, pp. 1463–1471. doi: 10.1002/2017gl075571.

Schuur, E. A. G. *et al.* (2009) 'The effect of permafrost thaw on old carbon release and net carbon exchange from tundra', *Nature Letters*, 459, pp. 556–559. doi: doi:10.1038/nature08031.

Schuur, E. A. G. *et al.* (2015) 'Climate change and the permafrost carbon feedback', *Nature Review*, 520, pp. 171–179. doi: 10.1038/nature14338.

Schwikowski, M. *et al.* (2004) 'Post-17th-Century Changes of European Lead Emissions Recorded in High-Altitude Alpine Snow and Ice', *Environmental Science and Technology*, 38, pp. 957–964. doi: 10.1021/es034715o.

Screen, J. A. and Simmonds, I. (2010) 'The central role of diminishing sea ice in recent Arctic temperature amplification', *Nature*, 464, pp. 1334–1337. doi: 10.1038/nature09051.

Segal, R. A., Lantz, T. C. and Kokelj, S. V (2016) 'Acceleration of thaw slump activity in glaciated landscapes of the Western Canadian Arctic', *Environmental Research Letters*, 11, pp. 1–12. doi: 10.1088/1748-9326/11/3/034025.

Semple, K. T. *et al.* (2004) 'Defining Bioavailability and Bioaccessibility of Contaminated Soil and Sediment is Complicated', *Environmental Science & Technology*, 38, pp. 228A-231A. doi: 10.1021/es040548w.

Shanley, J. B. and Bishop, K. (2012) 'Mercury in the Environment : Pattern and Process: Part 3', in Bank, M. S. (ed.) *Mercury in the Environment: Pattern and Process*. 1st edn. University of California Press, pp. 99–196. doi: 10.1525/california/9780520271630.001.0001.

Sharma, B. M. *et al.* (2015) 'Melting Himalayan glaciers contaminated by legacy atmospheric depositions are important sources of PCBs and high-molecular-weight PAHs for the Ganges floodplain during dry periods', *Environmental Pollution*, 206, pp. 588–596. doi: 10.1016/j.envpol.2015.08.012.

Sheppard, D. S., Deely, J. M. and Edgerley, W. H. L. (1997) 'Heavy metal content of meltwaters from the Ross Dependency, Antarctica', *New Zealand Journal of Marine and Freshwater Research*, 31, pp. 313–325. doi: 10.1080/00288330.1997.9516769.

Shogren, A. J. *et al.* (2019) 'Revealing biogeochemical signatures of Arctic landscapes with river chemistry', *Scientific Reports*, 9, pp. 1–11. doi: 10.1038/s41598-019-49296-6.

Søndergaard, J. *et al.* (2012) 'Mercury transport in a low-arctic river in Kobbefjord, West Greenland (64° N)', *Water, Air, and Soil Pollution*, 223, pp. 4333–4342. doi: 10.1007/s11270-012-1198-1.

Sonke, J. E. *et al.* (2018) 'Eurasian river spring flood observations support net Arctic Ocean mercury export to the atmosphere and Atlantic Ocean', *Proceedings of the National Academy of Sciences of the United States of America*, 115, pp. E11586–E11594. doi: 10.1073/pnas.1811957115.

Sprague, J. B. (2007) 'Great Wet North? Canada's Myth of Water Abundance', in Bakker, K. (ed.) *Eau Canada*. 1st edn. Vancouver: UBC Press, pp. 23–36.

Steinlin, C. *et al.* (2016) 'A Temperate Alpine Glacier as a Reservoir of Polychlorinated Biphenyls: Model Results of Incorporation, Transport, and Release', *Environmental Science and Technology*, 50, pp. 5572–5579. doi: 10.1021/acs.est.5b05886.

Stern, G. A. *et al.* (2012) 'How does climate change influence arctic mercury?', *Science of The Total Environment*, 414, pp. 22–42. doi: 10.1016/j.scitotenv.2011.10.039.

Stocker, T. F. *et al.* (2013) 'Climate Change 2013: The Physical Science Basis. Contribution of Working Group I to the Fifth Assessment Report of the Intergovernmental Panel on Climate Change', in Stocker, T. F. et al. (eds). Cambridge, United Kingdom and New York, NY, USA: Cambridge University Press, p. 115.

Streets, D. G. *et al.* (2011) 'All-Time Releases of Mercury to the Atmosphere from Human Activities', *Environmental Science & Technology*, 45, pp. 10485–10491. doi: 10.1021/es202765m.ALL-TIME.

Sun, S. *et al.* (2018) 'Insights into mercury in glacier snow and its incorporation into meltwater runoff based on observations in the southern Tibetan Plateau', *Journal of Environmental Sciences (China)*, 68, pp. 130–142. doi: 10.1016/j.jes.2018.03.033.

Sun, X. *et al.* (2017) 'The role of melting alpine glaciers in mercury export and transport: An intensive sampling campaign in the Qugaqie Basin, inland Tibetan Plateau', *Environmental Pollution*, 220, pp. 936–945. doi: 10.1016/j.envpol.2016.10.079.

Sun, X. *et al.* (2018) 'Mercury speciation and distribution in a glacierized mountain environment and their relevance to environmental risks in the inland Tibetan Plateau', *Science of the Total Environment*, 631–632, pp. 270–278. doi: 10.1016/j.scitotenv.2018.03.012.

Sun, Y. *et al.* (2020) 'Glacial Melt Inputs of Organophosphate Ester Flame Retardants to the Largest High Arctic Lake', *Environmental Science and Technology*, 54, pp. 2734–2743. doi: 10.1021/acs.est.9b06333.

Sunderland, E. M. and Selin, N. E. (2013) 'Future trends in environmental mercury concentrations: Implications for prevention strategies', *Environmental Health: A Global Access Science Source*, 12, pp. 1–5. doi: 10.1186/1476-069X-12-2.

Swennen, R. and Vandeginste, V. (2003) 'Genesis of zebra dolomites (Cathedral Formation : Canadian Cordillera Fold and Thrust Belt , British Columbia)', *Journal of Geochemical Exploration*, 78–79, pp. 571–577. doi: 10.1016/S0375-6742(03)00065-7.

Tarnocai, C. (2009) 'The Impact of Climate Change on Canadian Peatlands', *Canadian Water Resources Journal*, 34, pp. 453–466. doi: 10.4296/cwrj3404453.

Tennant, C. and Menounos, B. (2013) 'Glacier change of the Columbia Icefield, Canadian Rocky Mountains, 1919-2009', *Journal of Glaciology*, 59, pp. 671–686. doi: 10.3189/2013JoG12J135.

Beijer Institute *et al.* (1987) *Environmental impacts of coal mining and utilization.* In Chadwick M.J., Highton N.H., and Lindman N. (eds). Pergamon Press, pp. 171–217. doi: 10.1016/b978-0-08-031427-3.50002-5.

The Government of Canada, The Vuntut Gwitchin First Nation and The Government of the Yukon (1993) *Vuntut Gwitchin First Nation Final Agreement*. doi: 10.1017/CBO9781107415324.004.

Toohey, R. C. *et al.* (2016) 'Multidecadal increases in the Yukon River Basin of chemical fluxes as indicators of changing flowpaths, groundwater, and permafrost', *Geophysical Research Letters*, 43, pp. 12,120-12,130. doi: 10.1002/2016GL070817.

U.S. Environmental Protection Agency (1996) *Method 1669 Sampling Ambient Water for Trace Metals at EPA Water Quality Criteria Levels 20460*. Washington, D. C.

U.S. Environmental Protection Agency (2002) *Method 1631, Revision E: Mercury in water by oxidation, purge and trap, and cold vapor atomic fluorescence spectrometry*, *Epa 821-R-96-012*.

Ullrich, S. M., Tanton, T. W. and Abdrashitova, S. A. (2001) 'Mercury in the Aquatic Environment : A Review of Factors Affecting Methylation', *Environmental Science and Technology*, 31. doi: 10.1080/20016491089226.

US Environmental Protection Agency (2009) 'Environmental Chemistry, Transport and Fate', *Guidance for Reporting on the Environmental Fate and Transport of the Stressors of Concern in Problem Formulations*, p. 30.

VanLooy, J. A. and Vandeberg, G. S. (2019) 'Late summer glacial meltwater contributions to Bull Lake Creek stream flow and water quality, Wind River Range, Wyoming, USA', *Physical Geography*, 40, pp. 461–480. doi: 10.1080/02723646.2019.1565215.

Vermilyea, A. W. *et al.* (2017) 'Continuous proxy measurements reveal large mercury fluxes from glacial and forested watersheds in Alaska', *Science of the Total Environment*, 599–600, pp. 145–155. doi: 10.1016/j.scitotenv.2017.03.297.

Villa, S. *et al.* (2006) 'Organochlorine compounds in ice melt water from Italian Alpine rivers', *Ecotoxicology and Environmental Safety*, 63, pp. 84–90. doi: 10.1016/j.ecoenv.2005.05.010.

Wada, T. *et al.* (2011) 'Glacial effects on discharge and sediment load in the subarctic Tanana River Basin, Alaska', *Arctic, Antarctic, and Alpine Research*, 43, pp. 632–648. doi: 10.1657/1938-4246-43.4.632.

Wade, A. J. *et al.* (2012) 'Hydrochemical processes in lowland rivers: Insights from in situ, high-resolution monitoring', *Hydrology and Earth System Sciences*, 16, pp. 4323–4342. doi: 10.5194/hess-16-4323-2012.

Wasiuta, V. *et al.* (2019) 'Accumulating Mercury and Methylmercury Burdens in Watersheds Impacted by Oil Sands Pollution', *Environmental Science and Technology*, 53, pp. 12856–12864. doi: 10.1021/acs.est.9b02373.

Water Survey of Canada (2020) *Daily Discharge Graph for SUNWAPTA RIVER AT ATHABASCA GLACIER (07AA007) [AB] - Water Level and Flow - Environment Canada*. Available at: https://wateroffice.ec.gc.ca/report/historical_e (Accessed: 28 April 2020).

Wedepohl, H. K. (1995) 'The composition of the continental crust', *Geochimica et Cosmochimica Acta*, 59, pp. 1217–1232. doi: 10.1016/0016-7037(95)00038-2.

Willis, B. L. (1997) *The environmental effects of the Yukon Gold Rush, 1896-1906: Alterations to land, destruction of wildlife, and disease*. University of Western Ontario.

Yang, Z. *et al.* (2016) 'Warming increases methylmercury production in an Arctic soil', *Environmental Pollution*, 214, pp. 504–509. doi: 10.1016/j.envpol.2016.04.069.

YSI Inc. (2020) *Multiparameter water quality instrument - YSI EXO - EXO2 Sonde*. Available at: https://www.ysi.com/exo2 (Accessed: 28 April 2020).

Yukon Ecoregion Working Group (2004) 'Old Crow Flats', in Smith, C. A. S., Meikle, J. C., and Roots, C. F. (eds) *Ecoregions of the Yukon Territory: Biophysical Properties of Yukon Landscapes*. Summerland, British Columbia: Minister of Supply and Services Canada, pp. 115–122.

Yukon Placer Secretariat (2016) *Water Quality Monitoring Annual Report Klondike Watershed 2016*.

Zazula, G. D. *et al.* (2004) 'Late Pleistocene chronology of glacial Lake Old Crow and the north west margin of the Laurentide Ice Sheet', *Quaternary Glaciations - Extent and Chronology, Part II*. Edited by J. Ehlers and P. L. Gibbard, pp. 347–362. doi: 10.1016/S1571-0866(04)80207-0.

Zdanowicz, C. *et al.* (2018) 'Snowmelt, glacial and atmospheric sources of mercury to a subarctic mountain lake catchment, Yukon, Canada', *Geochimica et Cosmochimica Acta*, 238, pp. 374–393. doi: 10.1016/j.gca.2018.06.003.

Zemp, M. *et al.* (2019) 'Global glacier mass changes and their contributions to sea-level rise

from 1961 to 2016', *Nature*, 568, pp. 382–386. doi: 10.1038/s41586-019-1071-0.

Zhang, L., Wright, L. P. and Blanchard, P. (2009) 'A review of current knowledge concerning dry deposition of atmospheric mercury', *Atmospheric Environment*, 43, pp. 5853–5864. doi: 10.1016/j.atmosenv.2009.08.019.

Zhang, Y., *et al.* (2016) 'Observed decrease in atmospheric mercury explained by global decline in anthropogenic emissions', *Proceedings of the National Academy of Sciences of the United States of America*, 113, pp. 526–531. doi: 10.1073/pnas.1516312113.

Zolkos, S. *et al.* (2020) 'Mercury Export from Arctic Great Rivers', *Environmental Science and Technology*, 54, pp. 4140–4148. doi: 10.1021/acs.est.9b07145.

APPENDIX A

Table A.1. Raw chemical, discharge, and sonde data is attached electronically**.**

A.1. Sonde and Chemical Data

Dissolved oxygen, temperature, specific conductance, turbidity, and pH were measured using Hydrolab HL4 (OTT Hydromet, 2020) and EXO2 (YSI Inc., 2020) sondes. Sonde sensors were calibrated and maintained during grab sampling on a monthly basis. Measurements of each parameter were cross-validated during grab-sampling with alternate sondes at the time of grab sampling, and in the laboratory in grab-samples by electronic meters. Turbidity was measured using the nephelometric method; MDL: 0.1 NTU. Dissolved Oxygen was measured by a luminescent electronic meter; MDL: 0.1 mg/L. Specific Conductance was measured by conductivity meter with a platinum electrode; MDL: 0.4 µS/cm. pH was measured by an electronic meter with a glass electrode, calibrated with standard buffer solutions. Temperature was measured using a resistance thermometer.

An assessment of 30-minute resolution, 4 point mean smoothed sonde parameters reveals 3 periods of sonde sensor malfunction. (1) Data were suspended from analyses for turbidity from August 8 to September 11, 2017 due to turbidity sensor miscalibration (Hydrolab DS5X 46884). (2) Data were suspended from analyses for pH from July 10 to August 8, 2018 due to pH sensor malfunction (Sonde 14A103775). (3) All sonde-parameters were suspended from analyses from August 25 and September 12, 2018 due to emergence of the sonde from the stream. The sonde was discovered on the bank of the Sunwapta River during maintenance on September 12, 2018. The high temporal resolution data was inspected visually to determine at which date and time the

disturbance had occurred. Temperature, conductance, pH, and dissolved oxygen parameters each displayed a break in pattern at August 25th. Additionally, up to 1 h of data were discarded around periods of sonde service where readings showed a jump and return to the trend.

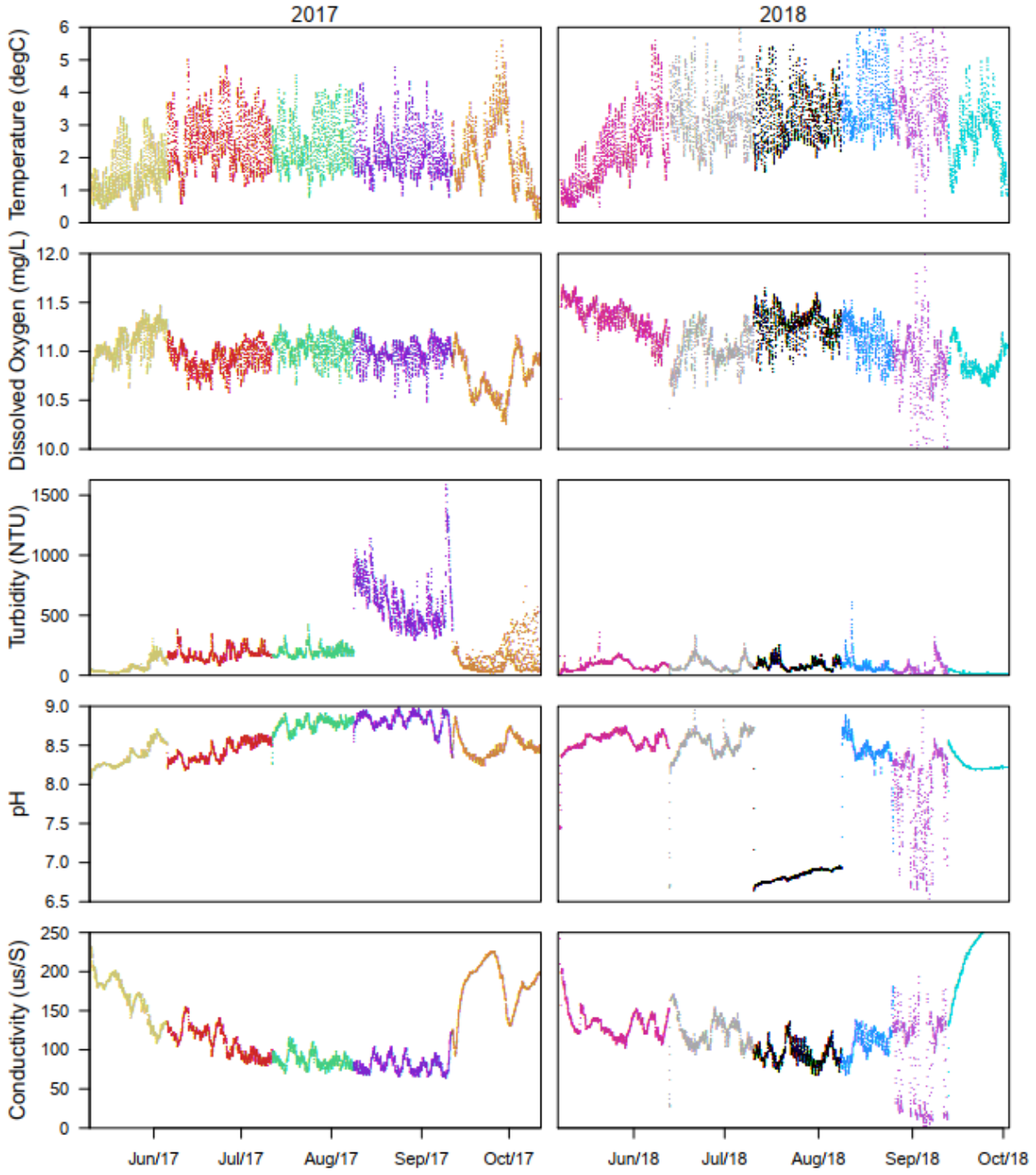

Figure A.1. Timeseries of raw sonde data at 4pt mean smooth presented at 30-minute resolution, pre-processing, for May 10 – Oct. 11, 2017; and May 7 – Oct. 2, 2018. Plot is coloured by intervals between sonde maintenance and calibration. Detachments in the trend indicates sensor malfunction.

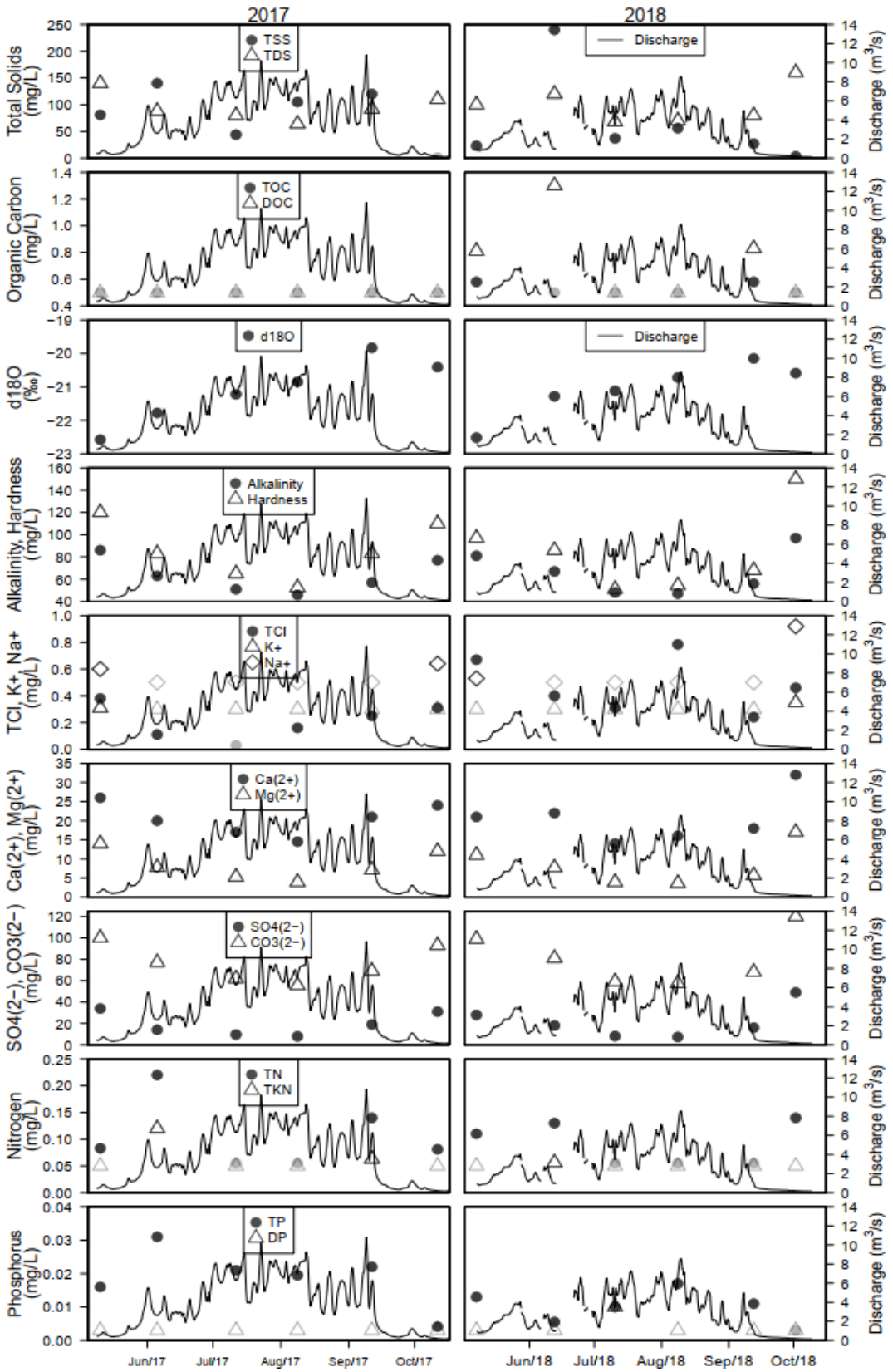

Figure A.2. Timeseries of chemical parameters (symbols) and discharge smoothed at 24h (line). Light grey points are plotted where parameters were at or below the method detection limit.

A.2. Principal Component Analysis

Table A.2. Scaled loadings from principal component analysis

	PC1	PC2	PC3	PC4
Temp	0.171	0.010	-0.012	-0.007
Q	0.157	0.049	-0.139	-0.141
pH	0.150	0.115	0.083	-0.062
TBe	0.149	-0.161	-0.001	-0.043
Turb	0.137	-0.020	-0.216	-0.224
THg	0.133	-0.125	0.155	0.102
TAl	0.128	-0.184	-0.070	-0.021
TCo	0.128	-0.187	0.023	0.020
TP	0.124	-0.081	-0.200	0.141
TPb	0.117	-0.188	0.106	0.001
TCr	0.117	-0.196	0.000	-0.018
TFe	0.115	-0.198	0.049	0.024
DAl	0.113	-0.108	-0.140	-0.231
TCu	0.112	-0.198	-0.003	-0.101
TV	0.112	-0.199	-0.052	-0.027
TTh	0.103	-0.208	0.020	-0.003
TAs	0.099	-0.202	0.120	0.064
TMn	0.099	-0.205	0.115	0.055
TSS	0.089	-0.181	0.023	0.030
TZn	0.081	-0.207	0.072	-0.127
DHg	0.075	-0.090	0.306	0.196
TNi	0.062	-0.178	-0.186	0.258
DO	0.053	-0.017	0.369	-0.025
TTi	0.048	-0.149	-0.150	0.014
TBa	0.047	-0.229	-0.020	0.032
TLi	0.032	-0.242	-0.040	0.023
TCa	0.016	-0.231	0.133	-0.015
DNi	-0.021	-0.044	-0.338	0.396
DMn	-0.030	0.087	0.263	0.329
DCo	-0.037	0.016	-0.231	0.500
TCl	-0.058	-0.004	0.321	0.083
TB	-0.108	-0.183	-0.157	-0.022
DTi	-0.125	-0.113	-0.192	-0.144
TMo	-0.133	-0.094	0.186	0.150
TSb	-0.137	-0.158	-0.034	0.164
NO^{3-}	-0.149	-0.133	0.046	-0.095
NO^{3-}+NO^{2-}	-0.151	-0.126	0.043	-0.116
TSr	-0.153	-0.145	0.093	0.014
TDS	-0.171	-0.098	-0.036	-0.054
DB	-0.172	-0.102	-0.067	0.041

Ca^{2+}	-0.174	-0.092	-0.045	-0.126
TU	-0.176	-0.103	0.047	-0.074
DLi	-0.180	-0.072	-0.100	0.094
DMo	-0.181	-0.077	0.037	0.052
Hard	-0.183	-0.080	-0.047	-0.087
DCa	-0.185	-0.064	0.012	-0.123
Bicarb	-0.187	-0.072	0.038	-0.021
TAlk	-0.187	-0.075	0.019	0.007
DBa	-0.187	-0.059	0.042	0.079
DMg	-0.188	-0.068	-0.046	-0.031
DU	-0.188	-0.064	0.024	-0.057
$SO4^{2-}$	-0.190	-0.043	-0.019	-0.089
DSr	-0.191	-0.057	0.033	-0.019
EC	-0.192	-0.051	0.009	-0.010

A.3. Simple Linear Regression

Data normality was checked visually using quantile-quantile plots (Fig. A.2) prior to conducting linear regression models on the data. No parameters were transformed. Linear regression was performed exclusively on pairwise complete observations, on post-processed data. Data were reduced to the largest common time interval between observations; missing values in pairwise comparisons were removed, and Pearson correlation coefficients (r) and p-values were computed. Concentrations were modelled at a higher temporal resolution using simple linear regression equations. Simple linear regression equations were generated between select elements and continuous parameters to model instantaneous flux and annual flux, and annual yield. The resultant regression equations were used to model element concentrations (Table A.3).

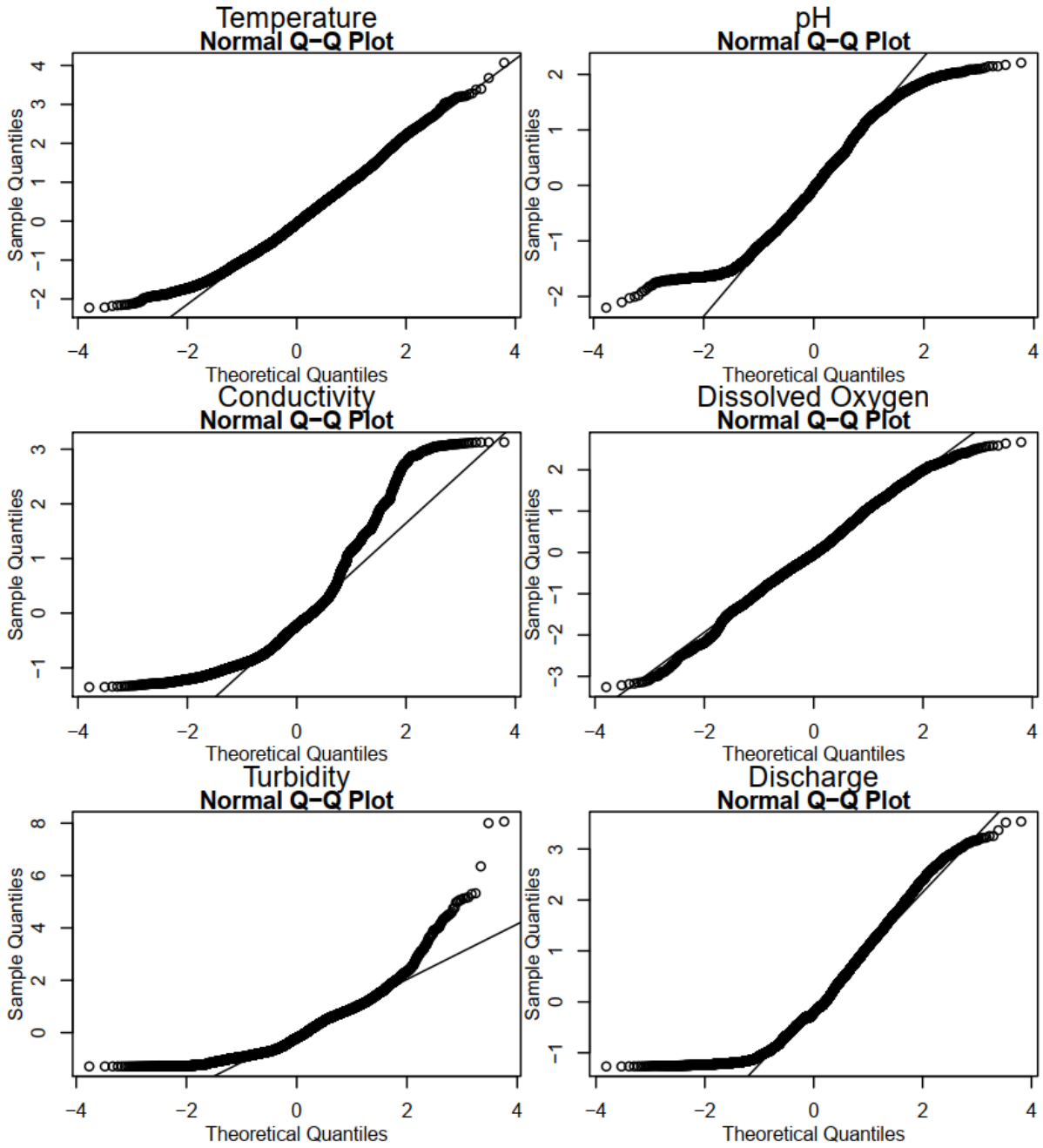

Figure A.3. Quantile-Quantile plots of sonde data. Turbidity and discharge displayed strongly right-skewed behaviour.

Table A.3. Simple Linear Regression equations, pearson correlation and p-values for select chemical parameters and the sonde parameter (turbidity or conductivity) identified in the principal component analysis (Figure 3.4, main text) as the most closely covaried.

Parameter	Slope & Modeling Parameter	Intercept	R	P-Value
TSS	0.2592 x Turbidity	+ 61.861	0.2446	4.96E-01
TAl	2.617 x Turbidity	+ 395.373	0.3863	2.41E-01
TPb	0.001116 x Turbidity	+ 0.6085	0.1416	6.78E-01
TCr	0.002990 x Turbidity	+ 0.5769	0.3359	3.12E-01
TAs	0.0001465 x Turbidity	+ 0.1432	0.0905	7.91E-01
THg	0.0004199 x Turbidity	+ 1.4545	0.2871	3.92E-01
TDS	0.4863 x Conductivity	+ 26.0019	0.9588	3.21E-06
TSr	0.7253 x Conductivity	+ 13.2882	0.8759	4.07E-04
DCa	0.07380 x Conductivity	+ 8.7757	0.9736	4.42E-07
TU	0.002631 x Conductivity	+ 0.009159	0.9618	2.30E-06

Table A.4. Extended table of simple linear regression Pearson correlations and p-values.

	Turbidity		Discharge		Conductivity	
	r	p-value	r	p-value	r	p-value
Water Temp	0.2676	4.262E-01	0.7186	1.273E-02	-0.8024	2.959E-03
pH	0.4226	1.953E-01	0.5744	6.457E-02	-0.7787	4.746E-03
Conductivity	-0.5184	1.023E-01	-0.8053	2.781E-03	1.0000	0.000E+00
DO	-0.2142	5.271E-01	0.1475	6.651E-01	-0.3560	2.825E-01
Turbidity	1.0000	0.000E+00	0.5902	5.594E-02	-0.5184	1.023E-01
Discharge	0.5902	5.594E-02	1.0000	0.000E+00	-0.8053	2.781E-03
N-NO2	-0.3142	3.467E-01	-0.6689	2.440E-02	0.8463	1.021E-03
N-NO2-NO3	-0.3367	3.114E-01	-0.6574	2.795E-02	0.8541	8.162E-04
DAl	0.4058	2.156E-01	0.5978	5.206E-02	-0.4321	1.844E-01
DAs	0.1867	6.055E-01	0.2577	4.723E-01	0.0354	9.226E-01
DB	-0.3865	2.404E-01	-0.6996	1.657E-02	0.9318	3.000E-05
DBa	-0.5323	9.184E-02	-0.8682	5.288E-04	0.9746	3.774E-07
DCa	-0.4208	1.975E-01	-0.7701	5.555E-03	0.9736	4.425E-07
DCo	-0.3334	3.163E-01	-0.1782	6.001E-01	0.1998	5.558E-01
DLi	-0.4163	2.028E-01	-0.7372	9.638E-03	0.9561	4.265E-06
DMn	-0.3278	3.251E-01	-0.3040	3.634E-01	-0.0384	9.108E-01
DMo	-0.4618	1.527E-01	-0.8237	1.830E-03	0.9683	9.992E-07
DNi	-0.1719	6.132E-01	-0.0494	8.852E-01	0.1983	5.590E-01
DSr	-0.4793	1.358E-01	-0.8212	1.942E-03	0.9934	8.955E-10
DTi	-0.2054	5.692E-01	-0.6633	3.653E-02	0.8350	2.645E-03
DU	-0.4452	1.700E-01	-0.7869	4.051E-03	0.9898	6.361E-09
TAg	-0.3135	4.114E-01	0.1050	7.880E-01	-0.1806	6.419E-01
TAl	0.3864	2.405E-01	0.3394	3.072E-01	-0.4697	1.449E-01
CaCO3	-0.4023	2.200E-01	-0.7522	7.569E-03	0.9806	1.116E-07
THg	0.2872	3.919E-01	0.4897	1.262E-01	-0.6588	2.750E-02
DHg	0.0270	9.371E-01	0.0403	9.063E-01	-0.5116	1.077E-01
Mg2+	-0.4109	2.093E-01	-0.7505	7.790E-03	0.9881	1.240E-08
Alkalinity	-0.4849	1.306E-01	-0.7996	3.135E-03	0.9946	3.626E-10
Bicarbonate	-0.4932	1.232E-01	-0.7963	3.356E-03	0.9928	1.330E-09
SO42-	-0.4137	2.059E-01	-0.7399	9.228E-03	0.9819	8.310E-08
TDS	-0.5094	1.095E-01	-0.7646	6.125E-03	0.9588	3.213E-06
TSS	0.2446	4.958E-01	-0.0775	8.316E-01	-0.1514	6.763E-01
Ca2+	-0.4227	1.953E-01	-0.7543	7.314E-03	0.9652	1.528E-06
TP	0.3961	2.278E-01	0.5522	7.820E-02	-0.5613	7.239E-02
TAs	0.0905	7.913E-01	0.0813	8.123E-01	-0.3286	3.237E-01
TB	-0.1657	6.263E-01	-0.5189	1.019E-01	0.6878	1.933E-02
TBa	0.0876	7.978E-01	-0.1052	7.581E-01	-0.0367	9.147E-01
TBe	0.3777	2.521E-01	0.4333	1.830E-01	-0.5907	5.570E-02
TCa	-0.0762	8.238E-01	-0.2873	3.917E-01	0.0958	7.793E-01
TCl	-0.5009	1.166E-01	-0.2383	4.804E-01	0.2552	4.488E-01
TCo	0.2302	4.959E-01	0.2635	4.337E-01	-0.4606	1.539E-01
TCr	0.3359	3.125E-01	0.2754	4.124E-01	-0.4305	1.862E-01
TCu	0.2453	4.672E-01	0.2333	4.900E-01	-0.3516	2.890E-01
TFe	0.1831	5.899E-01	0.1831	5.899E-01	-0.3954	2.287E-01

TLi	0.0463	8.925E-01	-0.1126	7.417E-01	0.0550	8.724E-01
TMn	0.0886	7.955E-01	0.0811	8.126E-01	-0.3241	3.309E-01
TMo	-0.5041	1.139E-01	-0.8047	2.817E-03	0.8599	6.880E-04
TNi	-0.0489	8.864E-01	0.0509	8.818E-01	-0.1086	7.505E-01
TPb	0.1416	6.779E-01	0.1946	5.663E-01	-0.4132	2.065E-01
TSb	-0.4630	1.515E-01	-0.6874	1.942E-02	0.8009	3.051E-03
TSr	-0.4792	1.358E-01	-0.8272	1.682E-03	0.8759	4.071E-04
TTh	0.2292	4.978E-01	0.1372	6.876E-01	-0.3357	3.129E-01
TTi	0.4149	2.045E-01	0.1913	5.731E-01	-0.1422	6.767E-01
TTl	0.4357	1.804E-01	0.2165	5.225E-01	-0.2987	3.723E-01
TU	-0.4645	1.501E-01	-0.7956	3.405E-03	0.9618	2.303E-06
TV	0.3510	2.898E-01	0.2457	4.664E-01	-0.3854	2.418E-01
TZn	0.0266	9.381E-01	0.0967	7.774E-01	-0.1923	5.711E-01

A.4. Comparisons of Flux and Yield Estimation Methods

Annual fluxes were estimated using three methods: (1) the product of daily discharge and daily concentration, modeled by simple linear regression with conductivity or turbidity, (2) the product of daily discharge and daily concentration, linearly interpolated between grab-sampling events, and (3) the product of mean annual discharge and mean annual concentration. The three estimates methods provide consistent results with %RSD < 20 % for conductivity, and %RSD < 15% for turbidity (Table A.4). Annual fluxes estimated using simple linear regression with conductivity are systematically lower than linear interpolated and mean-annual concentration estimates.

Table A.5. Mean annual flux estimates using three methods, and the % relative standard deviation between the estimates. The mean flux of 2017 and 2018 is presented.

Chemical Parameter	Simple Linear Regression Mean Flux	Linear Interpolation Mean Flux	Mean Annual Concentration Mean Flux	Estimate % RSD
	(Gg/yr)	**(Gg/yr)**	**(Gg/yr)**	**%**
TSS	4.5	4.0	3.4	15%
TDS	3.4	3.7	4.5	14%
DCa	0.7	0.8	0.9	11%
	(Mg/yr)	**(Mg/yr)**	**(Mg/yr)**	**%**
TAl	35.1	36.1	29.2	11%
TSr	4.0	4.3	5.7	20%
	(kg/yr)	**(kg/yr)**	**(kg/yr)**	**%**
TCr	45.8	47.5	40.1	9%
TPb	38.7	39.2	32.9	10%
TU	12.5	14.0	17.0	16%
TAs	7.5	8.1	7.3	5%
THg	0.10	0.10	0.09	8%

A.5. Comparisons of Mercury Flux and Yield Results to Literature

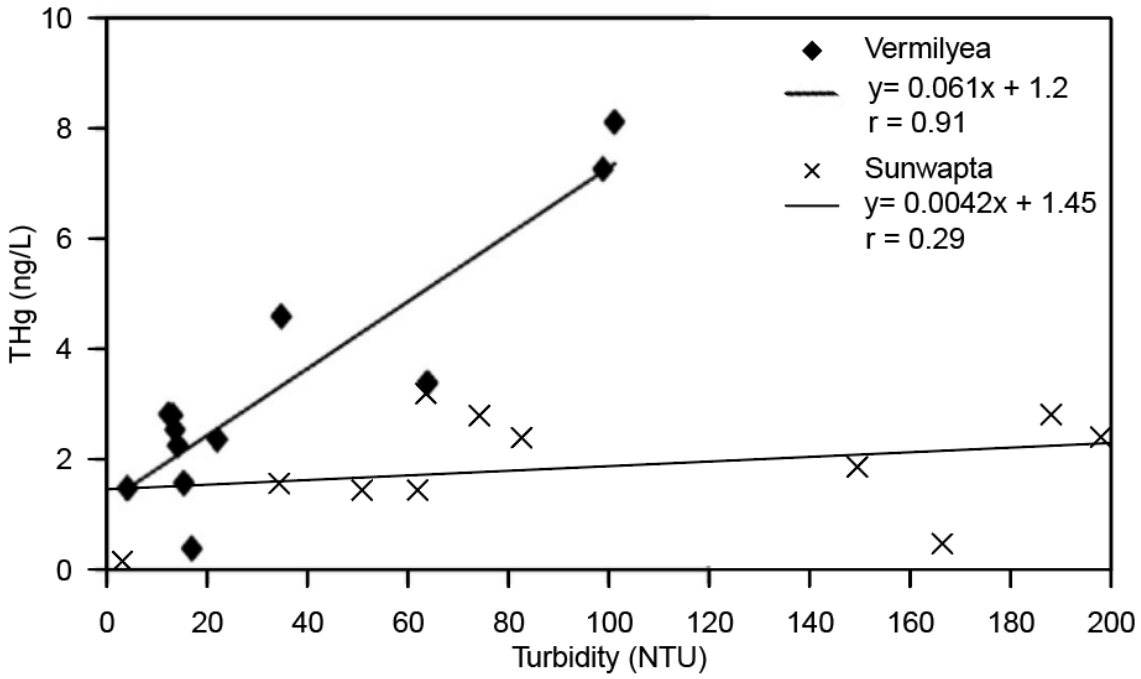

Figure A.4. Comparison of mercury-turbidity correlation at Sunwapta River and Lemon Creek, Alaska. Figure modified from Vermilyea et al., 2017.

Table A.6. Comparison of mercury yields across a range of geographic and physiographic catchment settings.

Source	Watershed Physiographic Description	Geographic Location	Yield ($g/km^2/yr$) (mean or range)	Watershed Identifier	Watershed Area (km^2)	Glacial Cover
This study	proglacial	Rocky Mountains, Canada	3.5 2.6 – 4.5	Sunwapta	29.3	70%
Vermilyea et al., 2017	proglacial	Coastal Alaska	19.9	Lemon Creek	32	55%
Sondergaard 2012	proglacial	Arctic, Greenland	0.45 0.2 – 0.5	Kobblefjord	32	6%
X. Sun et al., 2017	proglacial	Tibetan Plateau, proglacial station	0.99	Qugaqie Basin	7.4	27%
X. Sun et al., 2017	proglacial	Tibetan Plateau, downstream station	2.7	Qugaqie Basin	57.6	3%
St Pierre et al., 2019	proglacial	Arctic, Canada	1.7 0.57 – 3.88	Lake Hazen Proglacial tributaries	7156	41%
Zolkos et al., 2020	large arctic	Arctic, Russia	0.8	Ob	2990000	-
Zolkos et al., 2020	large arctic	Arctic, Russia	1.5	Yenisey	2400000	-
Zolkos et al., 2020	large arctic	Arctic, Russia	2.7	Lena	2430000	-
Zolkos et al., 2020	large arctic	Arctic, Russia	2.1	Kolyma	530000	-
Zolkos et al., 2020	large arctic	Arctic, USA	4	Yukon	830000	-
Schuster et al., 2011	large arctic	Alaska, USA	5.17	Yukon River	850000	-
Zolkos et al., 2020	large arctic	Arctic, Canada	1.6	Mackenzie	1680000	-
Emmerton et al., 2013	large arctic	Arctic, Canada	1.3 – 2.4	Mackenzie and Peel	1780000	-
Kirk & St. Louis, 2009	large prairie	Arctic, Canada	0.13	Churchill	281000	-
Kirk & St. Louis, 2009	large prairie	Arctic, Canada	0.13	Nelson	892000	-
Kirk & St. Louis, 2009	large prairie	Canadian Prairie	0.4	N. Sask. at Edmonton	28100	-
Vermilyea et al., 2017	forested/ wetland	Coastal Alaska	3.0 – 6.0	Peterson Creek	25	-
Brigham et al., 2009	forested	Ore., Wis., Fla., U.S.A.	0.87 – 4.36	selection	62 – 2630	-
Brigham et al., 2009	urban	Ore., Wis., Fla., U.S.A.	1.60 – 3.63	selection	64 – 115	-

A.6. References

Brigham, M. E. *et al.* (2009) 'Mercury cycling in stream ecosystems. 1. Water column chemistry and transport', *Environmental Science and Technology*, 43, pp. 2720–2725. doi: 10.1021/es802694n.

Emmerton, C. A. *et al.* (2013) 'Mercury export to the Arctic Ocean from the Mackenzie River, Canada', *Environmental Science and Technology*, 47, pp. 7644–7654. doi: 10.1021/es400715r.

Kirk, J. L. and Louis, V. L. S. (2009) 'Multiyear total and methyl mercury exports from two major sub-arctic rivers draining into Hudson Bay, Canada', *Environmental Science and Technology*, 43, pp. 2254–2261. doi: 10.1021/es803138z.

OTT Hydromet (2020) *Hydrolab HL4 Multiparameter Sonde*. Available at: https://www.ott.com/products/water-quality-2/hydrolab-hl4-multiparameter-sonde-54/ (Accessed: 28 April 2020).

Schuster, P. F. *et al.* (2011) 'Mercury export from the Yukon River Basin and potential response to a changing climate', *Environmental Science and Technology*, 45, pp. 9262–9267. doi: 10.1021/es202068b.

Søndergaard, J. *et al.* (2012) 'Mercury transport in a low-arctic river in Kobbefjord, West Greenland (64° N)', *Water, Air, and Soil Pollution*, 223, pp. 4333–4342. doi: 10.1007/s11270-012-1198-1.

St Pierre, K. A. *et al.* (2019) 'Drivers of Mercury Cycling in the Rapidly Changing Glacierized Watershed of the High Arctic's Largest Lake by Volume (Lake Hazen, Nunavut, Canada)', *Environmental Science and Technology*, 53, pp. 1175–1185. doi: 10.1021/acs.est.8b05926.

Sun, X. *et al.* (2017) 'The role of melting alpine glaciers in mercury export and transport: An intensive sampling campaign in the Qugaqie Basin, inland Tibetan Plateau', *Environmental Pollution*, 220, pp. 936–945. doi: 10.1016/j.envpol.2016.10.079.

Vermilyea, A. W. *et al.* (2017) 'Continuous proxy measurements reveal large mercury fluxes from glacial and forested watersheds in Alaska', *Science of the Total Environment*, 599–600, pp. 145–155. doi: 10.1016/j.scitotenv.2017.03.297.

YSI Inc. (2020) *Multiparameter water quality instrument - YSI EXO - EXO2 Sonde*. Available at: https://www.ysi.com/exo2 (Accessed: 28 April 2020).

Zolkos, S. *et al.* (2020) 'Mercury Export from Arctic Great Rivers', *Environmental Science & Technology*, 54, pp. 4140–4148. doi: 10.1021/acs.est.9b07145.

APPENDIX B

B.1. Site Descriptions

B.1.1. River Mouth

The Old Crow River mouth sampling site (67.5817º, -139.8020º) was located on a cobble-gravel point bar on the west bank of the river, at the base of a ~ 40 m-tall bluff, 1 km west of the village of Old Crow. The moderately consolidated sandy-silt bluff did not have appreciably organic-rich strata and was covered by very sparse vegetation (grass clumps and dogwood). Small colluvial cones were present at the base of the bluff, indicating that the bluff is actively eroding. Small intra-beds of gravelly material were present near river level (May 14, 2019). The river at the sample site is gravel-bedded, made up of well-rounded cobble to gravel sizes clasts. The river water was coloured dark brown throughout the year.

B.1.2. Slump Sampling Locations

1. TS1: 68.1008, -139.8351°
2. TS2: 67.8087°, -139.8864°
3. TS3: 67.8798°, -139.7617°
4. TS4: 67.9037°, -139.7106°

The four sampled thaw slumps sampled were comparable in size and setting, and were representative of other active and inactive slumps observed from the air. Retrogressive thaw slumps in this watershed formed along the cut banks of bluffs along the meandering river. The average thaw slump basin was ~30 – 50 m across, and headwall height was ~2 – 5 m. The thaw

slump lobes (mobilized sediment at river level) were variable in size (TS2 and TS3's lobes were submerged; TS1 and TS4's lobes extended ~10 – 15 meters into the river course). Slump headwalls were overhung by organic rich peats in the active layer of the ground-surface level. In-situ headwall sediments were dominated by clay and silt, and were very ice rich with exposed ice wedges and lenticular cryostructures. TS1 headwall sediment was carbonate in nature; TS2, TS3, TS4 headwall sediments were aluminosilicate in nature. The thawed debris in the thaw slump basins incorporated thawed ice rich silt sediment from the headwall as well as organic matter from the overhanging active layer.

B.1.3. Tributary Sampling Locations

We sampled water from eight tributary creeks to the Old Crow River, between July 21 and 28, 2019. Samples were collected 100 – 1000 m upstream of the tributary and Old Crow River confluence, along the tributary, in continuous flow.

1. Bilwaddy Creek Mouth: (68.1876°, -140.9075°) Upper Old Crow River tributary. Drains the mountainous northwestern portion of the watershed. Very minor alpine glacier contribution. Pebbly to sandy substrate. Shallow banks covered by sparse willow and conifers.
2. Thomas Creek Mouth: (68.1879°, -140.6534°) Many beaver dams and fallen trees which obstruct flow have been observed along the creek (Anderton, 2004). Drains the mountainous northern portion of the watershed. Muddy substrate.

3. Surprise Creek Mouth: (68.2268°, -140.4157°) Drains a large portion of the central-western OCF (Anderton, 2004); likely significant thermokarst lake connectivity during high precipitation. Densely vegetated and steep banks.
4. Timber Creek Mouth: (68.1688°, -139.9430°) Drains the central north-eastern portion of the OCF and a large portion of Vuntut National Park.
5. Black Fox Creek Mouth: (68.0570°, -139.5763°) Drains the north-eastern OCF. Banks were loosely vegetated by deciduous trees. Substrate was coarse grained.
6. Johnson Creek Mouth: (67.8346°, -139.7983°) Drains a large portion of the eastern OCF (Anderton, 2004). This tributary is the largest, highest flow tributary to the Old Crow River.
7. Schaeffer Creek Mouth: (67.8380°, -139.8504°) Sampled a kilometer upstream of the mouth. The flow speed was low and the water was a murky brown colour. Samples were collected 0.5 m from the right bank. Flow of water was obstructed by numerous fallen deciduous trees. The river substrate was organic rich, and thickly muddy. Schaeffer Creek drains many thermokarst lakes and wetlands (Anderton, 2004) from the central Old Crow Flats.
8. King Edward Creek Mouth: (67.8169°, -139.9428°) Was sampled a kilometer upstream. Flow speed was low, the stream colour was a murky red. Sample was collected by boat in the center of the bank. The banks had dense spruce vegetation cover. The sub-catchment area is the smallest of the tributaries sampled, and flows from the direction of Schaeffer Mountain.

Table B.1. Description of Tributary Creek sampling locations, listed in order of confluence with the Old Crow River Mainstem from upstream to downstream.

Sample ID	Location	GPS coordinate	Substrate	Vegetation	Sampling distance	Water Depth	Clarity	Flow speed	Distance from Mouth	Thermokarst Lake within Drainage
OCRT1	Bilwaddy	68.1876°, -140.9075°	gravelly	Sparse, willow and grass	1.5 m from left bank	0.4 m	v. clear	low	~200 m	Minimal
OCRT2	Thomas	68.1879°, -140.6534°	Muddy	Sparse; black spruce	0.5 m from R bank	1.0 m	brown; murky	strong	~100 m	Minimal
OCRT3	Surprise	68.2268°, -140.4157°	Treed, muddy	Densely vegetated, black spruce, v. steep bank	0.5 m from R bank	>2 m	brown; v. murky	v. low	~500 m	Substantial
OCRT4	Timber	68.1688°, -139.9430°	Silty	Densely treed and willow	1 m from L bank	>1 m	moderate	low	>1000 m	Minimal
OCRT5	Black Fox	68.0570°, -139.5763°	Sandy-pebbly	Deciduous	2 m from L bank	0.3 m	v. clear	moderate	~500 m	Minimal
OCRT6	Johnson	67.8346°, -139.7983°	Sandy-pebbly	Willow; deciduous	off sand bar in good flow	>2 m	v. clear	v. strong	>1000 m	Moderate
OCRT7	Schaeffer	67.8380°, -139.8504°	V. muddy, organic rich	Deciduous; many fallen trees	0.5 m from R bank	>1m	brown; murky	low	>1000 m	Substantial
OCRT14	King Edward	67.8169°, -139.9428°	Sampled by boat. Too murky to see	Dense black spruce cover, steep bank	center stream - by boat	>1m	red; v. murky	v. low	>1000 m	Minimal

B.2. Methodology

B.2.1. Additional Water Chemistry Analytical Information

River water samples were analyzed for routine parameters. Turbidity was analyzed using the Hack Laboratory Turbidimeter 2100N; US EPA Method 180.1. Measurements of pH, conductivity, and alkalinity were made using electrometric PC-Titrate instrumentation. Cations (Al, Ca, Fe, K, Mg, Na), were measured by inductively coupled argon plasma optical emission spectrometry. Anions (SO4, Cl) were measured by ion chromatography. Deuterium and $\delta^{18}O$ were measured by Picarro Isotope Analyzer L2130-I, laser spectroscopic analysis of liquid water samples, and are presented in δ-notation relative to VSMOW-standard. Nitrogen and phosphorus species were analyzed by Flow Injection Analysis on a Lachat QuickChem QC8500 FIA Automated Ion Analyzer by Method 353.2 4500-NH3-B,H, and 4500-P-G. 31 total and dissolved trace elements were analyzed by inductively coupled plasma mass spectrometry. Mercury was analyzed by oxidation, purge and trap, and Cold Vapor Atomic Fluorescence Spectrometry on a Tekran 2600 Total Mercury Analyzed using US EPA Method 1631E. Methylmercury was analyzed by Isotope Dilution, Distillation, Aqueous Ethylation, Purge and Trap, Gas Chromatography and Inductively Coupled Plasma Mass Spectrometry using a Tekran 2750 Methyl Mercury Distillation System, Tekran 2700 Methyl Mercury Analyzer, Agilent 7900 ICP-MS, using US EPA Method 1630. Filterable and nonfilterable residue concentrations (i.e., total dissolved and total suspended solids; TDS and TSS) were derived from masses of, respectively, evaporated, and dried materials of known original volumes.

B.3. Quality Control

B.3.1. Discards

Water chemistry samples' selenium and tin results were suspended from statistical analyses. Tin returned below detection for all sampling events. Selenium returned at precisely the method detection limit, or at only 2x the MDL above; making statistical inference unreliable.

B.3.2. Water Chemistry Quality Control

Total and routine parameters were collected in duplicate for the first three sampling events. Dissolved parameters were collected in duplicate on the June 4 sampling event. The average difference between duplicate concentrations was small (Table B.2). Water quality control field blank consisted of Milli-Q DI water transported from the University of Alberta to the site. Bottles were rinsed and filled at the shore of the river, and filtered in the field laboratory with QCDI water transported from the BASL (May, June, August, October) and Innotech (September) laboratories. Most parameters returned below detection for all 5 collection events. Of the 5 QCDI field blanks collected, concentrations of inorganic carbon, aluminum, and iron, were in excess of the MDL in 4 cases (Table B.2.); this suggests that a minor amount of dust-related contamination may have occurred during grab-sampling. Concentrations of dissolved solids, calcium, titanium, and zinc were in excess in 3 cases; nitrogen, organic carbon, the ions Ca, Fe, and elements Cu, Pb, Ni were in excess in 2 cases; and total P, Hg, Th, V, Ag, and As and the ions magnesium, sodium, and calcium were in excess in 1 case. The exceedances of the MDL were low in comparison to unknown parameter concentrations.

Table B.2. Water Chemistry QCDI Results; % of QCDI which exceed the method detection limit (MDL), the mean exceedance of the MDL, and the mean difference between duplicates.

Parameter	% QCDI >MDL	QCDI >MDL Mean	Mean dupl. dif. (original units)
NFR (mg/L) MDL <0.05	0%	-	15
TDS (mg/L) MDL <0.05	60%	6	7
TN (µg/L as N) MDL <6	40%	15	18
NO2+NO3 (µg/L as N) MDL <2	20%	7	5
TP (µg/L as P) MDL <1	20%	1	15
NH4 (µg/L as N) MDL <3	0%	-	6
SRP (µg/L as P) MDL <1	0%	-	
DIC (mg/L) MDL <0.2	80%	0.95	0.58
Ca (mg/L) MDL <0.01	40%	0.03	0.24
DOC (mg/L) MDL <0.1	40%	0.45	0.42
Mg (mg/L) MDL <0.01	20%	0.02	0.09
Na (mg/L) MDL <0.02	20%	0.02	0.02
Cl (mg/L) MDL <0.03	20%	0.42	0.34
Al (µg/L) MDL <3.6	0%	-	
K (mg/L) MDL <0.01	0%	-	0.03
SO4 (mg/L) MDL <0.04	0%	-	0.23
Aluminum, Total MDL <4 µg/L	80%	2.7	110
Iron, Total MDL <0.6 µg/L	80%	1.2	
Calcium, Total MDL <0.01 mg/L	60%	0.02	0.93
Titanium, Total MDL <0.03 µg/L	60%	0.08	0.11
Zinc, Total MDL <0.2 µg/L	60%	0.7	1.3
Chlorine, Total MDL <0.03 mg/L	40%	0.2	0.1
Copper, Total MDL <0.08 µg/L	40%	0.1	0.7
Lead, Total MDL <0.004 µg/L	40%	0.01	0.23
Nickel, Total MDL <0.03 µg/L	40%	0.05	0.6
Total Mercury (ng/L) MDL <0.06	20%	0.27	0.82
Arsenic, Total MDL <0.01 µg/L	20%	0.010	0.24
Silver, Total MDL <0.001 µg/L	20%	0.001	0.003
Thorium, Total MDL <0.002 µg/L	20%	0.005	0.11
Vanadium, Total MDL <0.007 µg/L	20%	0.010	0.57
Methyl Mercury (ng/L) MDL <0.01	0%	-	0.006
Antimony, Total MDL <0.008 µg/L	0%	-	0.01
Cadmium, Total MDL <0.01 µg/L	0%	-	0.02
Chromium, Total MDL <0.1 µg/L	0%	-	0.4
Selenium, Total MDL <0.2 µg/L	0%	-	-
Strontium, Total MDL <0.07 µg/L	0%	-	1.2
Thallium, Total MDL <0.002 µg/L	0%	-	0.003
Tin, Total MDL <0.06 µg/L	0%	-	
Uranium, Total MDL <0.002 µg/L	0%	-	0.035

B.3.3. Sediment Chemistry Quality Control

Table B.3. DMA-80 MESS-4 and Duplicate results

Sample ID	THg (µg/kg)	St. Dev.
	Reference Material	
MESS-4	81.4	2.9
	76.9	
	74.9	
	75.6	
	Duplicates	
Headwall	76.0	0.3
	75.6	
Basin-debris	74.0	1.3
	72.1	

Table B.4. ICP-MS MESS-4 Results and Certified Values, and the relative percent difference between 4 duplicate sets of unknowns.

Analyte	MESS-4 mean concentration	MESS-4 duplicate %	MESS-4 certified value	Relative Percent Difference Between Unknown Duplicates			
	mg/kg			in-situ	debris	active	basin
Sb	1.10	1.2%	1.07 ± 0.16	6.3%	4.5%	24.3%	0.4%
As	16.0	0.9%	21.7 ± 2.8	24.0%	4.6%	22.2%	0.4%
Be	1.91	16.8%	2.09 ± 0.28	53.2%	3.0%	2.4%	5.2%
Cd	0.16	1.7%	0.28 ± 0.04	9.1%	1.1%	3.9%	0.2%
Cr	107.5	0.2%	94.3 ± 1.8	45.5%	0.9%	30.1%	0.5%
Co	12.7	1.1%	13.0 ± 0.8	13.8%	0.2%	11.7%	1.5%
Cu	31.4	4.9%	32.9 ± 1.8	7.7%	1.8%	9.5%	0.7%
Pb	22.6	0.8%	21.5 ± 1.2	20.4%	0.6%	2.2%	0.6%
Li	75.9	1.9%	65.3 ± 6.8	66.0%	1.3%	29.7%	8.0%
Mn	301	3.8%	298 ± 14	14.8%	0.0%	7.2%	0.1%
Ni	37.1	4.2%	42.8 ± 1.6	21.8%	0.2%	19.0%	0.6%
Ag	0.6	0.4%	0.161 ± 0.024	14.7%	6.3%	18.3%	2.8%
Sr	133	2.8%	132 ± 8	12.6%	1.2%	14.0%	0.8%
Tl	1.04	5.1%	0.85 ± 0.10	37.5%	1.7%	4.5%	1.5%
Sn	2.87	5.3%	2.35 ± 0.12	31.6%	5.6%	31.4%	1.0%
U	3.9	2.7%	3.4 ± 0.4	18.2%	1.4%	18.1%	0.2%
V	250	0.7%	216 ± 8	45.8%	0.9%	25.1%	0.5%
Zn	135	5.1%	147 ± 6	132.2%	0.0%	20.8%	0.6%
	g/kg						
Al	85.5	2.8%	79.1 ± 2.0	47.5%	0.0%	22.9%	0.7%
Ca	11.8	0.4%	13.1 ± 0.6	23.7%	0.0%	4.4%	0.3%
Fe	59.9	2.0%	37.9 ± 1.6	22.0%	0.7%	12.6%	0.2%
Mg	15.4	3.5%	15.8 ± 1.2	11.5%	0.4%	24.1%	0.5%
P	1.16	6.8%	1.04 ± 0.16	6.0%	0.8%	14.5%	1.4%
K	28.6	1.2%	23.8 ± 1.0	45.7%	0.4%	4.8%	0.3%
Na	10.5	6.0%	12.6 ± 0.8	43.3%	0.0%	9.1%	0.1%
Ti	4.03	1.2%	3.84 ± 0.22	23.0%	1.4%	29.9%	0.8%

B.4. Results

B.4.1. Historic Discharge

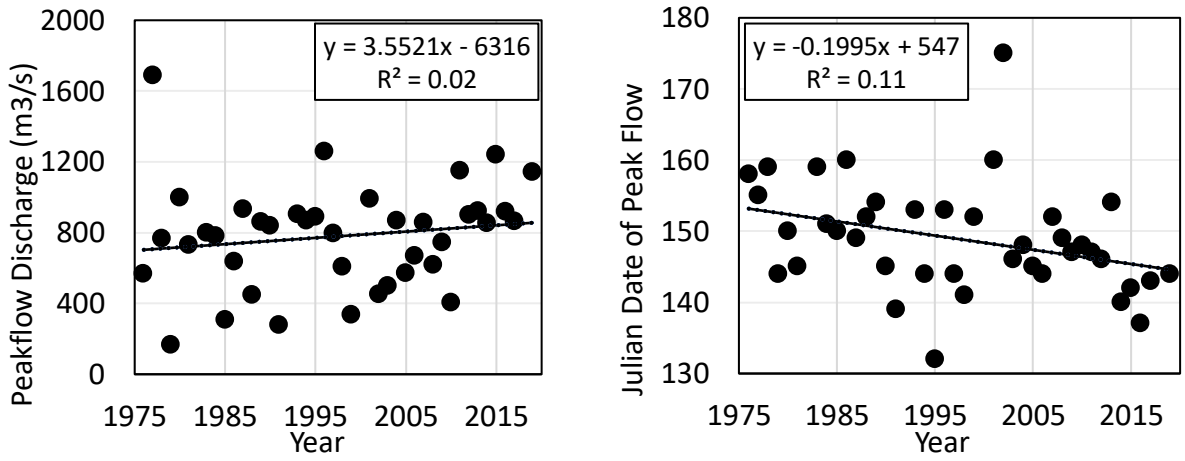

Figure B.1. Peak Freshet discharge magnitude and Julian date across the 42-year record at the Old Crow River mouth. No significant trend is observed in peak flow discharge magnitude. The date of peak freshet magnitude, however, has moved ~8 days earlier over the 42-year record.

B.4.2. Correlograms of Water Chemistry: River Mouth and River Basin in July

Table B.5. Correlation of Parameters at River Mouth

Parameter	TSS	DOC	Q	TSS*Q	DOC*Q	d18O	d2H	d-excess
Total Mercury (ng/L) MDL <0.06	0.87	0.73	0.88	0.76	0.88	-0.91	-0.80	0.75
Dissolved Mercury (ng/L) MDL <0.08	0.86	0.92	0.92	0.88	0.92	-0.82	-0.80	0.39
Methyl Mercury (ng/L) MDL <0.01	0.84	0.72	0.83	0.76	0.83	-0.83	-0.74	0.65
Dissolved Methyl Mercury (ng/L) MDL <0.01	0.46	0.60	0.44	0.37	0.43	-0.30	-0.22	0.56
NO2+NO3 (µg/L as N) MDL <2	0.54	0.90	0.57	0.40	0.58	-0.70	-0.56	0.75
NO2 (µg/L as N) MDL <1	-0.02	0.12	-0.03	-0.01	-0.02	-0.10	-0.23	-0.44
NH4 (µg/L as N) MDL <3	0.17	-0.01	0.22	0.29	0.23	-0.24	-0.41	-0.28
TN (µg/L as N) MDL <6	0.95	0.68	0.95	0.89	0.95	-0.95	-0.90	0.62
TDN (µg/L as N) MDL <6	0.49	0.80	0.55	0.43	0.57	-0.72	-0.77	0.26
TKN (µg/L as N) MDL <6	0.96	0.60	0.94	0.92	0.95	-0.92	-0.90	0.52
SRP (µg/L as P) MDL <1	-0.17	0.30	-0.17	-0.20	-0.17	0.17	0.19	-0.04
TP (µg/L as P) MDL <1	1.00	0.54	0.99	0.96	0.99	-0.94	-0.89	0.62
TDP (µg/L as P) MDL <2	0.69	0.63	0.72	0.63	0.73	-0.77	-0.86	0.17
Al (µg/L) MDL <3.6	0.88	0.70	0.92	0.87	0.92	-0.92	-0.90	0.52
Ca (mg/L) MDL <0.01	-0.43	-0.48	-0.46	-0.43	-0.48	0.47	0.64	0.19
K (mg/L) MDL <0.01	-0.17	-0.30	-0.19	-0.10	-0.19	0.15	-0.11	-0.69
Mg (mg/L) MDL <0.01	-0.30	-0.49	-0.34	-0.24	-0.34	0.32	0.16	-0.55
Na (mg/L) MDL <0.02	-0.11	0.11	-0.10	-0.17	-0.10	0.13	0.39	0.56
Cl (mg/L) MDL <0.03	0.57	0.42	0.60	0.57	0.60	-0.51	-0.34	0.69
SO4 (mg/L) MDL <0.04	-0.36	-0.24	-0.38	-0.39	-0.39	0.41	0.64	0.34
DOC (mg/L) MDL <0.1	0.51	1.00	0.56	0.41	0.57	-0.67	-0.58	0.57
DIC (mg/L) MDL <0.2	-0.47	-0.58	-0.50	-0.44	-0.51	0.50	0.59	-0.03
pH MDL <N/A	-0.66	-0.63	-0.70	-0.60	-0.70	0.75	0.68	-0.57
Alkalinity (mg/L) MDL <3	-0.50	-0.60	-0.52	-0.45	-0.53	0.56	0.62	-0.13
Cond (µS/cm) MDL <N/A	-0.48	-0.47	-0.51	-0.48	-0.52	0.52	0.70	0.18
Bicarbonate (mg/L as HCO3) MDL <N/A	0.65	0.98	0.73	0.56	0.74	-0.85	-0.88	0.65
Turbidity (NTU) MDL <N/A	0.98	0.59	0.97	0.93	0.97	-0.93	-0.84	0.69
TDS (mg/L) MDL <0.05	-0.47	-0.40	-0.50	-0.49	-0.51	0.51	0.71	0.23
NFR (mg/L) MDL <0.05	1.00	0.51	0.99	0.98	0.99	-0.93	-0.88	0.60
δ^2H (‰) MDL <N/A	-0.88	-0.58	-0.91	-0.87	-0.92	0.95	1.00	-0.37
$\delta^{18}O$ (‰) MDL <N/A	-0.93	-0.67	-0.95	-0.88	-0.96	1.00	0.95	-0.64
Aluminum, Total MDL <4 µg/L	1.00	0.53	0.99	0.97	0.99	-0.93	-0.88	0.61
Antimony, Total MDL <0.008 µg/L	0.68	0.05	0.65	0.68	0.64	-0.62	-0.71	0.11
Arsenic, Total MDL <0.01 µg/L	0.99	0.54	0.99	0.96	0.99	-0.95	-0.92	0.57
Barium, Total MDL <0.05 µg/L	0.92	0.26	0.89	0.91	0.88	-0.82	-0.81	0.43
Beryllium, Total MDL <0.003 µg/L	1.00	0.55	0.99	0.97	0.99	-0.94	-0.88	0.62
Bismuth, Total MDL <0.003 µg/L	0.92	0.35	0.91	0.93	0.90	-0.83	-0.82	0.47
Boron, Total MDL <0.2 µg/L	0.31	-0.16	0.26	0.36	0.26	-0.19	-0.37	-0.35
Cadmium, Total MDL <0.01 µg/L	1.00	0.52	0.99	0.97	0.99	-0.93	-0.87	0.63
Calcium, Total MDL <0.01 mg/L	-0.49	-0.62	-0.54	-0.49	-0.55	0.59	0.74	0.06
Chlorine, Total MDL <0.03 mg/L	-0.47	-0.42	-0.49	-0.39	-0.49	0.64	0.55	-0.57
Chromium, Total MDL <0.1 µg/L	1.00	0.54	0.99	0.97	0.99	-0.95	-0.90	0.61
Cobalt, Total MDL <0.002 µg/L	1.00	0.54	0.99	0.97	0.99	-0.94	-0.89	0.61
Copper, Total MDL <0.08 µg/L	0.99	0.54	0.99	0.97	0.99	-0.94	-0.89	0.62
Iron, Total MDL <6 µg/L	0.99	0.57	0.99	0.96	0.99	-0.95	-0.90	0.62
Lead, Total MDL <0.004 µg/L	1.00	0.50	0.99	0.98	0.99	-0.93	-0.89	0.57
Lithium, Total MDL <0.007 µg/L	0.93	0.36	0.90	0.90	0.89	-0.80	-0.69	0.70
Manganese, Total MDL <0.04 µg/L	1.00	0.52	0.99	0.98	0.99	-0.94	-0.90	0.58
Molybdenum, Total MDL <0.002 µg/L	-0.32	-0.75	-0.36	-0.21	-0.37	0.41	0.20	-0.72
Nickel, Total MDL <0.03 µg/L	0.98	0.59	0.98	0.95	0.98	-0.93	-0.85	0.68
Silver, Total MDL <0.001 µg/L	0.99	0.55	0.98	0.95	0.98	-0.94	-0.88	0.65
Strontium, Total MDL <0.07 µg/L	-0.52	-0.70	-0.56	-0.48	-0.57	0.63	0.74	-0.07
Thallium, Total MDL <0.002 µg/L	1.00	0.50	0.99	0.98	0.99	-0.93	-0.88	0.63
Thorium, Total MDL <0.002 µg/L	1.00	0.52	0.99	0.97	0.99	-0.94	-0.90	0.59
Titanium, Total MDL <0.03 µg/L	0.87	0.71	0.88	0.76	0.89	-0.94	-0.83	0.75

Uranium, Total MDL <0.002 µg/L	0.76	-0.05	0.72	0.79	0.71	-0.61	-0.57	0.41
Vanadium, Total MDL <0.007 µg/L	1.00	0.53	0.99	0.97	0.99	-0.94	-0.90	0.59
Zinc, Total MDL <0.2 µg/L	0.98	0.61	0.98	0.93	0.98	-0.94	-0.86	0.70

Table B.6. Correlogram of water chemistry across the basin, grab sampled in July; upstream, downstream, and tributary samples, and mouth.

Parameter	TSS	DOC	$\delta^{18}O$	$\delta^{2}H$	d-excess
Total Mercury (ng/L) MDL <0.06	0.62	-0.13	-0.33	-0.13	0.51
Dissolved Mercury (ng/L) MDL <0.08	-0.44	0.56	-0.02	0.02	0.07
Methyl Mercury (ng/L) MDL <0.01	-0.21	0.63	0.37	0.51	-0.16
Dissolved Methyl Mercury (ng/L) MDL <0.01	-0.54	0.81	0.54	0.50	-0.52
NO2+NO3 (µg/L as N) MDL <2	0.73	-0.10	-0.22	-0.16	0.25
NO2 (µg/L as N) MDL <1	0.55	-0.17	0.07	0.10	-0.03
NH4 (µg/L as N) MDL <3	-0.38	0.35	0.38	0.28	-0.43
TN (µg/L as N) MDL <6	0.24	0.51	0.52	0.53	-0.44
TDN (µg/L as N) MDL <6	0.12	0.62	0.64	0.63	-0.57
TKN (µg/L as N) MDL <6	-0.28	0.80	0.77	0.73	-0.72
SRP (µg/L as P) MDL <1	0.76	-0.46	-0.35	-0.37	0.29
TP (µg/L as P) MDL <1	0.81	-0.30	-0.18	-0.09	0.25
TDP (µg/L as P) MDL <2	0.33	0.40	0.30	0.29	-0.27
Al (µg/L) MDL <3.6	-0.27	0.66	-0.05	0.06	0.16
Ca (mg/L) MDL <0.01	0.39	-0.65	-0.81	-0.81	0.70
K (mg/L) MDL <0.01	-0.05	0.09	0.50	0.51	-0.43
Mg (mg/L) MDL <0.01	-0.09	-0.03	-0.20	0.04	0.44
Na (mg/L) MDL <0.02	-0.03	0.27	0.12	0.34	0.14
Cl (mg/L) MDL <0.03	0.60	-0.52	-0.32	-0.32	0.27
SO4 (mg/L) MDL <0.04	-0.06	-0.10	-0.39	-0.18	0.58
DOC (mg/L) MDL <0.1	-0.41	1.00	0.43	0.43	-0.37
DIC (mg/L) MDL <0.2	0.38	-0.65	-0.65	-0.75	0.46
pH MDL <N/A	0.19	-0.45	-0.42	-0.56	0.20
Alkalinity (mg/L) MDL <3	0.34	-0.64	-0.63	-0.76	0.42
Cond (µS/cm) MDL <N/A	0.30	-0.64	-0.86	-0.79	0.82
Turbidity (NTU) MDL <N/A	0.81	-0.30	-0.27	-0.12	0.41
TDS (mg/L) MDL <0.05	0.15	-0.47	-0.86	-0.81	0.81
NFR (mg/L) MDL <0.05	1.00	-0.41	-0.33	-0.29	0.34
$\delta^{2}H$ (‰) MDL <N/A	-0.29	0.43	0.95	1.00	-0.77
$\delta^{18}O$ (‰) MDL <N/A	-0.33	0.43	1.00	0.95	-0.93
Aluminum, Total MDL <4 µg/L	0.70	-0.32	-0.30	-0.11	0.48
Antimony, Total MDL <0.008 µg/L	0.60	-0.35	-0.12	-0.08	0.15
Arsenic, Total MDL <0.01 µg/L	0.29	0.54	0.52	0.53	-0.45
Barium, Total MDL <0.05 µg/L	0.21	-0.01	0.71	0.76	-0.56
Beryllium, Total MDL <0.003 µg/L	0.70	0.02	-0.24	-0.06	0.41
Bismuth, Total MDL <0.003 µg/L	0.00	0.14	0.54	0.55	-0.45
Boron, Total MDL <0.2 µg/L	-0.05	0.00	0.51	0.65	-0.29
Cadmium, Total MDL <0.01 µg/L	0.77	-0.10	-0.18	-0.06	0.29
Calcium, Total MDL <0.01 mg/L	0.22	-0.52	-0.78	-0.79	0.66
Chlorine, Total MDL <0.03 mg/L	0.08	-0.49	-0.11	-0.21	-0.02
Chromium, Total MDL <0.1 µg/L	0.61	0.01	-0.17	0.02	0.36
Cobalt, Total MDL <0.002 µg/L	0.62	0.08	-0.22	-0.04	0.39
Copper, Total MDL <0.08 µg/L	0.75	-0.11	-0.10	0.06	0.26
Iron, Total MDL <6 µg/L	0.70	0.15	0.06	0.19	0.09
Lead, Total MDL <0.004 µg/L	0.84	-0.39	-0.50	-0.36	0.58
Lithium, Total MDL <0.007 µg/L	0.05	-0.15	-0.34	-0.14	0.51
Manganese, Total MDL <0.04 µg/L	0.59	-0.03	-0.09	-0.02	0.16
Molybdenum, Total MDL <0.002 µg/L	0.28	-0.19	0.26	0.09	-0.42
Nickel, Total MDL <0.03 µg/L	-0.13	0.31	-0.27	-0.20	0.32
Silver, Total MDL <0.001 µg/L	0.73	-0.22	-0.27	-0.06	0.47
Strontium, Total MDL <0.07 µg/L	0.47	-0.79	-0.74	-0.72	0.66
Thallium, Total MDL <0.002 µg/L	0.39	0.03	-0.11	0.09	0.32
Thorium, Total MDL <0.002 µg/L	0.69	-0.01	-0.01	0.14	0.18
Titanium, Total MDL <0.03 µg/L	0.79	-0.26	-0.29	-0.12	0.44
Uranium, Total MDL <0.002 µg/L	0.45	-0.66	-0.73	-0.78	0.58
Vanadium, Total MDL <0.007 µg/L	0.71	-0.11	-0.12	0.05	0.29
Zinc, Total MDL <0.2 µg/L	0.72	-0.23	-0.32	-0.14	0.49

Aluminum, Dissolved MDL <0.4 µg/L	-0.25	0.24	-0.15	-0.12	0.17
Antimony, Dissolved MDL <0.09 µg/L	0.45	-0.78	-0.67	-0.76	0.50
Arsenic, Dissolved MDL <0.01 µg/L	-0.17	0.49	0.84	0.69	-0.92
Barium, Dissolved MDL <0.05 µg/L	-0.01	0.08	0.84	0.84	-0.74
Beryllium, Dissolved MDL <0.004 µg/L	-0.47	0.84	0.11	0.12	-0.09
Bismuth, Dissolved MDL <0.003 µg/L	-0.09	-0.13	0.28	0.30	-0.22
Boron, Dissolved MDL <0.2 µg/L	-0.08	0.04	0.53	0.68	-0.31
Cadmium, Dissolved MDL <0.002 µg/L	0.06	0.32	0.26	0.32	-0.16
Calcium, Dissolved MDL <0.03 mg/L	0.20	-0.54	-0.78	-0.81	0.67
Chlorine, Dissolved MDL <0.2 mg/L	0.09	-0.50	0.36	0.45	-0.22
Chromium, Dissolved MDL <0.3 µg/L	-0.32	0.48	0.16	0.02	-0.31
Cobalt, Dissolved MDL <0.006 µg/L	0.41	0.43	-0.20	0.06	0.39
Copper, Dissolved MDL <0.08 µg/L	-0.01	0.54	0.47	0.57	-0.30
Iron, Dissolved MDL <2 µg/L	-0.38	0.61	0.89	0.81	-0.89
Lead, Dissolved MDL <0.02 µg/L	-0.33	0.40	0.62	0.55	-0.62
Lithium, Dissolved MDL <0.02 µg/L	-0.12	-0.11	-0.31	-0.15	0.47
Manganese, Dissolved MDL <0.01 µg/L	-0.09	0.42	0.10	0.25	0.09
Molybdenum, Dissolved MDL <0.005 µg/L	0.29	-0.17	0.25	0.08	-0.43
Nickel, Dissolved MDL <0.03 µg/L	-0.42	0.83	0.42	0.51	-0.27
Strontium, Dissolved MDL <0.07 µg/L	0.41	-0.82	-0.76	-0.75	0.69
Thallium, Dissolved MDL <0.002 µg/L	-0.67	0.03	-0.56	-0.72	0.18
Thorium, Dissolved MDL <0.002 µg/L	0.03	0.41	0.19	0.19	-0.17
Titanium, Dissolved MDL <0.03 µg/L	0.04	0.19	0.22	0.34	-0.05
Uranium, Dissolved MDL <0.002 µg/L	0.46	-0.63	-0.73	-0.77	0.61
Vanadium, Dissolved MDL <0.006 µg/L	0.40	0.04	0.45	0.40	-0.47
Zinc, Dissolved MDL <0.3 µg/L	-0.41	0.41	0.23	0.30	-0.12

Table B.7. Electronic Appendix containing Raw Provisional 2019 discharge data, hydrochemistry data.

B.5. References

Anderton, I. (2004) *Porcupine River Watershed Fisheries Information Summary Report*. Whitehorse, YT.